2008

Assessment of oxygen sources and sinks in the northern Gulf of Mexico using stable oxygen isotopes

Zoraida Jazmin Quinones-Rivera
Louisiana State University and Agricultural and Mechanical College

ASSESSMENT OF OXYGEN SOURCES AND SINKS IN THE NORTHERN GULF OF MEXICO USING STABLE OXYGEN ISOTOPES

A Dissertation

Submitted to the Graduate Faculty of the
Louisiana State University and
Agricultural and Mechanical College
in partial fulfillment of the
requirements for the degree of
Doctor of Philosophy

in

The Department of Oceanography and Coastal Sciences

by
Zoraida J. Quiñones-Rivera
B.S., Tulane University, 1996
M.S., Louisiana State University, 2001
May 2008

For Björn

ACKNOWLEDGMENTS

This work was funded by the National Oceanographic and Atmospheric Administration Coastal Ocean Program grant for hypoxic studies (NA06OP0526; PI: D. Justić). I am thankful to my major professor, D. Justić, and my graduate committee and advisors; N. N. Rabalais, K. Rose, C. Li, A. Sluyter and B. Fry. I am particularly grateful to N. N. Rabalais for organizing and leading the shelfwide and monthly cruises, also funded by NOAA Coastal Ocean Program (NA06OP0528; PI: N. N. Rabalais). Z. J. Q. R. was supported by a grant from the J. Bennett Johnston Science Foundation. N. N. Rabalais provided surface PAR, oxygen, salinity, and temperature data that were incorporated in this work. R. E. Turner provided Secchi depth readings and B. Fry provided isotope laboratory facilities. The crews of the *R/V Pelican* and *R/V Acadiana* provided important technical field support. I thank N. Atilla, A. Barker, B. Cole, V. Gudatti, J. Lee, and C. Milan, for their assistance in the field and laboratory, as well as N. N. Rabalais, N. Ostrom and three anonymous reviewers for their helpful comments on Chapter 2 (Quiñones-Rivera et al. 2007). Last but not least, I thank my parents, Dorisoraida and Jose Antonio, and my dear sister Doris.

TABLE OF CONTENTS

ABSTRACT

Coastal hypoxia (< 2 mg O_2 L^{-1}) represents a global problem that continues to worsen as nutrient fluxes to these areas increase. The second largest zone of human-induced hypoxia is located on the Louisiana continental shelf where hypoxic bottom waters commonly occur during summertime. This region is strongly impacted by the large flux of freshwater and nutrients from the Mississippi River, which influences both biological and physical processes that control oxygen dynamics. Yet, based on oxygen concentration measurements alone, it is difficult to separate the effects of biological factors from physical factors. To address this problem, I used a dual budget approach to assess the importance of oxygen sources and sinks on the Louisiana continental shelf. The dual budget was based on using stable oxygen isotopes ($\delta^{18}O$) in combination with conventional oxygen concentration measurements. To analyze temporal trends, surface and bottom water samples were collected monthly between July 2001 and July 2003 along an onshore-offshore transect. For better spatial resolution, shelfwide sampling was conducted extending from the Mississippi River Delta to the Louisiana-Texas border in the month of July of 2001, 2002, and 2003. Oxygen saturations values ranged between 180% at the surface and almost 0% close to the bottom with a corresponding range of $\delta^{18}O$ values from 15‰ to 50‰. Biological parameters were important during all seasons for surface oxygen dynamics. The effects of physical factors were less apparent, except during severe physical disturbances. Bottom water oxygen dynamics showed clear seasonal signals of high oxygen depletion and larger contributions of benthic respiration during the summer, which corresponded to the strong stratification of the water column. In bottom waters, summer oxygen depletion was predominantly due to benthic respiration, accounting for about 73%, 80% and 60% of the total oxygen loss for 2001, 2002 and 2003 respectively. Model estimates of production/respiration

(P/R) ratio during the July shelfwide cruises indicated that surface waters were productive with an average calculated P/R above 1. Depth stratified sampling (5 m intervals), which started in July 2002, showed that productivity in the mixed layer (5 to 10 m) was not homogeneous. Calculated P/R exceeded 1 only in the surface layer, while at 5 m P/R was approximately 1 and at a depth of 10 m, P/R was less than 1. Additionally, hypoxic conditions were only detected within 5 m of the bottom sediments. The dual budget approach yielded new estimates of productivity dynamics in surface waters and of sediment oxygen demand in bottom waters.

For the first time, this study provided routine insight into productivity and respiration dynamics over large temporal and spatial scales. This could not have been accomplished using traditional methods because they commonly rely on time-consuming incubations. The study has shown that respiration dynamics in bottom waters vary seasonally with higher contribution of benthic respiration during stratified summer conditions and prevalent water column respiration during fall and winter. In contrast, seasonality in surface waters was less pronounced as productivity was more dependent on (salinity-inferred) nutrient supply than climatic forcing.

CHAPTER 1
INTRODUCTION

The northern Gulf of Mexico is presently the site of the second largest human-caused coastal hypoxic zone (<2 mg O_2 L^{-1}) in the world's oceans. Often referred to as the "dead zone", hypoxic bottom waters can cover an area up to 22,000 km^2 (Rabalais et al. 2007). The development of hypoxia is probably a recent phenomenon (~30 to 50 years), primarily due to increased nutrient inputs from the Mississippi River, in addition to strong water column stratification. The Mississippi River drains over 40% of the lower forty-eight United States (Milliman & Meade 1983) into the Gulf of Mexico. In the last fifty years, the concentrations of nitrate and phosphate in the river have doubled. This increase in nutrient inputs has been linked to an increase in primary production across the Louisiana continental shelf (Turner & Rabalais 1991, 1994). Along with the increase in nitrogen, a decrease in silica has shifted the Si:N ratio close to the Redfield ratio (1:1), and therefore nutrients are now balanced for optimal growth of phytoplankton (Turner & Rabalais 2003). Consequently, large nutrient flux from the river strongly enhances shelf primary productivity, leading to increased algal biomass in surface waters that sinks to the bottom in form of cell aggregates, fecal material and dead algae. Decomposition of this organic matter in the lower stratified water layers and bottom sediments fuels oxygen consumption and decreases oxygen concentrations via bacterial respiration. Changing riverine nutrient concentrations and ratios have impacted not only the primary productivity, but also the productivity of higher trophic levels (Turner et al. 1998).

Development of hypoxia is also sensitive to climate anomalies, such as droughts and floods, which can cause large interannual variations in severity and areal extent of hypoxia. During the drought of 1988, the Mississippi River had a 52 yr record-low discharge and while

hypoxia formed in early summer, a large continuous hypoxic zone did not develop due to lack of stratification. On the other hand, during the Great Flood of 1993, the areal extent of hypoxia showed a two-fold increase with respect to the average year (Rabalais et al. 1994). Overall, there is a strong relationship between river discharge, nutrients loads and extent of hypoxia (Turner et al. 2006). With respect to seasonality, hypoxic bottom waters can be prevalent from March through October (Rabalais et al. 1991). Spring is usually characterized by increased Mississippi River discharge, which is associated with high nutrient flux to coastal waters. There is typically a one month lag between the peak in riverine nutrient flux and the peak in net primary productivity (Justić et al. 1995). Following the increase in primary production across the continental shelf, hypoxic conditions begin to set in during late spring so that by summer hypoxia usually reaches its peak. In addition to biological processes, physical stratification of the water column is necessary to maintain hypoxic conditions. A strong pycnocline forms due to the difference in density between lighter fresh river water and heavier marine water. When a strong pycnoclyne is present, oxygen re-supply by the atmosphere to bottom waters becomes negligible. Except for the occasional storm, summers in the northern Gulf of Mexico are calm and devoid of wind driven mixing. Hypoxia typically does not dissipate until early fall, when frontal passages are common and strong physical mixing brings bottom waters into contact with surface waters and the atmosphere, causing re-oxygenation of the water column.

Despite of considerable monitoring and modeling carried out since 1985, the oxygen budget of the Gulf of Mexico's hypoxic zone is not well known. This is because conventional oxygen budgets based on oxygen concentration measurements are not particularly helpful in distinguishing the effects of physical and biological factors. A decrease in bottom oxygen content, for example, may be a result of benthic or water-column respiration. Similarly, an

increase in the oxygen content may be an effect of in situ photosynthesis, or a consequence of oxygen influx due to advection or diffusion. Hence, in conventional oxygen budgets, the effects of biological factors are masked by the effects of physical factors, and vice-versa.

To improve the understanding of oxygen dynamics in the northern Gulf of Mexico, I pursued a new, stable-isotope-based approach that allows separating the effects of key biological and physical processes on oxygen dynamics. In combination with conventional oxygen concentration measurements, oxygen budgets developed with stable isotopes ($\delta^{18}O$, expressed in ‰) can help define sources and sinks of oxygen among major processes that take place in aquatic systems. Such processes are air-sea gas transfer, photosynthesis, respiration and mixing. Regions of strong oxygen cycling, such as the highly productive Mississippi River plume and its associated oxygen-depleted bottom waters, are expected to have strong oxygen isotope signals accompanying the strong oxygen concentration dynamics. Atmospheric oxygen has a $\delta^{18}O$ value of 23.5‰ in the global earth atmosphere (Dole et al. 1954). In a purely physical system, oxygen entering the water column from the atmosphere leads to dissolved oxygen with a $\delta^{18}O$ value of 24.2‰, caused by a relatively small equilibrium isotope effect of about 0.7‰ (Benson & Krause 1984, Figure 1.1). Super-saturation caused by physical mixing or bubble injection would not further affect the $\delta^{18}O$ value. On the other hand, biological processes such as photosynthesis and respiration change $\delta^{18}O$ values from this 24.2‰ starting point. Due to the absence of fractionation (Guy et al. 1993), oxygen derived from aquatic primary production has an isotopic value equivalent to the ambient water (near 0‰ for seawater). Therefore, addition of photosynthetic oxygen will lower the $\delta^{18}O$ of dissolved oxygen in the water. Water column respiration removes isotopically depleted (light) oxygen, usually with a large fractionation effect of -15 to -21‰ (Kroopnick 1975, Bender and Grande 1987, Guy et al. 1989, Quay et al. 1993,

1995), and the net effect leads to increased $\delta^{18}O$ values of the residual dissolved oxygen pool. On the other hand, oxygen that is respired within the bottom sediments (benthic respiration) has a very small fractionation effect, ranging from 0 to -3‰ (Brandes & Devol 1997), and a substantial contribution of benthic respiration in bottom water samples would significantly reduce the net fractionation effect. As a result, the information from the dual analysis of oxygen concentrations and stable isotope values can help us to better understand oxygen dynamics beyond what can be determined by concentration measurements alone.

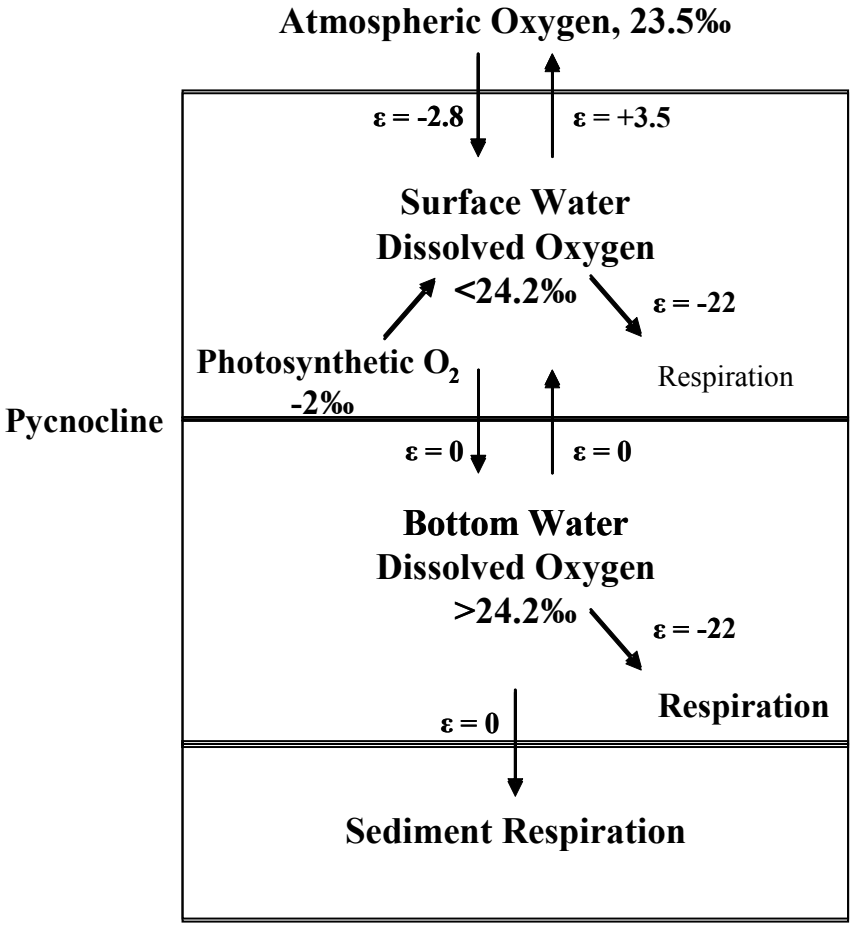

Figure 1.1 Conceptual model of oxygen isotopic values for the Gulf of Mexico's hypoxic zone during stratified summer conditions. The ε symbols accompanying arrows are per mil fractionation factors (changes in $\delta^{18}O$) expected during reactions and transfers. Isotopic values are representative values taken from this study and literature sources (Kroopnick 1975; Bender and Grande 1987; Guy et al. 1989, 1993; Knox et al. 1992; Quay et al. 1993, 1995; Brandes and Devol 1997).

Based on published studies (see above) and laboratory experiments, I developed and parameterized a dual-budget model (oxygen concentrations and stable isotopes) for surface waters that allowed me to calculate the ratio of production to respiration (P/R), and gross and net primary production across the Louisiana continental shelf. Subsequently the model was used for bottom waters to calculate the relative contribution of benthic versus water column respiration.

In chapter 2, spatial (shelfwide cruise 2001) and temporal (seasonal) patterns of $\delta^{18}O$ are discussed and compared to the dynamics of oxygen concentrations for surface and bottom waters. In addition, P/R and productivity values are calculated in surface waters, while for bottom waters, the relative importance of benthic versus water column respiration is calculated; spatial and temporal patterns are evaluated for both. Chapter 3 explores how interannual variability in various biological and physical factors affects seasonal and interranual oxygen dynamics. Additionally, by using multivariate analyses the importance of biotic (concentrations of particulate organic carbon and nitrogen, C:N ratio) and abiotic parameters (pH, temperature, salinity) is tested to explain the observed variability in productivity and P/R patterns in surface waters. The focus of chapter 4 is the sensitivity analysis of the developed budget models to test how variations in input parameters affect model outcomes. Tested parameters for the surface model were the $\delta^{18}O$ value of water, fractionation factor during water column respiration (ε), and wind speed. For the bottom model, I analyzed the sensitivity of calculated contribution of benthic respiration to changes in fractionation factor of water column respiration (ε), and the input of oxygen from benthic primary production and mixing. Model scenarios were run for both seasonal and annual variations in input parameters.

STUDY AREA AND SAMPLING DESIGN

The study area encompassed the Louisiana-Texas continental shelf, which is strongly influenced by the Mississippi River and the Atchafalaya River that deliver 98% of total freshwater input into the northern Gulf of Mexico (Dinnel & Wiseman 1986). At river mile 315 (Old River Control Structure), approximately 30% of the Mississippi River water is diverted into the Atchafalaya River, that drains about 200 km west of the Mississippi River delta into the Gulf of Mexico. Both river plumes form the Louisiana Coastal Current, which flows westward along the Louisiana coast and then southward along the Texas coast. Due to salinity gradients, a strong seasonal pycnocline ($\Delta\sigma_t = 4$ - 10 kg m^{-3}) develops between April to October (Rabalais et al. 1991) that separates surface and bottom waters. Primary productivity in surface waters is high and ranges from 290 to 329 g C m^{-2} yr^{-1} (Sklar & Turner 1981, Lohrenz et al. 1990). This results in a high carbon flux to the sediments, due to the shallowness of the region (~20 m on average), over 50% of the sedimenting primary production reaches the bottom sediments (Rabalais et al. 1991).

Field sampling was conducted between July 2001 and July 2003 by participating in monthly oceanographic cruises, which are the core of the Hypoxia Research Program led by Dr. Nancy Rabalais. Sampling yielded two years of almost continuous monthly data including three shelfwide cruises (July of 2001, 2002, and 2003). For the shelfwide cruises, the sampling grid was composed of thirteen transects extending across the width of the shelf, starting west of the birdfoot delta to the Texas-Louisiana border (Figure 1.2). Each transect extends 40 to 120 km in the inshore-offshore direction and has between six to ten stations ranging from 5 to 60 m in depth. Monthly cruises were conducted along transect C that is located approximately 100 km to the west of the Mississippi River Delta (Figure 1.2). From July 2001 to June 2002 surface and

bottom water samples were collected from all stations within all transects. Starting in July 2002, samples were collected in 5 m depth intervals at stations with water depths of 10, 20, and 30 m within each transect. Monthly sampling along transect C was conducted to investigate the seasonal variability of oxygen concentration and isotopic signatures throughout the development and dissipation of hypoxia in the northern Gulf of Mexico.

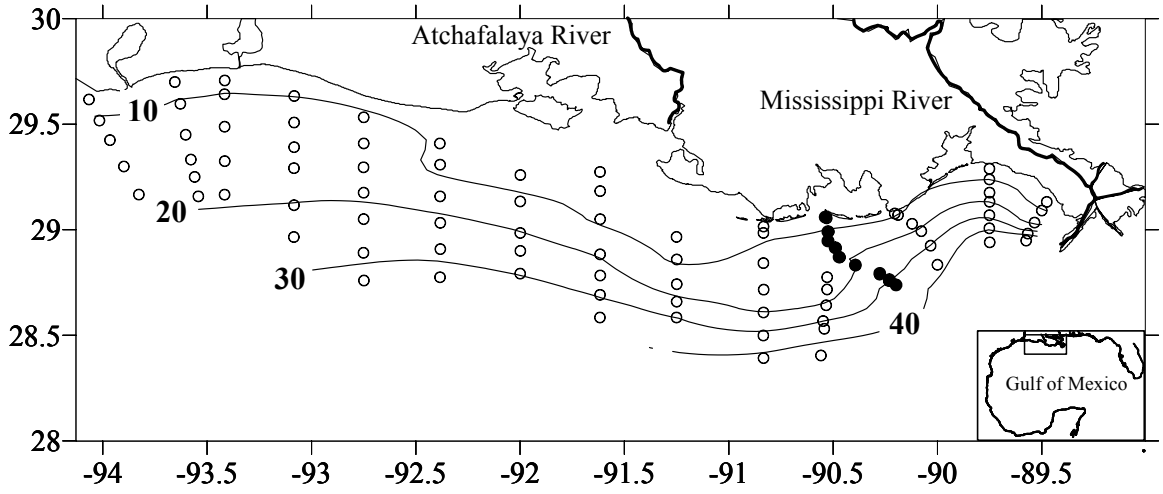

Figure 1.2 Map of the study area off the Louisiana coast showing depth contours (m), the station grid and location of transect C sampled each month, August 2001 to June 2002 (closed circles).

Shelfwide cruises are normally scheduled during the second half of July, which frequently is the peak of hypoxia in the Gulf of Mexico. The shelfwide cruises are crucial for examining the variation of oxygen dynamics on a large spatial scale. In addition, shelfwide cruises make it possible to examine not only the influence of the Mississippi River, but also the Atchafalaya River, which delivers approximately 30% of the total freshwater input into the northern Gulf of Mexico. During July, hypoxia thrives across the continental shelf, due to nutrient-enhanced primary production and strong stratification. Hypoxia varies spatially as a result of differences in respiration of accumulated organic matter that reflects distance from the river plumes. In respect to physical constraints, inner stations are more isolated from non-

hypoxic water masses, while in outer, peripheral stations hypoxia is often less severe due to a larger bottom water oxygen pool, and the potential for lateral oxygen input and mixing from oxygen rich off-shore waters.

REFERENCES

Bender, ML, Grande K (1987) Production, respiration and the isotope geochemistry of O_2 in the upper water column. Global Biogeochem Cycles 1:49-59

Benson BB, Krause D (1984) The concentration and isotopic fractionation of oxygen dissolved in fresh water and seawater in equilibrium with the atmosphere. Limnol Oceanogr 29:620-632

Brandes JA, Devol AH (1997) Isotopic fractionation of oxygen and nitrogen in coastal marine sediments. Geochim Cosmochim Acta 61:1793-1802

Dinnel S, Wiseman WJ Jr (1986) Freshwater on the Louisiana shelf. Cont Shelf Res 6:765-784

Dole M, Lane GA, Rudd DP, Zaukelies DA (1954) Isotopic composition of atmospheric oxygen and nitrogen. Geochim Cosmochim 6:65-78

Guy RD, Berry JA, Fogel ML, Hoering TC (1989) Differential fractionation of oxygen isotopes by cyanide-resistant and cyanide-sensitive respiration in plants. Planta 177:483-491

Guy RD, Fogel ML, Berry JA (1993) Photosynthetic fractionation of the stable isotopes of oxygen and carbon. Plant Physiol 101:47-47

Justić D, Rabalais NN, Turner RE (1995) Stoichiometric nutrient balance and origin of coastal eutrophication. Mar Poll Bull 30:4146

Kiddon J, Bender ML, Marra J (1995) Production and respiration in the 1989 North Atlantic spring bloom: and analysis of irradiance dependent changes. Deep-Sea Res 42:553-576

Knox M, Quay PD, Wilbur D (1992) Kinetic isotope fractionation during air-water gas transfer of O_2, N_2, Ch_4, and H_2. J Geophys Res 97:20335-20343

Kroopnick PM (1975) Respiration, photosynthesis, and oxygen isotope fractionation in oceanic surface water. Limnol Oceanogr 20:988-992

Lohrenz SE, Dagg MJ, Whitledge TE (1990) Enhance primary production in the plume/oceanic interface of the Mississippi River. Cont Shelf Res 10:639-664

Milliman JD, Meade RH (1983) World-wide delivery of river sediment to the ocean. J. Geol. 91:1-21

Quay PD, Emerson S, Wilbur DO, Stump C (1993) The δ ^{18}O of dissolve O_2 in the surface waters of the subarctic Pacific: A tracer of biological productivity. J Geophys Res 98:8447-8458

Quay PD, Wilbur DO, Richey JE, Devol AH, Benner R, Forsberg BR (1995) The ^{18}O:^{16}O of dissolve oxygen in rivers and lakes in the Amazon basin: Determining the ratio of respiration to photosynthesis rates in freshwaters. Limnol Oceanogr 40:718-729

Rabalais NN, Turner RE, Wiseman WJ Jr (1991) A brief summery of hypoxia on the northern Gulf of Mexico continental shelf: 1985-1988, p. 35-47. In R.V. Tyson and T.H. Pearson (eds.), Modern and ancient continental shelf anoxia. Geol Soc Spec Publ 58, London

Rabalais NN, Wiseman WJ Jr, Turner RE (1994) Comparison of continuous records of near-bottom dissolve oxygen from the hypoxia zone along the Louisiana coast. Estuaries 17:850-861

Rabalais NN, Turner RE, Justic D, Dortch Q, Wiseman WJ Jr (1999) Characterization of hypoxia: Topic 1 Report for the integrated assessment of hypoxia in the Gulf of Mexico. NOAA Coastal Ocean Program Decision Analysis Series No. 15, NOAA Coastal Ocean Program, Silver Springs, Maryland

Sklar FH, Turner RE (1981) Characteristics of phytoplankton production off Barataria Bay in an area influenced by the Mississippi River. Contrib Mar Sci 24:93-106

Turner RE, Rabalais NN (1991) Changes in the Mississippi River water quality this century – Implications for coastal food webs. BioScience 41:140-147

Turner RE, Qureshi N, Rabalais NN, Dortch Q, Justic D, Shaw RF, Cope J (1998) Fluctuating silicate:nitrate ratios and coastal plankton food webs. Proc Natl Acad Sci USA 95:13048-13051

Turner RE, Rabalais NN (2003) Linking landscape and water quality in the Mississippi River basin for 200 years. BioScience 52:139-148

Turner RE, Rabalais NN, and Justić D (2006) Predicting summer hypoxia in the northern Gulf of Mexico: riverine N, P, and Si loading. Mar Poll Bull 52:139-148

CHAPTER 2
PARTITIONING OXYGEN SOURCES AND SINKS IN A STRATIFIED, EUTROPHIC COASTAL ECOSYSTEM USING STABLE OXYGEN ISOTOPES

INTRODUCTION

Eutrophication is often manifested in the presence of noxious algal blooms and bottom water hypoxia (< 2 mg O_2 L^{-1}), which have been reported from a variety of coastal and estuarine ecosystems (Officer et al. 1984, Justić et al. 1987, Rabalais & Turner 2001). The extent and severity of eutrophication phenomena have increased during the second half of the 20th century (Hickel et al. 1993, Turner & Rabalais 1994, Diaz & Rosenberg 1995), generally coinciding with increased use of fertilizer in the watersheds and higher nitrogen and phosphorus concentrations in freshwaters (Rabalais & Turner 2001). During the last 50 years, the concentration of total phosphorus and dissolved inorganic nitrogen in the Mississippi River increased two and three-fold, respectively (Turner et al. 2003). In response to increased nutrient loading and eutrophication, the northern Gulf of Mexico is presently the site of the largest and most severe coastal hypoxic zone in the western Atlantic Ocean (Rabalais et al. 2002), which typically persists from April through October, and extends between 5 and 60 km offshore. Abundance and diversity of demersal species are drastically reduced under hypoxic conditions (Pavella et al. 1983), and mass mortalities are known to occur among benthic infauna when bottom oxygen concentration decreases below 0.5 mg L^{-1} (Rabalais & Turner 2001).

Hypoxia develops as a synergistic product of biological and physical factors. Nutrient-enhanced surface primary productivity results in high carbon flux to the lower water column and sediments. Decomposition of this material in bottom waters and sediments fuels oxygen consumption via bacterial respiration and decreases oxygen concentrations. Stability of the water column, due to a salinity- and temperature-controlled pycnocline, prevents vertical

diffusive oxygen flux and prevents re-oxygenation of lower water masses by the atmosphere (Wiseman et al. 1997, Justić et al. 1996). On the other hand, wind-induced mixing in fall and winter brings hypoxic waters into contact with the atmosphere and re-oxygenates the water column. This synergism of biological and physical factors complicates the development of accurate oxygen budgets. For example, a decrease in bottom oxygen content may be a result of either sediment- or water-column respiration. Also, an increase in oxygen content may be a consequence of *in situ* photosynthesis, oxygen influx from the atmosphere, or mixing with adjacent water masses. As a result, studies based on oxygen concentration measurements alone (Justić et al. 1996) reveal only limited information about the importance of individual oxygen sources and sinks.

In recent years, a second approach for measuring oxygen dynamics has been developed that uses stable oxygen isotopes ($\delta^{18}O$) in addition to conventional oxygen concentrations. Most work with oxygen isotopes has focused on open ocean systems, including the North Atlantic (Kroopnik 1975), the subarctic Pacific (Quay et al. 1993), and the subtropical Pacific (Bender & Grande 1987). Freshwater $\delta^{18}O$ studies include those conducted in the Amazon Basin (Quay et al. 1995) and the Great Lakes (Ostrom et al. 2005). No studies have been performed in river dominated, nutrient rich, and stratified coastal waters. However, regions of intense oxygen cycling, such as the highly productive Mississippi River plume and its associated oxygen-depleted bottom waters, are expected to have highly variable $\delta^{18}O$ signals accompanying the strong fluctuations in oxygen concentrations.

Atmospheric oxygen has a $\delta^{18}O$ value of 23.5‰ (Dole et al. 1954, recent work by Barkan & Luz 2005 suggested a $\delta^{18}O$ value of 23.9‰ for atmospheric oxygen to be more accurate, but for this study I will retain a value of 23.5‰ to be consistent with the referenced literature). In a

purely physical system, oxygen entering the water column from the atmosphere leads to dissolved oxygen with a $\delta^{18}O$ value of 24.2‰, due to a relatively small net equilibrium isotope effect of 0.7‰ (Knox et al. 1992, Figure 2.1). Biological processes, such as photosynthesis and respiration, change $\delta^{18}O$ values from this 24.2‰ starting point. Due to the absence of fractionation in photosynthesis (Guy et al. 1993), oxygen derived from aquatic primary production has an isotope value equivalent to the oxygen of the ambient water (near 0‰ for seawater). Therefore, addition of photosynthetic oxygen in marine systems will lower the $\delta^{18}O$ of dissolved oxygen in the water from 24.2‰ towards 0‰. Water column respiration removes isotopically depleted (light) oxygen, usually with a large fractionation effect (ε) of -15 to -25‰ (Kroopnick 1975, Bender & Grande 1987, Guy et al. 1989, Quay et al. 1993, 1995, Luz et al. 2002). Hence, respiratory fractionation results in increased $\delta^{18}O$ values for the residual dissolved oxygen pool. Oxygen that is respired within the bottom sediments (hereafter referred to as benthic respiration) has a very small fractionation effect, ranging from 0 to -3‰ (Brandes & Devol 1997). Thus, a substantial contribution of benthic respiration in bottom water samples would significantly reduce the net fractionation factor.

The objectives of this study were to describe $\delta^{18}O$ dynamics for the hypoxic zone in the northern Gulf of Mexico, and to assess the relative importance of key physical and biological processes affecting hypoxia. I investigated how the use of $\delta^{18}O$ measurements could enhance the understanding of oxygen dynamics above the level achievable with oxygen concentration measurements alone. This study showed that the dual budget approach with both $\delta^{18}O$ and oxygen concentration measurements yielded new estimates of productivity dynamics in surface waters and of sediment oxygen demand in bottom waters.

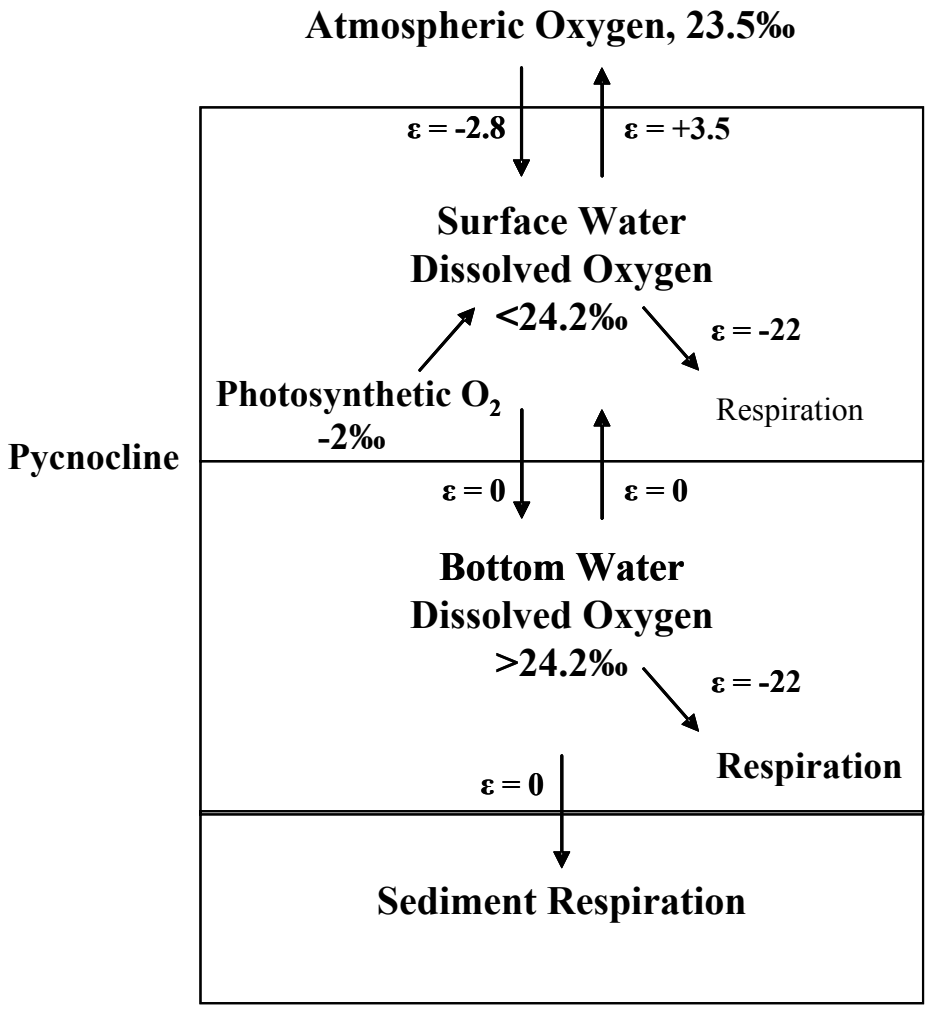

Figure 2.1 Conceptual model of oxygen isotopic values for the Gulf of Mexico's hypoxic zone during stratified summer conditions. The ε symbols accompanying arrows are per mil fractionation factors (changes in $\delta^{18}O$) expected during reactions and transfers. Isotopic values are representative values taken from this study and literature sources (Kroopnick 1975; Bender and Grande 1987; Guy et al. 1989, 1993; Knox et al. 1992; Quay et al. 1993, 1995; Brandes and Devol 1997).

STUDY AREA

The study area encompasses the Louisiana inner to mid continental shelf waters (Figure 2.2). This region is strongly influenced by the Mississippi and Atchafalaya Rivers, which together account for 98% of the total freshwater input into the Gulf of Mexico (Dinnel & Wiseman 1986). Plumes of the two rivers form the Louisiana Coastal Current, a highly stratified

current that flows westward along the Louisiana coast and continues southward along the Texas coast. A strong seasonal pycnocline ($\Delta\sigma_t$ = 4 - 10 kg m^{-3}) persists from April to October, largely due to salinity gradients. Intense wind mixing caused by frontal passages and storms can disrupt this stratification, resulting in partial or complete mixing of the water column (Wiseman et al. 1997). Primary productivity for this continental shelf region is high and averages approximately 300 g C m^{-2} yr^{-1} (Sklar & Turner 1981, Lohrenz et al. 1990). Due to the shallow water column in this region (approximately 5 to 40 m), nutrient-enhanced surface primary productivity results in high carbon flux to the sediments, and approximately 50% of the carbon produced *in situ* fuels this vertical flux (Rabalais & Turner 2001).

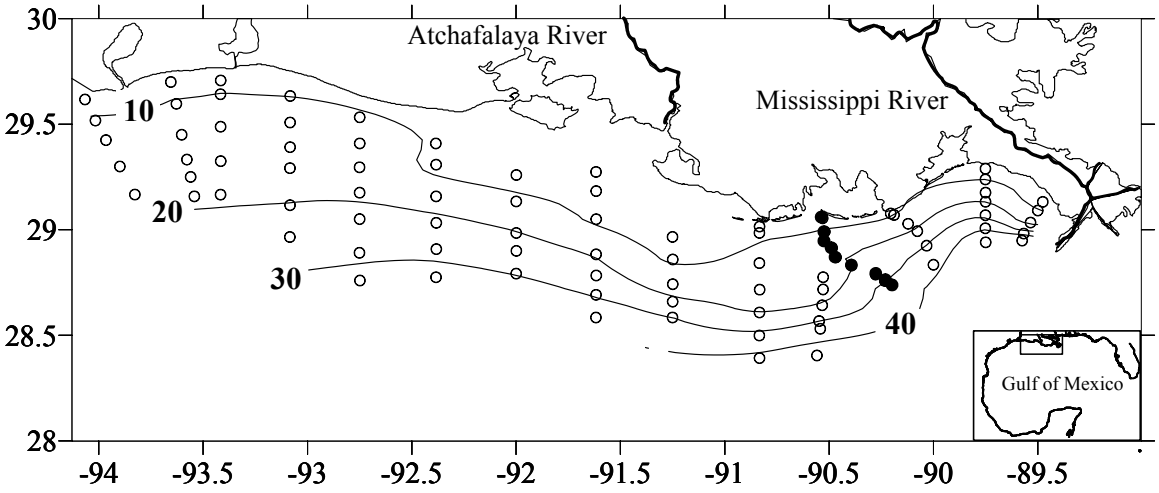

Figure 2.2 Map of the study area off the Louisiana coast showing depth contours (m), the station grid and location of transect C sampled each month, August 2001 to June 2002 (closed circles).

METHODS

Field Sampling

The sampling grid consisted of twelve transects across the width of the coastal shelf, from the Mississippi River birdfoot Delta west to the Texas-Louisiana border (Figure 2.2). Each

transect extended 40 to 60 km offshore and included six to ten stations ranging in depth from 5 to 60 m. During a six-day shelfwide cruise in July 2001, surface and bottom water samples were collected at each station within each transect. In addition, from August 2001 to May 2002, surface and bottom water samples were collected during monthly monitoring cruises at each station along transect C, 90 km west of the Mississippi River delta (Figure 2.2).

During the shelfwide cruise, Secchi depth readings (black and white disc, 25 cm diameter) were collected at stations that were sampled between 7:00 am and 7:00 pm, which approximately covered the time period from 6 hours before to 6 hours after apparent noon.

A 5L PVC Niskin sampler was used to collect bottom water samples and a plastic bucket for surface water. For surface samples, the bucket was placed sideways onto the water surface. Once it started sinking, the bucket filled passively with water, avoiding intrusion of atmospheric oxygen into the sample water due to turbulent mixing. Surface water samples were collected approximately 10 cm below the surface, while bottom water samples were collected within one meter of the bottom sediments. Subsequently, 125 ml Wheaton glass bottles were carefully filled using plastic Tygon tubing. The tubing was either attached to the Niskin sampler (bottom samples) or water was siphoned directly from the bucket (surface samples), and bottles were allowed to overflow at least twice their volume to exclude air bubbles. After filling, the bottles were immediately poisoned with 0.5 ml 6N HCl (Miyajima et al. 1995), sealed with heavy rubber stoppers (Bellco Glass, 20 mm), crimped, and stored in the dark.

Isotope Analyses

Immediately after return to the laboratory, samples were prepared for analysis by means of headspace equilibration (Kampbell et al. 1989, Miyajima et al. 1995). A headspace was created by injecting 10 ml of ultra pure helium into inverted bottles while allowing 10 ml of

sample water to drain out a small needle (BD brand, precision glide 23G1). The helium was injected at the bottom of the inverted sample bottle using a 15 cm long stainless steel needle that was attached to a 20 ml syringe (BD brand general use). Before injection, the syringe was flushed five times with ultra pure helium to avoid contamination with atmospheric oxygen. Subsequently, samples were stored in the dark at 5 °C for 1 to 4 weeks. To ensure equilibration of the dissolved gases with the headspace, samples were placed in a shaker (100 rpm, room temperature) for at least 12 hours before isotope analyses.

For the actual analysis, a sub-sample of the headspace was injected through a septum into a helium stream. At a flow rate of 120 mL min^{-1}, the sample traveled through a trap filled upstream with ascarite to absorb CO_2 and downstream with magnesium perchlorate to absorb water, and a 2 m packed GC column (molecular sieve, 5 Angstrom pore size) for separation of O_2 and N_2 for on-line, continuous flow isotope ratio measurements. To optimize signal strength, the amount of headspace injected varied with the dissolved oxygen concentration in the sample, which was measured in the field using a Hydrolab instrument (Hach Company). Accordingly, 1, 3, or 5 mL of headspace were injected for dissolved oxygen concentration of > 7, 7 - 2, or < 2 mg L^{-1}. Before each injection, the syringe (BD brand general use, Luer-Lok tip) was flushed five times with ultra pure helium and subsequently pressurized (150 kpa) using a three-way stopcock. After a new needle (BD brand, precision glide 23G1) was attached, the syringe was opened to release pressure and expel any air, quickly adjusted to the desired injection volume, which was injected into the headspace. After thoroughly mixing the ultra pure helium with the headspace, the desired amount of sample was withdrawn and immediately injected into the helium stream for analysis.

The gas analysis system allowed sequential elution of oxygen and nitrogen gases, so that concentrations of both dissolved oxygen and nitrogen could be calculated using the peak areas of mass 32 and 28, measured respectively in a downstream isotope ratio mass spectrometer (IRMS). The peak areas were calibrated using laboratory standards prepared in the same manner as samples, but air equilibrated, artificial seawater was used as water source. Artificial seawater was prepared by adding 33.75 g L^{-1} of NaCl to distilled water in a 4 liter glass beaker, then stirring overnight to achieve equilibration. The stirring speed was adjusted to obtain a small vortex of < 5 cm height to avoid supersaturation. After equilibration and just prior to filling these bottles with standard seawater, I added 2000 μmol $L^{-1}$of $NaCO_3$ in order to match the dissolved inorganic carbon concentration (DIC) of natural seawater.

Procedural blanks were prepared in the same way as procedural artificial seawater standards, but to obtain zero-oxygen water, 50 g L^{-1} Na_2SO_3 were added (Kampbell et al. 1989). The average oxygen concentration of zero-oxygen blanks was 0.007 mg L^{-1} (±0.002 standard deviation, n = 32), which corresponded to 0.1% and 0.3% of the average surface (7.0 mg L^{-1}) and bottom (2.1 mg L^{-1}) oxygen concentration during the shelfwide cruise, respectively. Accordingly, oxygen concentrations and isotopic values for all samples were corrected by subtraction and mass balance, respectively.

The isotope values of oxygen ($\delta^{18}O$ expressed as ‰ relative to standard mean ocean water, SMOW) were determined using a Finnigan Thermoquest Delta plus IRMS. As primary standard I used air (Dole et al. 1954) with a known $\delta^{18}O$ value of 23.5‰ (± 0.17‰ standard deviation, n = 89). The saturated artificial seawater used as procedural standard gave the expected $\delta^{18}O$ value of 24.2‰ (± 0.21‰ standard deviation for $\delta^{18}O$, n = 83) as well as accurate

dissolved oxygen and nitrogen concentrations, whereby the saturation concentrations were calculated according to Weiss (1970) using known temperature and salinity.

To investigate the precision of the analyses, I collected replicate samples for surface and bottom water (n = 19) during the cruise in October 2001. The average difference for oxygen concentrations and $\delta^{18}O$ values were 0.11 mg L^{-1} (± 0.16 standard deviation) and 0.05‰ (± 0.04 standard deviation), respectively.

Because headspace injections were not carried out using high precision syringes, inaccurate injection volumes (± 0.1 mL) sometimes affected oxygen concentration measurements. Depending on the injection volume (1 to 5 mL), this injection error varied between ±2 to ±10% of the ambient oxygen concentrations. The largest potential for error was related to extremely supersaturated surface water samples due to their small injection volumes (1 mL), while bottom water samples with the largest injection volume (5 mL) were the least affected. Nevertheless, based on the fact that dissolved nitrogen gas is generally inactive and should be close to 100% saturation in water samples, the parallel measurement of oxygen and nitrogen concentrations from the same sample allowed us to calculate the magnitude of over- or under-estimation of nitrogen gas concentrations due to injection errors in the samples. Saturation levels for dissolved oxygen and nitrogen were calculated according to Weiss (1970), by obtaining temperature and salinity readings taken with the Hydrolab at the approximate time and depth of sampling. Subsequently, I could correct the amounts of oxygen based on N_2 saturation levels in individual samples, assuming that dissolved nitrogen was 100% saturated:

$$[O_2]_{N2\text{-corrected}} = 100 * [O_2]_{measured} / N_2\text{-saturation}_{measured}$$

This correction was solely a volumetric correction affecting oxygen concentrations, and as such did not affect the $\delta^{18}O$ values and did not entail any $\delta^{18}O$ correction.

Note that the assumption of nitrogen being inactive holds true for surface waters, which are generally not supersaturated by more than 2% (Benson & Parker 1961, Craig & Hayward 1987, Emerson et al. 1999). For bottom water samples, intense denitrification producing N_2 could have increased the dissolved nitrogen concentrations above saturation levels. Actually, a trend of increasing nitrogen concentrations at low levels of oxygen was observed (Figure 2.3), whereby the average N_2 super-saturation in bottom water samples was approximately 7%. Still, even a 10% N_2 supersaturation would only have a small effect on the oxygen correction, e.g., a measured oxygen concentration of 1.0 mg L^{-1} would change to 0.9 mg L^{-1}. For future studies, O_2/Ar ratios should be used instead of O_2/N_2 as Ar gas is truly inert and would further reduce uncertainties, especially for bottom water samples.

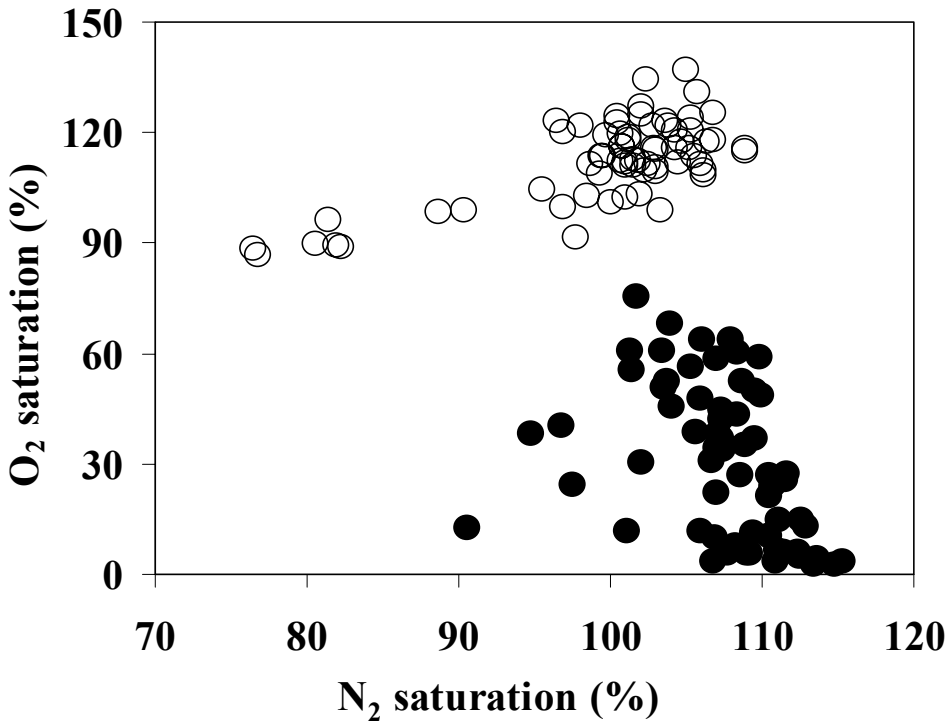

Figure 2.3 Relationship between measured oxygen and nitrogen saturation for surface (open circles) and bottom samples (closed circles) collected during the shelfwide cruise, July 2001.

Overall, I made this adjustment of oxygen concentrations based on nitrogen saturation levels because the correction significantly improved the data set so that the laboratory oxygen concentration estimates better matched the field Hydrolab measurements (which were routinely calibrated vs. Winkler measurements during all cruises). Thus, after these corrections, the r^2 value of calculated O_2 concentrations versus measured Hydrolab values for the 2001 shelfwide cruise samples increased overall from 0.92 to 0.97, while for surface and bottom values individually, the r^2 increased from 0.66 to 0.83 and 0.80 to 0.96, respectively. The lower final r^2 values for surface samples can be explained by the smaller range of oxygen concentrations from about 6 to 8 mg L^{-1} (with the exception of five samples exceeding 10 mg L^{-1}), while bottom water O_2 concentrations were between 0.5 and 7.0 mg L^{-1}. As this was the first attempt to measure both oxygen isotopes and concentration from the same IRMS analysis, the Winkler-calibrated Hydrolab data were important to validate the reliability of the calculations. Even though oxygen concentrations were acquired shipboard using a Hydrolab, I made the oxygen corrections to the laboratory analyses as described above, and then relied on the laboratory oxygen concentration measurements for reasons of consistency.

To obtain a fractionation factor for water column respiration that was representative for this system, surface water that was collected during three cruises along transect C was incubated (October 2002, March and July 2003). For each incubation experiment, 12 sample bottles were filled with surface water from a single bucket haul at station C6b. While 3 samples were immediately preserved with HCl to stop biological activity (t_0), 9 bottles were closed without preservation. These 9 samples were then incubated in the dark to only allow respiration, and at each of three subsequent time steps (t_1, t_2, and t_3) 3 more samples were preserved. Subsequently,

I calculated an average system-specific fractionation factor for water column respiration (-22.0 ±0.7‰, Figure 2.4), according to Mariotti et al. 1981 (see below).

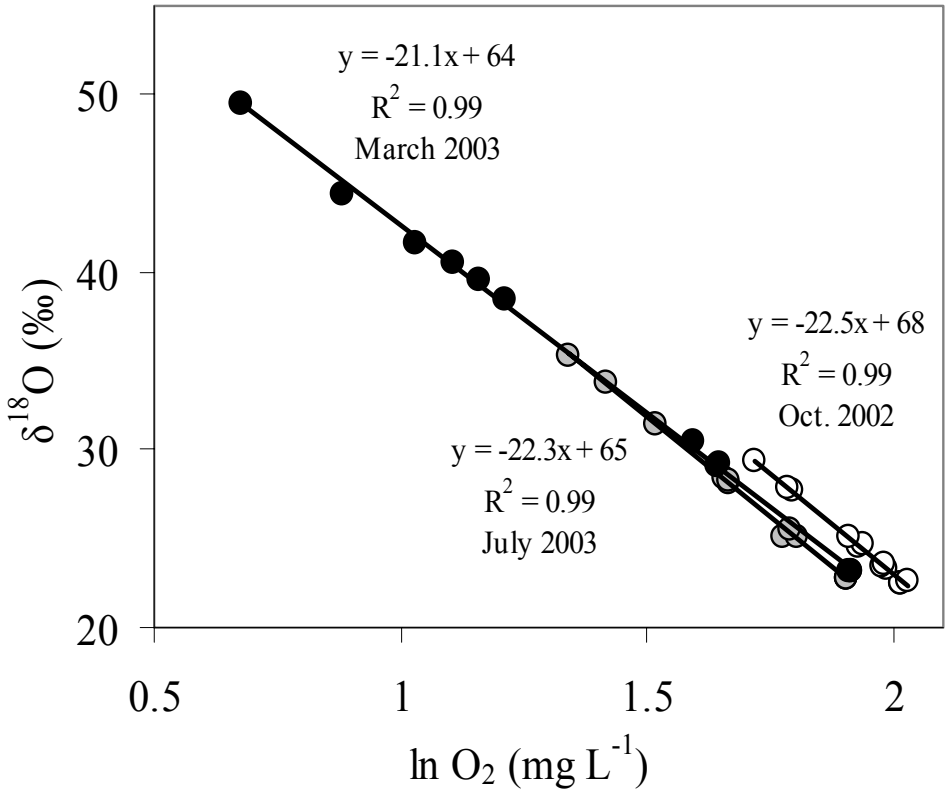

Figure 2.4 Experimentally determined fractionation factors for water column respiration in surface waters on the Louisiana continental shelf. Samples were collected at station C6b along transect C in October 2002, and in March and July of 2003. Incubation times were 37, 26, and 8 days, respectively. The negative slope of the linear regression represents the fractionation factor (Mariotti et al. 1981).

Modeling Approach

To evaluate oxygen dynamics recorded in the combined measurements of oxygen concentrations and $\delta^{18}O$ values, I developed a finite difference model equivalent to that used by Bender & Grande (1987), with sequential steps for mixing, fractionation, and air-sea gas exchange (Fry 2006). The mixing pertains to new oxygen added from photosynthesis or gas invasion, and the fractionation pertains to oxygen removed by respiration or gas evasion. Isotope

mixing can be understood as a weighted average, while isotopic fractionation for respiration can be described by logarithmic distillation equations (Mariotti et al. 1981). The eight sequential equations used in each time step of the model were as follows:

1. Oxygen Gain during Photosynthesis: $S_{S1} = S_{INITIAL} + C_P$
2. Isotope Mixing during photosynthesis: $\delta_{S1}S_{S1} = \delta_{INITIAL}S_{INITIAL} + \delta_P C_P$
3. Oxygen Gain during Invasion: $S_{S2} = S_{S1} + C_I$
4. Isotope Mixing during Invasion: $\delta_{S2}S_{S2} = \delta_{S1}S_{S1} + \delta_I C_I$
5. Oxygen Loss during Respiration: $S_{S3} = S_{S2} - C_R$
6. Isotope Fractionation during Respiration: $\delta_{S3} = \delta_{S2} + \varepsilon_R \ln((S_{S2} - C_R)/S_{S3})$
7. Oxygen Loss during Evasion: $S_{S4} = S_{S3} - C_E$
8. Isotope Fractionation during Evasion: $\delta_{S4} = \delta_{S3} + \varepsilon_E \ln((S_3 - C_E)/S_4)$

where δ is the $\delta^{18}O$ value, S is % saturation of oxygen, ε_R and ε_E are the fractionation factors (negative in sign, Mariotti et al. 1981) associated with respiration and evasion, C is the change in oxygen saturation associated with photosynthesis, respiration, or air-sea gas transfer, and subscripts are as follows: P = new oxygen added from photosynthesis, I = new oxygen added by invasion, R = oxygen removed by respiration, E = oxygen removed by evasion. In practice, these equations are linked in a row of calculations in a spreadsheet, then the last values of a row are used as initial values for the next row, i.e., S_4 and δ_{S4} from the end of one row become the initial values of the next row (Fry 2006), so that one row represents a complete cycle of photosynthesis + invasion + respiration + evasion accumulated in one time interval. To complete the parameterization of these models, I selected the following values: $\delta^{18}O$ value of -2‰ for new photosynthetic oxygen (based on average salinity of 30, assuming mixing of Mississippi River water with a value of -7‰ (Kendall, personal communication) with full strength salinity water of

0‰), $\delta^{18}O$ value of 24.2‰ for invading atmospheric oxygen (Knox et al. 1992), ε_R = -22‰ for respiration in surface waters (average value from three incubation experiments, see above), ε_R = 0‰ for respiration in sediments (Brandes & Devol 1997), and ε_E = -3.5‰ (derived from data presented in Knox et al. 1992).

Model runs typically started from initial conditions of 100% oxygen saturation and 24.2‰ $\delta^{18}O$ set by equilibration with the atmosphere. The equations were propagated over 100-10000 time intervals using incremental changes in concentration for photosynthesis, (C_P), respiration, (C_R), and air-sea gas exchange (C_I and C_E), and resulting curves were fit to experimental data as shown in Figs. 2.5 and 12 (below).

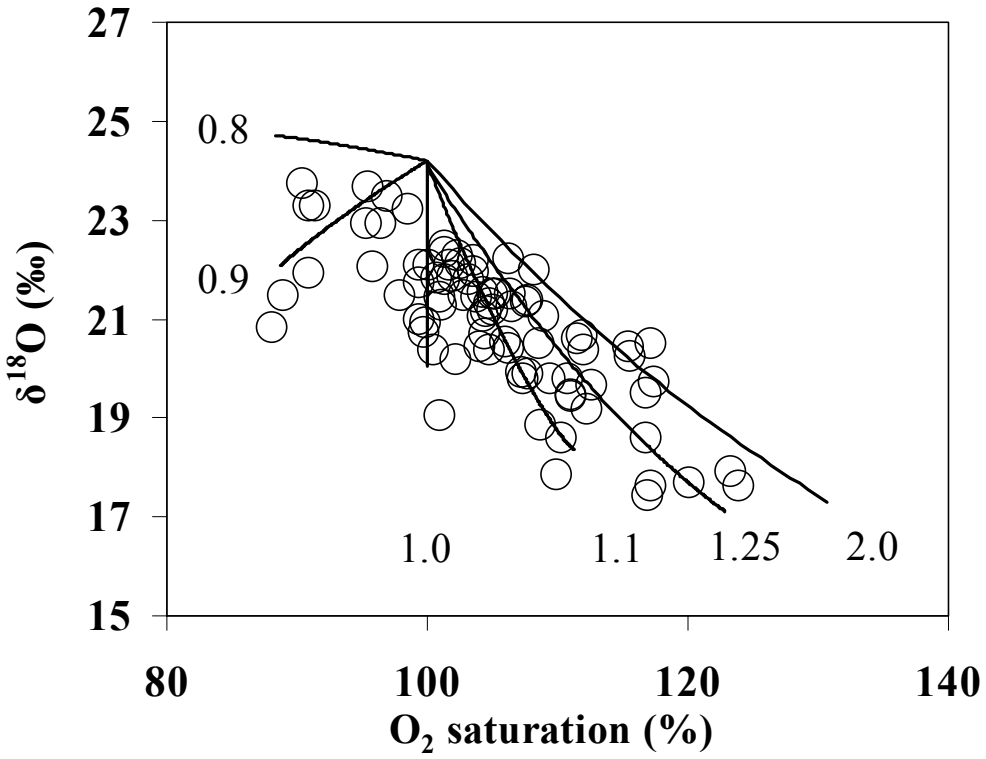

Figure 2.5 Relationship between oxygen saturation and $\delta^{18}O$ for surface water samples collected during the shelfwide cruise, July 2001. Lines represent oxygen saturation and $\delta^{18}O$ values modeled for production to respiration ratios (P/R) between 5.0 and 0.8. Data points of stations with O_2 saturation greater that 140% (n = 4) were above the P/R = 5 line and could not be modeled.

These finite difference models were used to estimate P/R ratios (hereafter, P/R) in surface waters, and respiration dynamics in bottom waters. To estimate P/R for individual samples of surface water, I started from a fixed point of air-equilibrated seawater (100% saturation, 24.2‰ $\delta^{18}O$). The respiration rate was held constant at 0.07 mg O_2 L^{-1} h^{-1}, which was the average decrease in O_2 concentration during three consecutive nights (PAR = 0) during the July 2001 shelfwide cruise. The r^2 between oxygen concentration and time for these nights was 0.54, with the first night-time period excluded from the regression due to the large inhomogeneity of surface water masses near the mouth of the Mississippi River. Air-sea gas exchange was dependent on oxygen saturation levels and wind speed (Stigebrandt 1991), which was 5.5 m sec^{-1} (± 2.1 standard deviation) during the sampling period from July 21 to 26, 2001 (measured shipboard using a RM Young 05103 Wind Monitor).

I found little evidence for benthic photosynthesis or gas exchange with the upper water column for bottom waters in the sampling area (see below), and I refocused this model to estimate fractionations associated with respiration only, assuming benthic photosynthesis and gas exchange to be zero. This respiration-only formulation of the model generated curves from a starting point of air-equilibrated seawater (100% saturation, 24.2‰ $\delta^{18}O$) that intersected individual data points depending on the fractionation factor used during respiration (ε_R in equation 6 above). Estimates of the individual ε_R fractionation factors were used to partition the sources of respiration, with sediment respiration expected to occur with no fractionation, and respiration in bottom waters expected to occur with a fractionation of -22‰. Thus, the estimated ε_R values were intermediate between 0‰ ($\varepsilon_{benthic}$) and -22‰ ($\varepsilon_{water\ column}$) with values closer to 0‰ indicating stronger sediment respiration, according to the formula:

$$\%\ \text{benthic respiration} = 100 * (\varepsilon_{observed} - \varepsilon_{water\ column}) / (\varepsilon_{benthic} - \varepsilon_{water\ column})$$

Nevertheless, to investigate the potential impact that benthic photosynthesis or gas exchange with the upper water column could have had on bottom water oxygen dynamics, I included equations 1 through 4 (photosynthesis and invasion; evasion was not included as bottom waters were always undersaturated) into the model for bottom waters. Per time step, I allowed 20% of the respired oxygen to be added back into bottom waters by either benthic photosynthesis or gas exchange with the upper water column, whereby the $\delta^{18}O$ values for these two oxygen sources were respectively -2 and 21‰ (average $\delta^{18}O$ value of surface waters during this study). Subsequently, I re-calculated the $\delta^{18}O$ vs. O_2 saturation curves for these scenarios and compared them to the original model that was based on respiration only.

All spatial diagrams were developed using Surfer Version 8.02 (Golden Software, Inc.). The spatial interpolation between individual sampling points was performed using the kriging technique. In the interpolations, I used standard features of the software to account for variable spacing between stations and transects.

RESULTS

Seasonal Trends

Monthly sampling along transect C (Figure 2.2) showed strong seasonal variability of oxygen concentrations and $\delta^{18}O$ throughout the development and dissipation of hypoxia. Comparisons of fall and summer transects illustrate these seasonal patterns. In fall and winter, shorter days, and strong winds, along with reduced river discharge and reduced nutrient loading, usually favor relatively low primary productivity and high aeration of shallow (< 100 m) Gulf waters. In October, oxygen in both surface and bottom waters was at saturation and $\delta^{18}O$ values were very close to 24.2‰, the expected value for air-equilibrated seawater (Figure 2.6). On the other hand when fairly calm summertime conditions prevailed in August, surface phytoplankton

blooms developed and produced oxygen supersaturation, while bottom waters became depleted in oxygen, with saturation declining to near-zero levels (Figure 2.6). Along with these intense changes in oxygen concentrations, there were strong, but inverse changes in $\delta^{18}O$. Surface $\delta^{18}O$ values were below 24.2‰ when oxygen was supersaturated, while in bottom waters when oxygen concentrations were low, I observed high $\delta^{18}O$ values up to 50‰ (Figure 2.6). Overall, I found a strong negative (or inverse) correlation between oxygen concentrations and $\delta^{18}O$ values during this seasonal study.

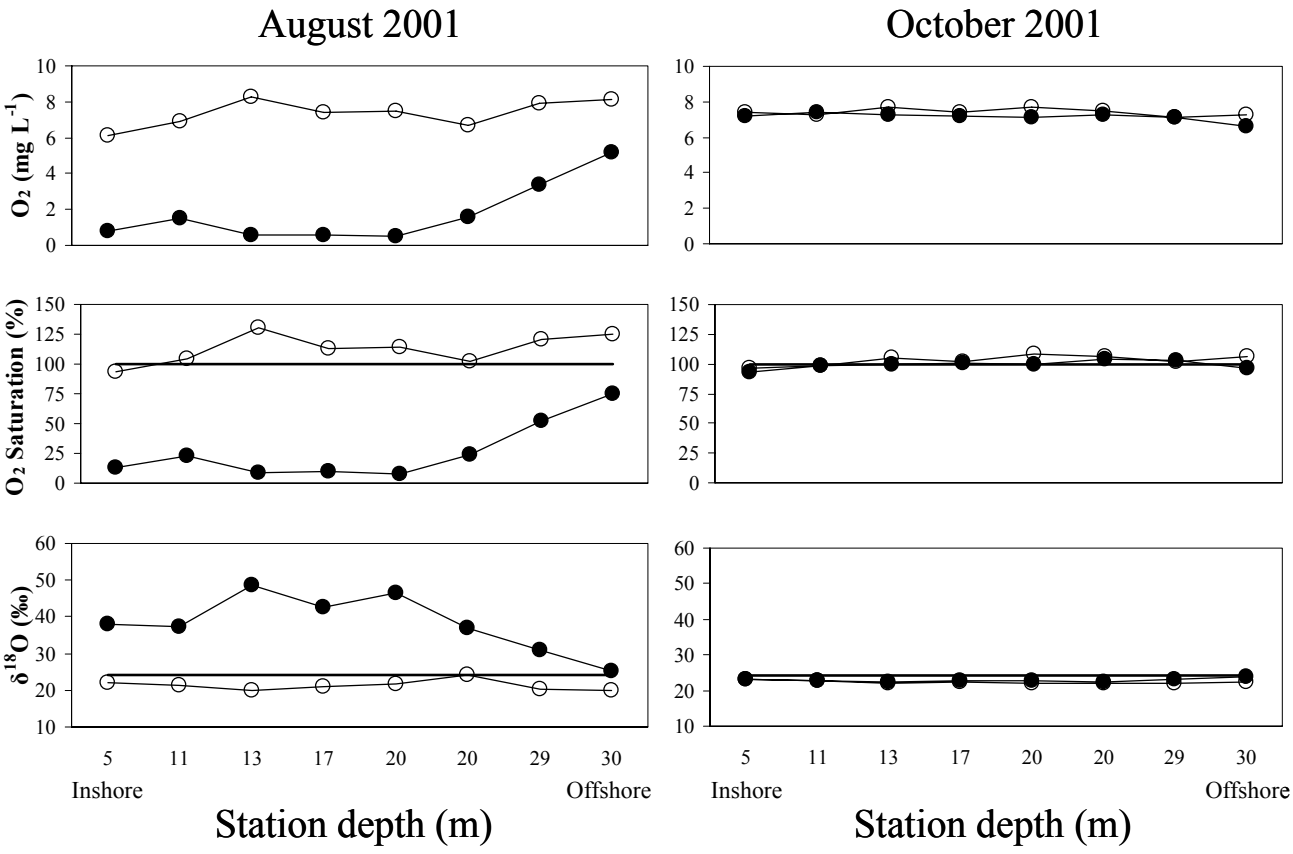

Figure 2.6 Oxygen concentration, oxygen saturation, and $\delta^{18}O$ for surface (open circles) and bottom samples (closed circles) for transect C, August and October 2001. Horizontal lines in the bottom panels represent air-equilibrated values.

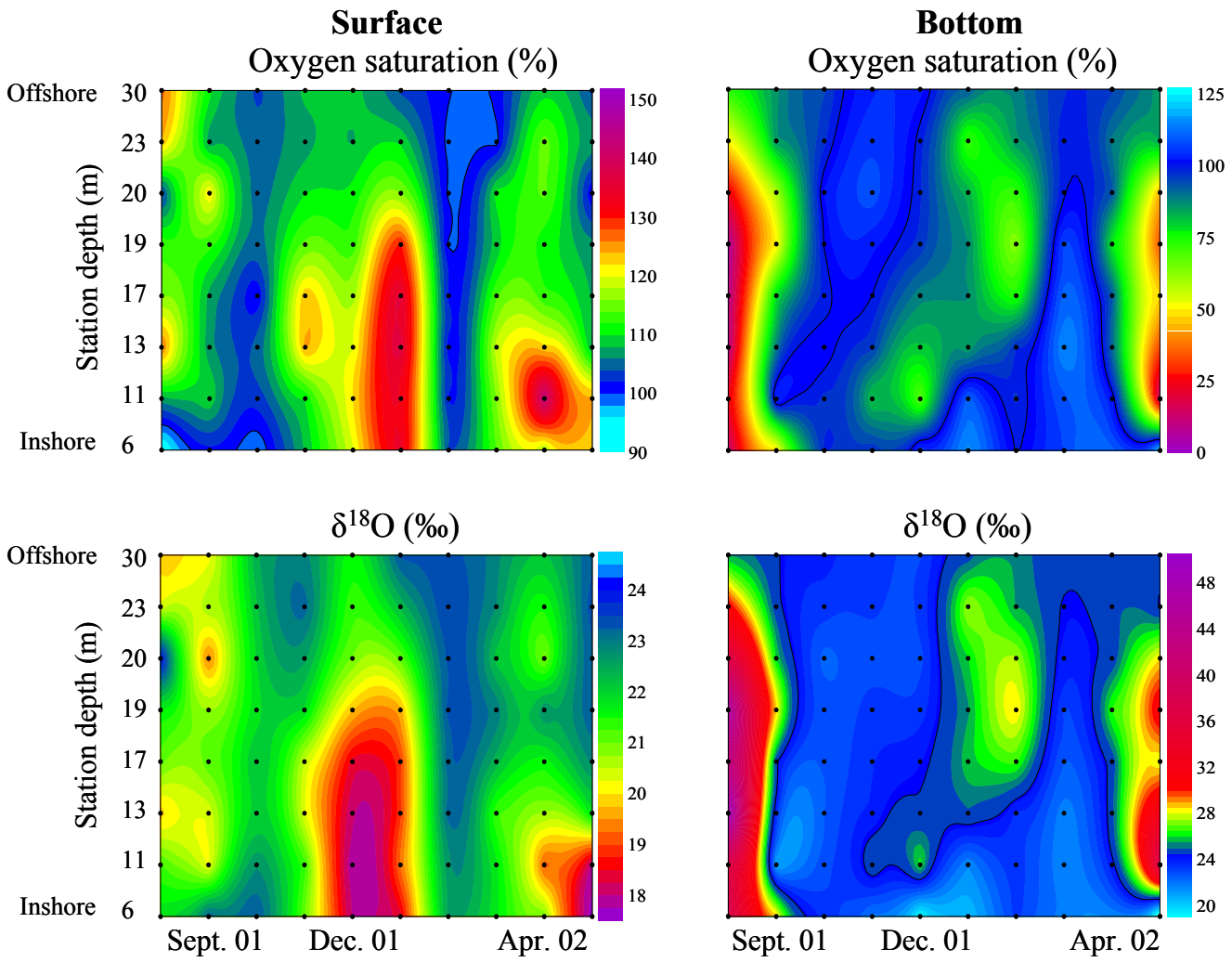

Figure 2.7 Oxygen saturation and $\delta^{18}O$ for surface and bottom samples for transect C, August 2001 to June 2002. The black reference lines represent air-equilibrated values.

Beyond these obvious seasonal contrasts, I observed interesting variations in oxygen concentrations and $\delta^{18}O$ on a shorter time scale when monthly sampling showed that oxygen depletion could also occur in winter (Figure 2.7). During calm periods in winter, oxygen saturation in surface waters often exceeded 130%, and bottom water oxygen saturation could drop to 60% (Figure 2.7). Accordingly, at higher oxygen concentrations in surface waters, $\delta^{18}O$ values decreased to about 18‰, while at lower concentrations in bottom waters $\delta^{18}O$ values increased to 28‰ (Figure 2.7). Only recurring, strong physical mixing was capable of re-

oxygenating the whole water column, with well-mixed conditions observed in October 2001 and February-March 2002. Overall, the system was quite dynamic in respect to oxygen concentrations and $\delta^{18}O$ values, displaying intense spatial variations in addition to month-to-month variations. For example, the location of minimum oxygen (Figure 2.7) moved from onshore during November and December 2001 (water depths less than 15 m) to offshore in January and February of 2002 (stations between 20 and 30 m water depth).

Surface Water Dynamics in July 2001

During the shelfwide cruise in July 2001, oxygen concentrations of surface waters were always high, generally exceeding 100% saturation. The highest concentrations of 10 to 14 mg L^{-1} were observed near the mouth of the Mississippi River, while elsewhere the oxygen concentrations were between 6 and 8 mg L^{-1} (Figure 2.8). Due to the continuous 24-h sampling scheme, a diurnal pattern was observed across the shelf in surface waters, i.e., high oxygen concentrations (indicated by green shading, top panel Figure 2.8) generally occurred during the late afternoon, while lower oxygen concentrations occurred at night and in the early morning, but also in some offshore areas (Figure 2.8). Surface $\delta^{18}O$ values were almost always lower than 24.2‰, the value for air-equilibrated water. At the sites of highest O_2 concentrations, isotope values were below 20‰, consistent with high rates of primary production. The diurnal pattern observed in oxygen concentrations was even more pronounced for isotope values, with lowest $\delta^{18}O$ values observed in the late afternoon (Figure 2.8).

The P/R surface model performed well and captured most of the observed variability in O_2 concentration vs. $\delta^{18}O$, as out of 72 stations that were sampled, I could generate P/R values for 68 of them. Only for stations near the mouth of the Mississippi River where O_2 saturation exceeded 150%, P/R could not be resolved, even though oxygen supersaturation suggested that

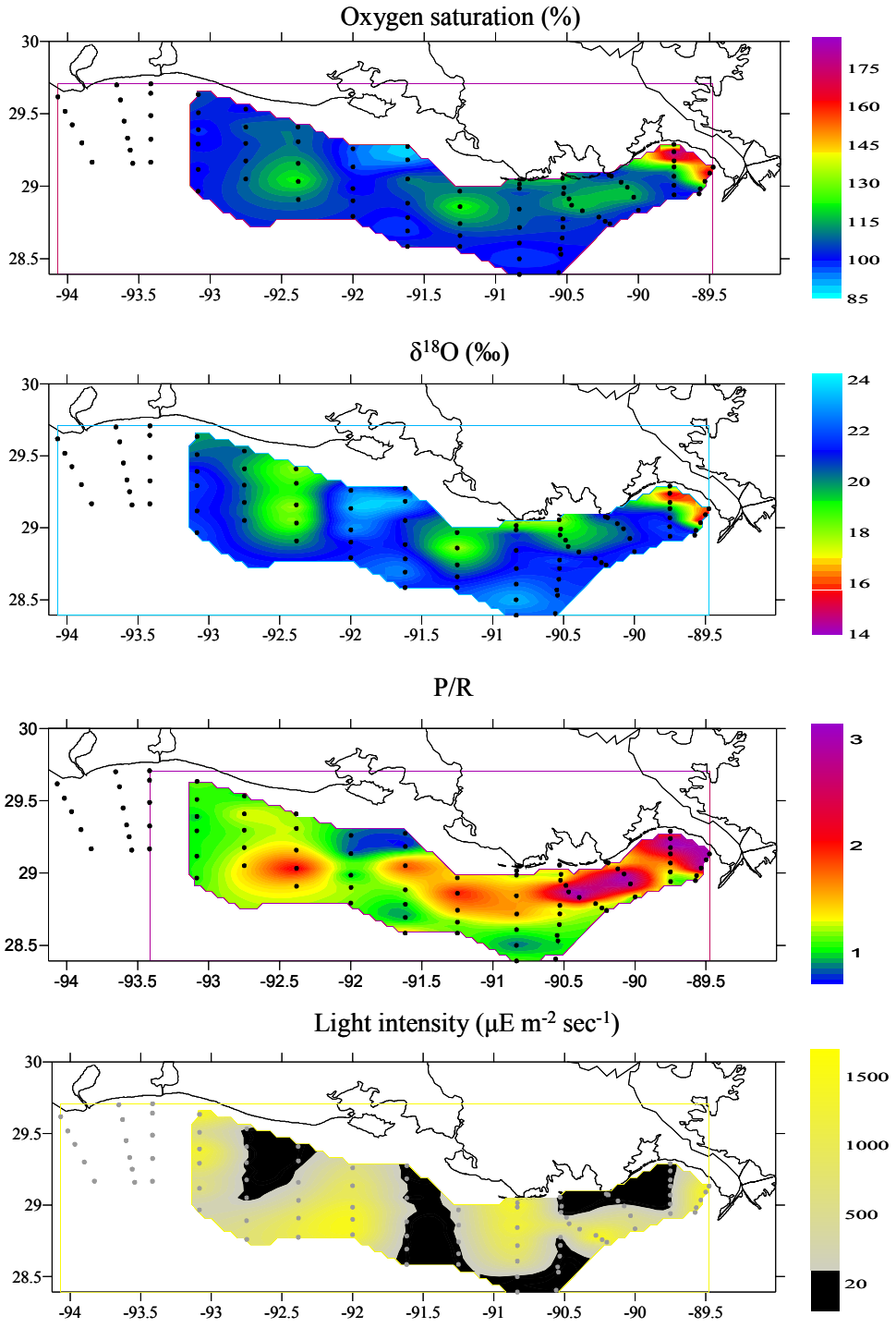

Figure 2.8 Oxygen saturation, $\delta^{18}O$, P/R, and light intensity for surface samples collected during the shelfwide cruise, July 2001. Black circles show the sampling grid. P/R values that could not be resolved (four stations near the mouth of the Mississippi River where O_2 saturation exceeded 150%) were set to 3 to facilitate visual perception of the spatial P/R pattern.

P/R at these stations was rather high. Calculated P/R values of surface samples for the shelfwide cruise in July 2001 generally exceeded 1 (Figure 2.8), which is in good agreement with the observed O_2 supersaturation and $\delta^{18}O$ values below 24.2‰. Average (median) P/R was 1.12 and the 10^{th} and 90^{th} percentiles were 0.94 and 1.64, respectively. The highest P/R values were found near the mouth of the Mississippi River (> 2), and in the central part of the Louisiana continental shelf at stations with water depths between 10 and 30 m (~ 1.3). Nevertheless, this pattern was disrupted near the mouth of the Atchafalaya River, where I encountered P/R values below 1. Because of the nature of this model (see Modeling approach), P/R values did not show the diurnal signal that was observed in oxygen concentrations and $\delta^{18}O$ time series. Rather, the calculated P/R values reflect longer-term rather than 24-hour oxygen cycling, as the magnitude of the effects of production (difference between $\delta^{18}O$ of ambient water and dissolved oxygen) and respiration (ε) on $\delta^{18}O$ values were roughly similar, at approximately 22‰. Assuming a respiration rate of 0.07 g O_2 m^{-3} h^{-1} and an oxygen-to-carbon ratio of 3.47 by weight (Redfield ratio * ratio of g mol^{-1} O_2 / g mol^{-1} C; 1.3 * 2.66 = 3.47), the P/R values of 0.94, 1.12, and 1.64 (10^{th} percentile, median, 90^{th} percentile) would translate into surface net primary productivities of -0.03, 0.06, and 0.31 g C m^{-3} day^{-1}, respectively, while gross primary production would amount to 0.46, 0.54, and 0.79 g C m^{-3} day^{-1}, respectively.

Bottom Water Dynamics in July 2001

Bottom water oxygen concentrations were always below 4 mg L^{-1}, and hypoxia (dissolved oxygen < 2 mg L^{-1}) was most severe at shallow inshore and mid stations with water depths up to 30 m (Figure 2.9). Hypoxia was especially pronounced in two areas that were located approximately 100 km west of the Mississippi River and 100 km west of the Atchafalaya Rivers. Bottom $\delta^{18}O$ values were usually higher than 24.2‰, particularly in hypoxic waters

where $\delta^{18}O$ values could exceed 40‰. The highest $\delta^{18}O$ values were found in the two hotspots approximately 100 km west of the Mississippi and Atchafalaya Rivers at water depths of 20-30 m, coinciding with the lowest oxygen concentrations (Figure 2.9).

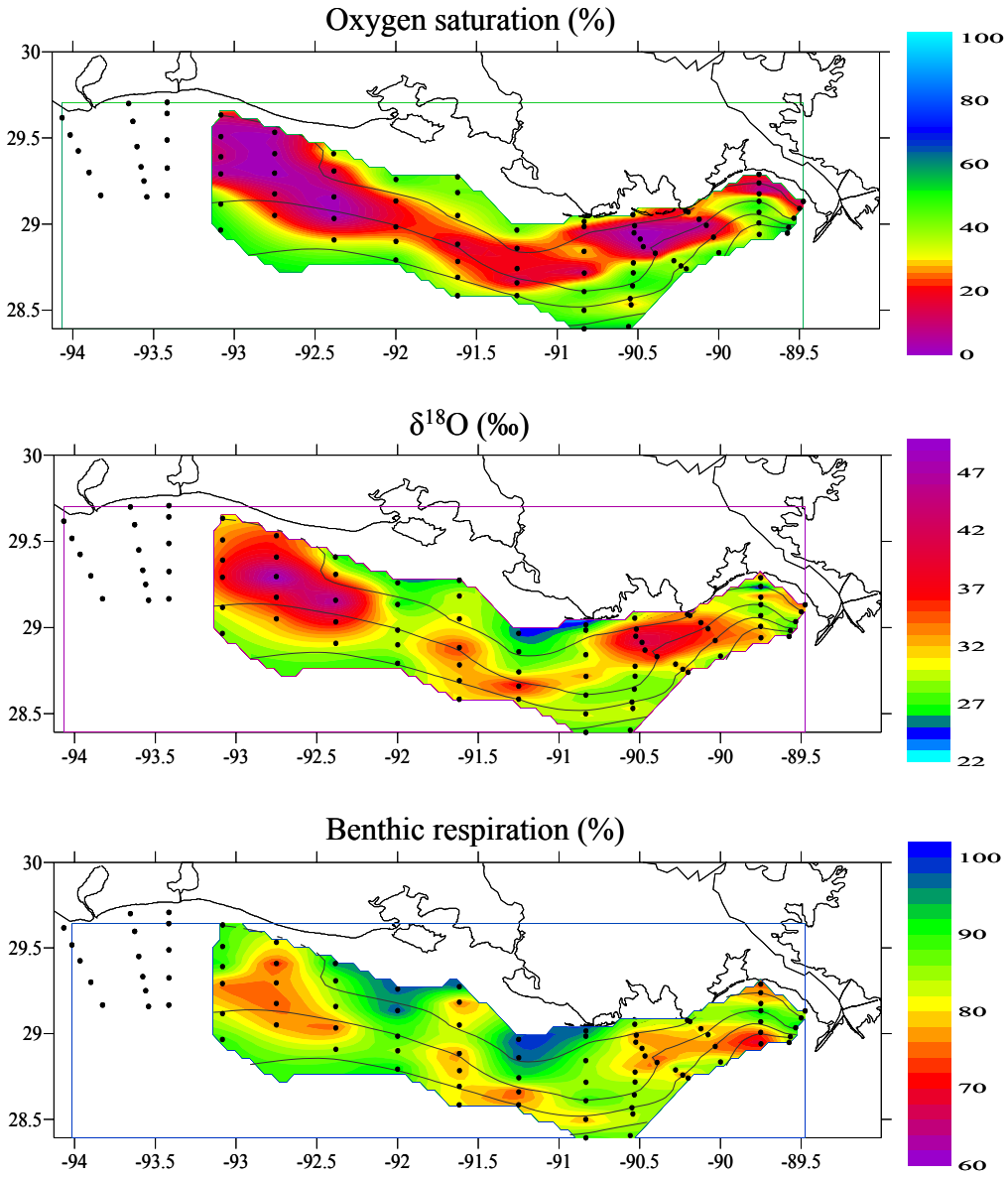

Figure 2.9 Oxygen saturation, $\delta^{18}O$, and spatial distribution of benthic respiration for bottom samples collected during the shelfwide cruise, July 2001. Values for benthic respiration were obtained from a mixing model (see Methods), with 100% water column respiration consistent with a -18‰ respiratory fractionation and 100% benthic respiration consistent with 0‰ fractionation. Black circles show the sampling grid, lines indicate depth as in Fig 1.

For respiration in bottom waters, the calculated fractionation factor for all samples combined was -6‰ (Figure 2.10), which is noticeably less than the -22‰ value that I measured for water column respiration (from incubation experiments). According to the mixing model that separated the effects of benthic versus water column respiration as components of total respiration in bottom waters, I estimated that respiration partitioned 73% to benthic and 27% to water column processes. In addition, water column contributions to total respiration never exceeded 40%. However, the small variation in water column contribution resulted in interesting spatial patterns, with the overall, somewhat counterintuitive result that water column respiration had larger contributions in areas of very intense hypoxia (Figure 2.9). The most intense benthic respiration was found near the mouth of the Atchafalaya River at water depths below 10 m.

DISCUSSION

I found very large fluctuations in oxygen concentrations and $\delta^{18}O$ values along the productive coastal shelf adjacent to the Mississippi River delta, which indicated that biological processes were very important and dominated oxygen dynamics during summer stratification. In fact, in 2001 the Mississippi River discharge was very high, and I observed the largest hypoxic area on record, exceeding 20,000 km^2 (Rabalais et al. 2002). Importantly, the variability of oxygen concentrations versus $\delta^{18}O$ values was not random, but rather enhanced the understanding of oxygen dynamics beyond previous studies that relied on the use of concentration measurements alone.

Surface Water Dynamics

The combined use of oxygen concentrations and $\delta^{18}O$ values allowed us to estimate P/R values and, subsequently, net and gross primary productivity across the Louisiana continental shelf. These large-scale measurements would not be possible with traditional, more time-

consuming incubations using either ^{14}C or ^{18}O additions (Lohrenz et al. 1999, Grande et al. 1989). The estimates of surface net primary productivity ranged from roughly 0 to 0.8 g C m^{-3} day^{-1}, approximately one order of magnitude lower than values that were measured by ^{14}C incubations between 1988 and 1992 across the Louisiana shelf (0 -10 g C m^{-2} day^{-1}, Lohrenz et al. 1999). The lower values of this study were likely due to the fact that I estimated productivity for the surface layer (approximate depth of 1 m), while Lohrenz et al. (1999) reported depth-integrated primary production for the mixed layer with a depth of generally 5 to 10 m. Assuming no significant light limitation throughout the mixed layer, these values can be transformed from g C m^{-3} day^{-1} to g C m^{-2} day^{-1} by multiplying with a factor of 5 to 10. Then, productivity estimates in this study would be only slightly lower than measurements performed by Lohrenz et al. (1999); especially since ^{14}C incubations results usually exceed net primary production (Grande et al. 1989). On the other hand, Justić et al. (1996) calculated average (1985 - 1992) net primary productivities for May and July of 1.0 and 0.04 C m^{-2} day^{-1}, respectively using oxygen concentration budgets. The high Mississippi River discharge in 2001 - that also occurred later in the year than usual - could probably be the reason that the July 2001 estimates were more representative of productive spring conditions rather than the usually less productive summer conditions.

The spatial pattern of high P/R and productivity near the mouth of the Mississippi River and along the central part of the shelf was consistent with the Mississippi River as major nutrient and freshwater source (Rabalais & Turner 2001) and the westerly transport due to the Louisiana-Texas current (Wiseman et al. 1997). The exceptionally low P/R values at the mouth of the Atchafalaya River might be caused by a combination of shallow water depth, high turbulence, and high turbidity, which would limit productivity despite high nutrient concentrations.

Absolute values of P/R and productivity estimates were susceptible to changes in respiration rate and fractionation factor (ε) during respiration. The determined respiration rate of 0.07 mg L^{-1} h^{-1} appears reasonable for the encountered warm and organic-rich bottom waters, as it corresponds to the upper range of values reported by Dortch et al. (1994) for coastal and estuarine system across the world. Typical fractionation factors reported in previous studies bracket the fractionation value (-22‰) and range from -15 to -25‰ found in this study (Kroopnick 1975, Bender & Grande 1987, Guy et al. 1989, Quay et al. 1993, 1995, Luz et al. 2005). Some of the described variability in net fractionation factors in aquatic systems is likely due to processes that generally occur during light respiration. For example, the importance of Mehler reaction (ε = -15‰), alternative oxidase pathway (ε = -31‰), and photorespiration (ε = -21‰) relative to total respiration will affect the net fractionation factor (Luz et al. 2002). Yet, assuming ε to be -18 or -25‰ (instead of the measured -22‰), P/R and productivity estimates would only be slightly lower and higher, respectively (Table 2.1), and the spatial patterns would remain the same. Furthermore, calculated P/R values are in good agreement with measured P/R values for a number of coastal ocean systems (ranging from about 0.8 to 4; Williams et al. 1999, Smith & Kemp 2001). Hence, calculated P/R and productivity values are generally consistent with productivity patterns in surface shelf waters.

Table 2.1 Model results of P/R and gross and net primary production for fractionation factors of 18, 22, and 25‰. Respiration rate was held constant at 0.07 mg O_2 L^{-1} h^{-1} for all three scenarios.

Fract. factor (ε_R)	**P/R**					**Gross primary production (g C m^{-3} day^{-1})**					**Net primary production (g C m^{-3} day^{-1})**				
%tile	10th	25th	med.	75th	90th	10th	25th	med.	75th	90th	10th	25th	med.	75th	90th
-18‰	0.89	1.11	1.22	1.45	2.17	0.44	0.54	0.60	0.71	1.06	-0.05	0.05	0.11	0.22	0.57
-22‰	0.94	1.06	1.12	1.24	1.64	0.46	0.51	0.54	0.60	0.79	-0.03	0.03	0.06	0.12	0.31
-25‰	0.96	1.03	1.07	1.32	1.32	0.46	0.50	0.52	0.79	0.64	-0.02	0.01	0.03	0.08	0.15

Yet, because of the nature of this model, P/R values are estimates at this time, with no P or R measurements made during the 2001 shelfwide cruise that would directly confirm or refute these values. The modeling approach used to generate these P/R values was simplistic, assuming that P and R are always coupled in essentially daytime conditions. Also, an alternative interpretation of P and R dynamics could not be rejected, namely that P/R values varied over a smaller range (e.g., 0.9 to 1.4), with larger "apparent P/R" variations due to increases in the fractionation factor for respiration, ε_R (-15 from -25‰) rather than changes in P or R. The total range in ε_R fractionation values from a variety of aquatic and terrestrial environments can extend considerably beyond the central -22‰ fractionation factor assumed for this model, from about -4 to -32‰ (Lane and Dole 1956, Kroopnick 1975, Bender & Grande 1987, Guy et al. 1989, Kiddon et al. 1993, Quay et al. 1993, 1995). Still, larger P/R values and larger fractionation factors would both reflect higher productivity in supply-demand isotope models (Fry 2006), and an overall conservative conclusion from the modeling is that the P/R map of Figure 8 is likely correct in relative terms of areas of lower and higher productivity, even if there is some uncertainty about the absolute P/R values. Given these caveats, direct experimental determinations of P and R during future cruises will be needed to better constrain the P/R model estimates generated with oxygen concentration and oxygen isotope measurements.

Bottom Water Dynamics

The combined oxygen concentration and $\delta^{18}O$ measurements of bottom water samples let us differentiate between water column respiration and benthic sediment respiration. For bottom water samples, I observed an overall net fractionation factor of -6‰ (Figure 2.10), considerably smaller than the measured -22‰ ε_R value for water column respiration. Results of the mixing model indicated that benthic respiration was clearly the dominant sink for dissolved oxygen,

whereby respiration in the bottom waters was about 3/4 sediment-driven and 1/4 water-column-driven. This result is in good agreement with previous work by Dortch et al. (1994), who came to the similar conclusion by measuring enzymatic respiratory electron-transport-system activity (ETS) on the Louisiana continental shelf in July 1991. The dominance of benthic respiration is likely related to the relatively shallow water depth and high sedimentation rates of phytoplankton cells and fecal pellets (Dortch et al. 2001). Consistent with this conclusion, I found that benthic respiration was strongest in shallow water (less than 10 m; Figure 2.9).

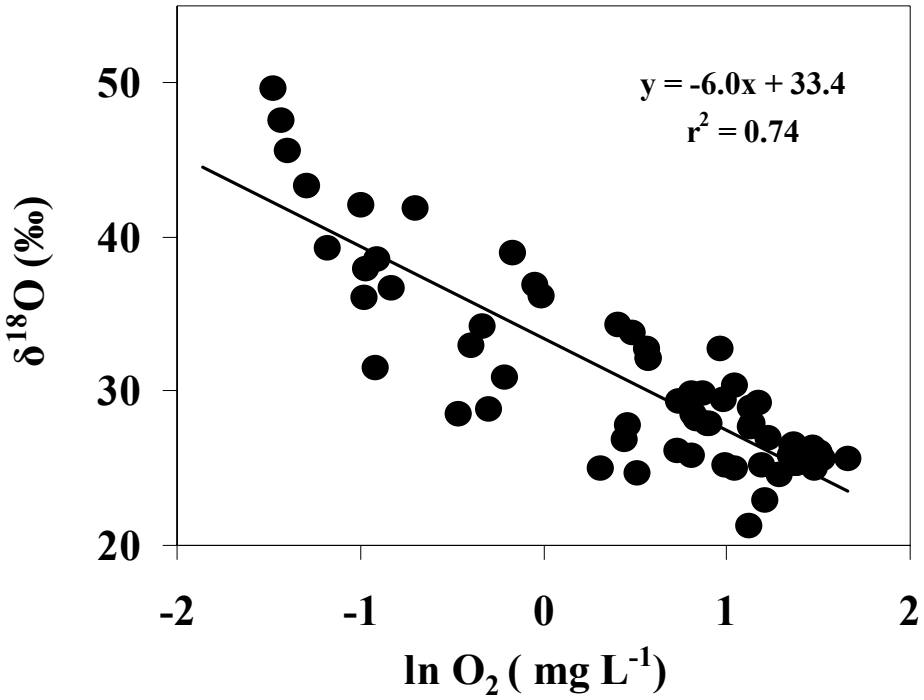

Figure 2.10 Relationship between $\delta^{18}O$ and ln (O_2 concentration) for bottom samples collected within 1 m of the sediment during the shelfwide cruise, July 2001. The slope of the regression line represents the overall average fractionation factor (ε, ‰) due to respiration in bottom water samples.

Calculations of the contribution of benthic respiration to total respiration were based on the assumptions that oxygen inputs to bottom waters from photosynthesis and mixing were negligible during summertime conditions, i.e., the system was isolated or closed to inputs and

exports. These assumptions are supported by the following three findings. First, the vertical oxygen transport across the pycnocline in the inner section of the hypoxic zone is small during the peak of summer stratification (Justić et al. 1996). Second, a strong tidal signal, which would indicate horizontal transport, is not present in the periodograms of oxygen data series from station C6B (Rabalais et al. 1994). The maximum lateral displacement of water parcels that can be expected due to diurnal and semidiurnal currents in the study area is only about 3 km (Rabalais et al. 1994), which is not likely to affect the inner section of a 60 km wide hypoxic zone. Third, benthic photosynthesis, which can potentially re-supply significant amounts of oxygen lost by respiration in coastal waters (Dortch et al. 1994, Jahnke et al. 2000), was likely not an important oxygen source for bottom waters in July 2001. At that time, light conditions in bottom waters were unfavorable for benthic primary production because Secchi depths were relatively shallow so that little light reached benthic sediments (Figure 2.11). Sediments were usually deeper than 2-3x Secchi depths, with depths exceeding 2x Secchi depth usually being considered to be below compensation depth for phytoplankton growth (Wetzel 2001). Moderate oxygen inputs due to benthic photosynthesis or oxygen-rich surface water would have slightly reduced the estimate of benthic respiration. Nevertheless, even a 20% addition from either source (e.g. conditions reported for July 1991 by Dortch et al. (1994)) to the ambient bottom water concentrations would not have had a strong effect on the calculations of the contribution of benthic respiration (Figure 2.12). Somewhat smaller or larger fractionation factor for water column respiration, such as -18‰ or -25‰ (Kroopnick 1975, Bender & Grande 1987, Guy et al. 1989, Quay et al. 1993) would have changed the contribution of benthic respiration as well. Still, in those cases the average contributions of benthic respiration would remain high (66% and 76%, respectively) and the sediment would be the dominant sink for oxygen. On the other hand,

a fractionation factor > 0‰ for benthic respiration would have underestimated the contribution of benthic respiration, e.g. an ε value of -3‰ would have increased the average contribution of benthic respiration from 73 to 84%. Brandes & Devol (1997) performed benthic chamber incubations in Puget Sound and measured fractionation factors between -1 to -4‰ for dissolved oxygen. However, the overlaying water in these experiments remained unfiltered and still contained particles that could have contributed to water column respiration, which would explain the measured non-zero fractionation factor.

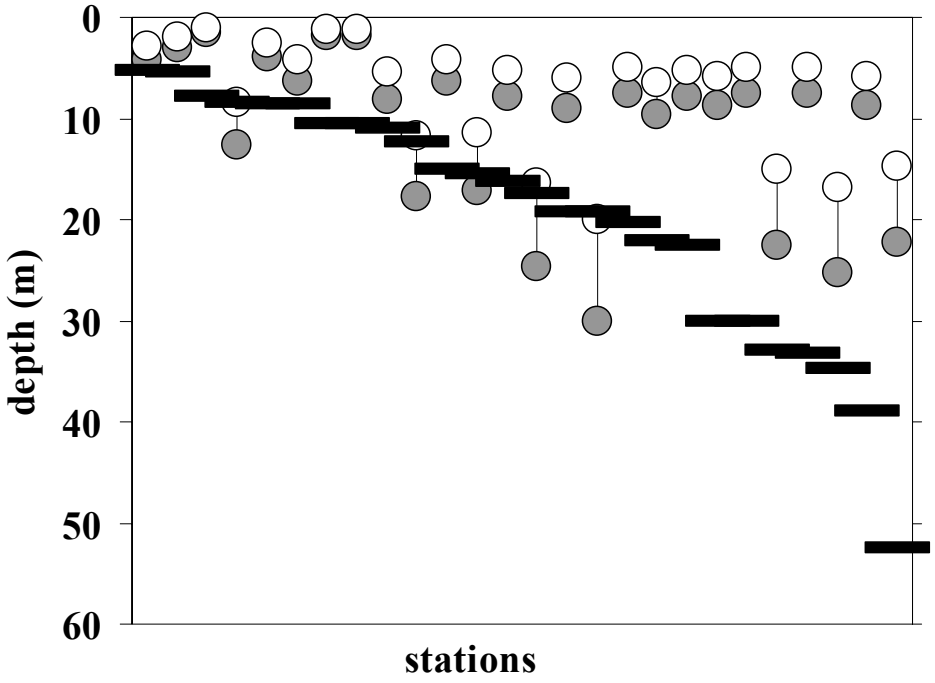

Figure 2.11 Relationship between 2x Secchi depth (open circles) and 3x Secchi depth (close circles) versus station depth (m, black bars) for the shelfwide cruise, July 2001.

The assumed respiration rate of 0.07 mg L^{-1} h^{-1} might have overestimated the actual respiration rate in bottom waters as previous research indicated that respiration rates in surface waters frequently exceed those in bottom waters (Dortch et al. 1994). Nevertheless, beyond the

analyses shown in Figure 2.12, the conclusions derived from this model that separates water-column and benthic respiration in bottom waters only depended on the fractionation factor of respiration (ε), but were insensitive to the actual respiration rates. A lower respiration rate would lead to the same combinations of oxygen concentration and $\delta^{18}O$ values, but at a later time. In conclusion, calculated contributions of benthic respiration to total respiration could vary somewhat, but the overall importance of benthic respiration and its spatial patterns remain the same.

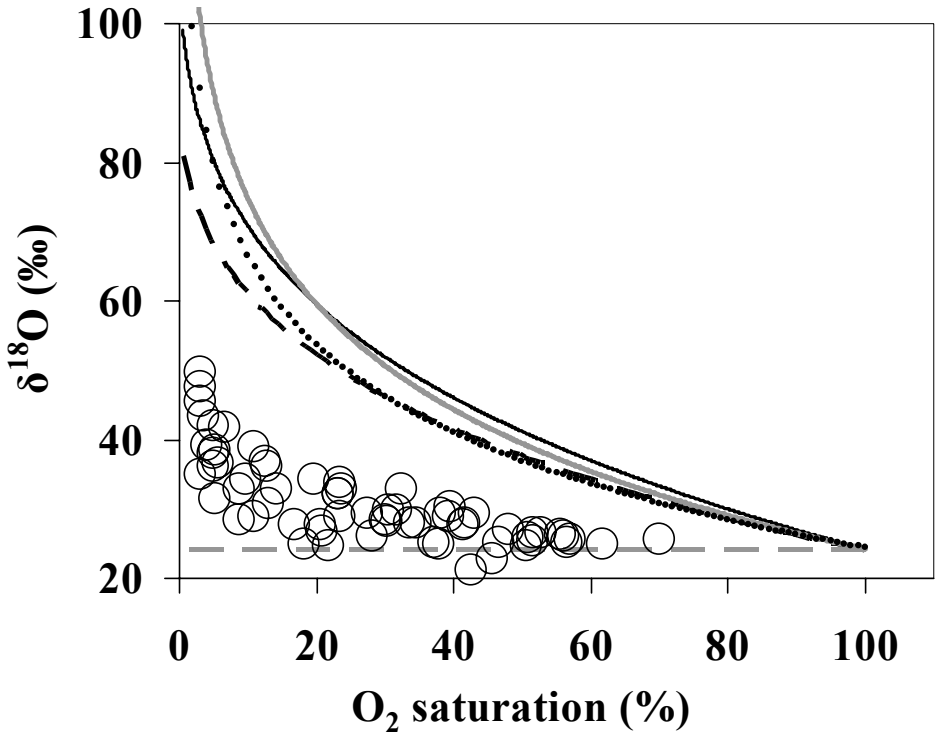

Figure 2.12 Relationship between oxygen saturation and $\delta^{18}O$ for bottom water samples (open circles) collected during the shelfwide cruise, July 2001. The dashed gray horizontal line represents 100% benthic respiration in the absence of new oxygen inputs, while curved lines represent alternate model scenarios, as follows: 1) grey line: -22‰ fractionation during water column respiration in a closed system with no oxygen inputs; 2) solid black line: as scenario 1, with a 20% oxygen addition from oxygen-rich surface water; 3) black dashed line: as scenario 1, with a 20% oxygen addition from benthic photosynthesis; 4) dotted line: as scenario 1, but a fractionation factor of -18‰ during water column respiration. The closer a sample is to the lower horizontal line, the larger is the contribution of benthic respiration.

The spatial distribution of benthic versus water column respiration indicated that the contribution of water column respiration was larger in areas of intense hypoxia. It is possible that benthic respiration due to the accumulation of organic material on the sediment surface could be relatively similar across the shelf. Areas of high production could contribute further to oxygen loss by water column respiration due to the increased amount of sinking particles. Hence, this combined respiration would then lead to more severe hypoxia along with larger contributions of water column respiration. This assumption is also supported by increased P/R in the central part of the Louisiana shelf, which should result in increased particle flux to the lower water column. Similar to the low P/R values, the highest contribution of benthic respiration in the vicinity of the Atchafalaya River delta might be a result of high turbidity in these areas (due to high concentrations of suspended phytoplankton and sediment) in combination with a relatively shallow water column of generally less than 10 m. The lack of particle flux due to low in situ production and a reduced depth as potential site for water column respiration would favor the dominance of benthic respiration at the shallower stations. Reduced oxygen concentrations in areas of strong hypoxia may also impose a diffusional limitation on sediment respiration rates, increasing the apparent importance of water column respiration.

REFERENCES

Barkan E, Luz B (2005) High precision measurements of $^{17}O/^{16}O$ and $^{18}O/^{16}O$ ratios in H_2O. Rapid Commun Mass Spectrom 19:3737-3742

Bender ML, Grande K (1987) Production, respiration and the isotopic geochemistry O_2 in the upper water column. Global Biogeochem Cycles 1:49-59

Benson BB, Parker DM (1961) Nitrogen/argon isotope ratios in aerobic sea water. Deep-Sea Res 7:237-264

Brandes JA, Devol AH (1997) Isotopic fractionation of oxygen and nitrogen in coastal marine sediments. Geochim Cosmochim Acta 61:1793-1802

Craig H, Hayward T (1987) Oxygen supersaturation in the ocean: biological versus physical contributions. Science 235:199-202

Diaz RJ, Rosenberg R (1995) Marine benthic hypoxia: A review of its ecological effects and behavioural responses of benthic macrofauna. Oceanogr Mar Biol Annu Rev 33:245-303

Dinnel S, Wiseman WJ Jr (1986) Freshwater on the Louisiana shelf. Cont Shelf Res 6:765-784

Dole M, Lane GA, Rudd DP, Zaukelies DA (1954) Isotopic composition of atmospheric oxygen and nitrogen. Geochim Cosmochim 6:65-78

Dortch Q, Turner RE, Rowe GT (1994) Respiration rates and hypoxia on the Louisiana shelf. Estuaries 17:862-872

Dortch Q, Rabalais NN, Turner RE, Qureshi NA (2001) Impacts of changing Si/N ratios and phytoplankton species composition. In: Rabalais NN, Turner RE (eds) Coastal Hypoxia: consequences for living resources and ecosystems. Coastal and Estuarine Studies 58, American Geophysical Union, Washington D.C., p. 37-48

Emerson S, Stump C, Wilbur D, Quay P (1999) Accurate measurement of O_2, N_2, and Ar gases in water and the solubility of N_2. Mar Chem 64:337-347

Fry B (2006) Stable Isotope Ecology. Springer, New York.

Grande KD, Williams PJ, Marra J, Purdie DA, Heinemann K, Eppley RW, Bender ML (1989) Primary production in the North Pacific gyre: a comparison of rates determined by the ^{14}C, O_2 concentration and ^{18}O methods. Deep-Sea Res 36:1621-1634

Guy RD, Berry JA, Fogel ML, Hoering TC (1989) Differential fractionation of oxygen isotopes by cyanide-resistant and cyanide-sensitive respiration in plants. Planta 177:483-491

Guy RD, Fogel ML, Berry JA (1993) Photosynthetic fractionation of the stable isotopes of oxygen and carbon. Plant Physiol 101:47-47

Hickel W, Mangelsdorf P, Berg J (1993) The human impact in the German Bight: eutrophication during three decades (1962-1991). Helgol Meeresunters 47:243-263

Jahnke RA, Nelson JR, Marinelli RL, Eckman JE (2000) Benthic flux of biogenic elements on the southeastern US continental shelf: influence of pore water advective transport and benthic microalgae. Cont Shelf Res 20:109-127

Justić D, Legović T, Rottini-Sandrini L (1987) Trends in the oxygen content 1911-1984 and occurrence of benthic mortality in the northern Adriatic Sea. Estuar Coast Shelf Sci 25:435-445

Justić D, Rabalais NN, Turner RE (1996) Effects of climate change on hypoxia in coastal waters: A doubled CO_2 scenario for the northern Gulf of Mexico. Limnol Oceanogr 41:992-1003

Kampbell DH, Wilson JT, Vandergrift SA (1989) Dissolve oxygen and methane in water by a GC headspace equilibration technique. Intern J Environ Anal Chem 36:249-257

Kiddon, J, Bender ML, Orchardo J, Caron DA, Goldman JC, Dennett M (1993) Isotopic fractionation by respiring marine organisms. Global Biogeochem Cycles 7:679-694

Knox M, Quay PD, Wilbur D (1992) Kinetic isotope fractionation during air-water gas transfer of O_2, N_2, Ch_4, and H_2. J Geophys Res 97:20335-20343

Kroopnick PM (1975) Respiration, photosynthesis, and oxygen isotope fractionation in oceanic surface water. Limnol Oceanogr 20:988-992

Lane GA, Dole M (1956) Fractionation of oxygen isotopes during respiration. Science 123:574-576

Lohrenz SE, Dagg MJ, Whitledge TE (1990) Enhanced primary production in the plume/oceanic interface of the Mississippi River. Cont Shelf Res 10:639-664

Lohrenz SE, Fahnenstiel GL, Redalje DG, Lang GA, Dagg MJ, Whitledge TE, Dortch Q (1999) Nutrients, irradiance, and mixing as factors regulating primary production in coastal waters impacted by the Mississippi River plume. Cont Shelf Res 19:1113-1141

Luz B, Barkan E, Sagi Y, Yacobi Y (2002) Evaluation of community respiratory mechanisms with oxygen isotopes: A case study in Lake Kinneret. Limnol Oceanogr 47:33-42

Mariotti A, Germon JC, Hubert P, Kaiser P, Letolle R, Tardieux A, Tardieux P (1981) Experimental determination of nitrogen kinetic isotope fractionation: Some principles; illustration for the denitrification and nitrification processes. Plant and Soil 62:413-430

Miyajima T, Yamada T, Hanba YT (1995) Determining the stable isotope ratio of total dissolved inorganic carbon in lake water by GC/C/IRMS. Limnol Oceanogr 40:994-1000

Officer CC, Biggs RB, Taft JL, Cronin LE, Tyler M, Boynton WR (1984) Chesapeake Bay anoxia: origin, development and significance. Science 223:22-27

Ostrom NE, Carrick HJ, Twiss MR (2005) Evaluation of primary production in Lake Erie by multiple proxies. Oecologia 145:669-669

Pavella JS, Ross JL, Chittenden ME Jr (1983) Sharp reduction in abundance of fishes and benthic macroinvertebrates in the Gulf of Mexico off Texas associated with hypoxia. Northeast Gulf Sci 6:167-173

Quay PD, Emerson S, Wilbur DO, Stump C (1993) The $\delta^{18}O$ of dissolved O_2 in the surface waters of the Subarctic pacific: A tracer of biological productivity. J Geophys Res 98:8447-8458

Quay PD, Wilbur DO, Richey JE, Devol AH, Benner R, Forsberg BR (1995) The ^{18}O:^{16}O of dissolved oxygen in rivers and lakes in the Amazon basin: Determining the ratio of respiration to photosynthesis rates in freshwaters. Limnol Oceanogr 40:718-729

Rabalais NN, Turner RE (eds) Coastal Hypoxia: consequences for living resources and ecosystems. Coastal and Estuarine Studies 58, American Geophysical Union, Washington D.C., 463pp

Rabalais NN, Turner RE, Scavia D (2002) Beyond science into policy: Gulf of Mexico hypoxia and the Mississippi River. BioScience 52:129-142

Rabalais NN, Wiseman WJ Jr, Turner RE (1994) Comparison of continuous records of near-bottom dissolved oxygen from the hypoxic zone along the Louisiana coast. Estuaries 17:850-861

Sklar FH, Turner RE (1981) Characteristics of phytoplankton production off Barataria Bay in an area influenced by the Mississippi River. Contrib Mar Sci 24:93-106

Smith EM, Kemp WM (2001) Size structure and production/respiration balance in a coastal plankton community. Limnol Oceanogr 46:473-485

Stigebrandt A (1991) Computations of oxygen fluxes through the sea-surface and the net production of organic matter with application to the Baltic and adjacent seas. Limnol Oceanogr 36:444-454

Turner RE, Rabalais NN (1994) Evidence for coastal eutrophication near the Mississippi River delta. Nature 368:619-621

Turner RE, Rabalais NN, Justić D, Dortch Q (2003) Global patterns of dissolved N, P and Si in large rivers. Biogeochemistry 64:297-317

Weiss R (1970) The solubility of nitrogen, oxygen and argon in water and seawater. Deep-Sea Res 17:721-735

Wetzel RG (2001) Limnology - lake and river ecosystems. Academic Press.

Williams PJB, Bowers DG, Duarte CM, Agosti S, delGiorgio PA, Cole JJ (1999) Regional carbon imbalances in the oceans. Science 284:1735b

Wiseman WJ Jr, Rabalais NN, Turner RE, Dinnel SP, MacNaughton A (1997) Seasonal and interannual variability within the Louisiana coastal current: stratification and hypoxia. J Mar Syst 12:237-248

CHAPTER 3
QUANTIFYING THE EFECTS OF PHYSICAL AND BIOLOGICAL FACTORS ON SEASONAL OXYGEN DYNAMICS IN A STRATIFIED, EUTROPHIC COASTAL ECOSYSTEM

INTRODUCTION

Like many other coastal areas worldwide, the northern Gulf of Mexico experienced the effects of eutrophication in the last half of the 20th century (Boesch 2002, Rabalais et al. 2002a, 2007). The most notable symptoms of eutrophication in this area are extensive surface algal blooms and the annual formation of a large hypoxic zone during summer. Hypoxia (< 2 mg O_2 L^{-1}) develops in bottom waters as a synergistic product of high stability of the water column and nutrient-enhanced surface productivity. Elevated surface productivity results in a high vertical carbon flux that ultimately fuels benthic and water column respiration (Rabalais & Turner 2001). Although the areal extent of hypoxia (usually mapped in late July, Rabalais et al. 2007) varies annually, it is tightly coupled to freshwater discharge and nitrogen and phosphorus loads of the Mississippi and Atchafalaya Rivers (Turner et al. 2006). Model hindcasts (Scavia et al. 2004, Justić et al. 2002, Turner et al. 2006) indicated that large scale hypoxia is a recent phenomenon, and is unlikely to have occurred before the 1970s, the period when the use of nitrogen-based fertilizer in the Mississippi River watershed increased dramatically (Turner and Rabalais 1991, Boesch 2002).

Even though nitrate-N flux is the strongest predictor for the bottom area of summer hypoxia, this relationship only holds true when the water column is well stratified and re-supply of oxygen into bottom waters is minimal (Rabalais et al. 1991). Stratification in summer months is usually strong, but tropical storms and hurricanes have the potential to completely mix the water column and replenish previous oxygen deficits in the lower water column (Wiseman at al.

1997, Rabalais et al. 2007). Consequently, in years when such high wind events occur, measured areal extent of hypoxia is generally much smaller than predicted (Turner et al. 2006).

Besides identifying the causes of hypoxia, there has been a considerable effort to better understand oxygen dynamics within this system. For example, primary production measurements have been conducted frequently (Sklar & Turner 1981, Lohrenz et al. 1990, 1999), and benthic respiration rates were determined (Rowe et al. 1992, Dortch et al. 1994, Turner et al. 1998, Rowe et al. 2002). More recently, the combined use of oxygen concentration and stable isotope measurements was used to improve the understanding of oxygen cycling in the northern Gulf of Mexico (Chapter 2). In equilibrium with the atmosphere, dissolved oxygen has a stable isotope value of 24.2‰ (Benson & Krause 1984, Knox et al. 1992), but photosynthesis and respiration can lead to significantly lower and higher $\delta^{18}O$ values, respectively. Decreasing $\delta^{18}O$ values in response to photosynthesis are due to the addition of isotopically depleted (light) oxygen that is derived from ambient water to the existing dissolved oxygen (DO) pool (Guy et al. 1986, 1993), whereby $\delta^{18}O$ of the source water in coastal marine systems ranges from 0‰ to about -3‰. In contrast, respiration preferentially removes light oxygen with a large fractionation factor (ε) of -15 to -25‰ (Kroopnick 1975, Quay et al. 1995, Luz et al. 2002, Hendricks et al. 2004, Chapter 2), which results in increased $\delta^{18}O$ values for the residual DO pool. Yet, oxygen that is respired within bottom sediments (hereafter referred to as benthic respiration) has a very small fractionation effect, ranging from 0 to -3‰ (Brandes & Devol 1997), and a substantial contribution of benthic respiration in bottom waters would significantly reduce the net fractionation factor. By applying this stable isotope technique to the Louisiana continental shelf, in Chapter 2, I estimated the ratios of production and respiration (P/R) in surface waters and quantified the relative contributions of water column and benthic respiration in bottom waters.

Model estimates for July 2001 indicated that surface waters across the Louisiana shelf were highly productive with a median P/R of 1.12 and net primary production of 0.06 g C m^{-3} day^{-1}. In contrast, in bottom waters oxygen depletion was severe and predominantly driven by benthic respiration, which accounted for about 3/4 of the total oxygen loss. This first application of oxygen stable isotope technique to productive coastal marine systems was very promising as it not only compared well to traditionally measured production estimates, but also added valuable new information on oxygen dynamics on the Louisiana continental shelf.

Here I build upon the work presented in Chapter 2 to further explore how physical (wind, salinity, water temperature, pH) and biological (concentrations and C:N ratios of particulate organic matter) parameters affect the seasonal and interannual oxygen dynamics. The previous study focused only on surface and bottom waters, but I now use measurements throughout the water column. Finally, the shelfwide summer cruises in July 2001, 2002 and 2003 followed comparable nutrient inputs from the Mississippi River, which should have resulted in similar areal extents of hypoxia in all three years (Turner et al. 2006). Yet, in late June of 2003, tropical storm Bill stirred up the water column across the Louisiana continental shelf, which gave us the opportunity to contrast the effects of a recent high wind event on oxygen dynamics relative to otherwise calm summertime conditions.

METHODS

Field Sampling

The sampling grid consisted of 14 transects across the width of the coastal shelf from the Mississippi River birdfoot delta westwards past the Texas-Louisiana border (Figure 3.1). Each transect extended 40 to 60 km offshore and included six to ten stations ranging in depth from 5 to

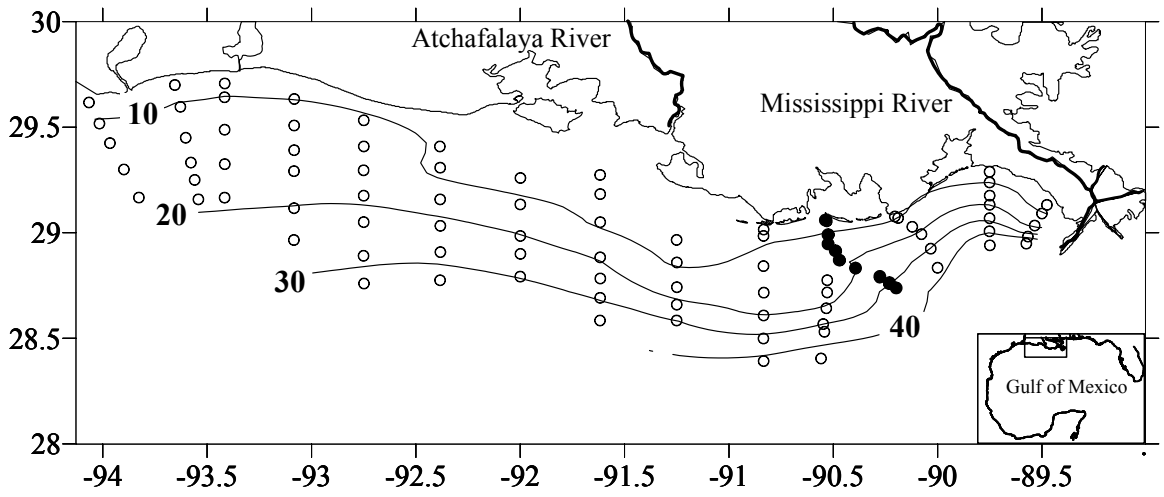

Figure 3.1 Map of the study area off the Louisiana coast showing depth contours (m), the station grid and location of transect C sampled each month, July 2001 to July 2003 (closed circles).

50 m. During the shelfwide cruises in July 2002 and July 2003, water samples were collected in 5-m depth intervals at stations with water depths of approximately 10, 20, and 30 m. In addition, in July 2003, surface water samples were collected at all stations that were visited during the survey. Moreover, from August 2002 to June 2003, seasonal samples were collected (5 m depth intervals at stations with water depths of approximately 10, 20, and 30 m) during monthly cruises along transect C, 90 km west of the Mississippi River delta (Figure 3.1).

I used a 5 L PVC Niskin sampler to collect sub-surface water samples and a plastic bucket for surface water. For surface samples, the bucket was placed sideways onto the water surface. Once it started sinking, the bucket filled passively with water, avoiding intrusion of atmospheric oxygen into the sample water due to turbulent mixing. Surface water samples were collected approximately 10 cm below the surface, while subsurface samples were collected at specific depths or within one meter of the bottom sediments. Subsequently, 125 ml Wheaton glass bottles were carefully filled using plastic Tygon tubing. The tubing was either attached to the Niskin sampler (bottom samples) or water was siphoned directly from the bucket (surface

samples), and bottles were allowed to overflow at least twice their volume to exclude air bubbles. After filling, the bottles were immediately poisoned with 1.0 ml 6N HCl (Miyajima et al. 1995), sealed with heavy rubber stoppers (Bellco Glass, 20 mm), crimped, and stored in the dark (Chapter 2).

From January 2002 to July 2003 surface water was also analyzed for concentrations of particulate organic carbon (POC) and nitrogen (PON). Particulates were collected on pre-combusted (450 ºC, 6 hours) GF/F filters, which were kept frozen until return to the laboratory where they were dried overnight at 60 ºC. The analyses were conducted using an elemental analyzer (Carlo Erba 1500) that was coupled to a Finnigan Thermoquest Delta plus XP isotope ratio mass spectrometer (see Wissel et al. 2005 for details).

Routinely temperature, salinity, and pH readings were collected using a Hydrolab multi-probe (Hach Instruments). Temperature was used to test if seasonality (e.g. summer vs. winter) was important for oxygen dynamics. Salinity was used as a proxy for nutrient availability in the study area. This was possible because the Mississippi River is both the major nutrient and freshwater source for this coastal region (> 95%, Dunn 1996; Goolsby, 1999). Similarly, elevated pH values were used as an indicator of enhanced surface productivity (Wetzel 2001).

To evaluate potential light penetration that could have affected bottom water oxygen dynamics (Chapter 2), Secchi depth readings (black and white disc, 25 cm diameter) were taken between 6 hours before until 6 hours after apparent noon.

Stepwise multiple linear regressions were performed (SYSTAT 10) to identify physical and biological parameters that had a significant influence on surface oxygen dynamics ($\delta^{18}O$ and P/R), both for seasonal and shelfwide cruises. Biological parameters included in the regressions were POC, PON, Chl *a* and molar C:N ratio, and physical parameters were pH, temperature, and

salinity. All independent variables were normally distributed, except concentrations of POC and PON, for which a log-transformation was performed; the p-value for variable inclusion and retention during stepwise regressions was 0.05. Highly correlated independent variables (e.g. POC and PON) were never included into the same model, because after selection of the first independent variable, the second variable did not improve the model fit any further at p 0.05. Hence, the variance inflation factors for all models were always below 2. Accordingly, conclusions that were drawn for POC were most likely applicable to PON as well.

Isotope Analyses

Immediately after return to the laboratory, samples were prepared for analysis by means of headspace equilibration (Chapter 2). A headspace was created by injecting 10 ml of ultra pure helium into inverted bottles while allowing 10 ml of sample water to drain out a small needle. Before injection, the syringe was flushed five times with ultra pure helium to avoid contamination with atmospheric oxygen. Subsequently, samples were stored in the dark at 5 °C for 1 to 4 weeks. To ensure equilibration of the dissolved gases with the headspace, samples were placed in a shaker (100 rpm, room temperature) for at least 12 hours before isotope analyses.

A 8-port Valco switching valve was used to accommodate the two-GC system ((Wissel et al. submitted), whereby the 8-port valve and the second GC were part of a computer controlled gas handling device (GasBench II, ThermoFinnigan). The first GC was upstream of the switching valve and the second GC column was in a loop that could be switched in and out of the main flow. While out of the main flow, the second GC was flushed by a slow flow of helium. CO_2 was retained on the first upstream column, while the other two gases (O_2 and N_2) passed

onto the second, downstream column. Flow paths were then changed to achieve optimal elution of all three gases.

To start the actual analysis, a sample was obtained from the headspace by first injecting an equal amount of helium into the headspace, flushing the syringe (5 mL, BD brand general use, Luer-Lok tip; BD brand needle, precision glide 23G1) five times to mix the headspace and then withdrawing the sample. This headspace-sample gas was then immediately injected through a Supelco septum (Thermogreen LB-2, 6 mm; 20651) into the sample train consisting of a water removal trap filled with magnesium perchlorate, a 2 m GC column (stainless steel, Costech # 051080) for CO_2 separation from N_2 and O_2, and a downstream 2 m GC column (stainless steel, 5 Angstrom mesh size, Costech # 051088) for separating N_2 and O_2. An additional second trap filled 50% with ascarite and 50% with magnesium perchlorate was placed before the second GC column to remove traces of CO_2 and water, respectively, that otherwise could interfere with oxygen and nitrogen isotope measurements. Both GC columns were kept at room temperature.

Carbon dioxide slowly passed onto the first GC column, while oxygen and nitrogen quickly eluted onto the second GC column, which was then switched from a high flowrate (200 mL min^{-1}) to a slow flow of 120 mL min^{-1}. These two gases were effectively parked onto this second, slow-flow column while measurement continued with the carbon dioxide analysis. Switching out the second GC column greatly increased the flow through the first GC column and rapidly eluted the carbon dioxide for isotopic measurement. After completion of the carbon dioxide measurement, the second column was switched back in-line and oxygen and then nitrogen isotope measurements were made sequentially.

The gas analysis system allowed sequential elution of oxygen, nitrogen, and carbon dioxide gases, so that concentrations of dissolved gases could be calculated using the peak areas

of mass 32, 28, and 44, measured respectively in a downstream isotope ratio mass spectrometer (the results of CO_2 analyses will be reported elsewhere). The peak areas were calibrated using laboratory standards prepared in the same manner as samples, but air equilibrated, artificial seawater was used as the water source (Chapter 2). Procedural blanks were prepared in the same way as procedural artificial seawater standards, but to obtain zero-oxygen water, 50 g L^{-1} Na_2SO_3 were added (Kampbell et al. 1989). The average oxygen concentration of zero-oxygen blanks was 0.006 mg L^{-1} (±0.002 standard deviation, $n = 46$). Accordingly, oxygen concentrations and isotopic values for all samples were corrected by subtraction and mass balance, respectively.

The isotope values of oxygen ($\delta^{18}O$ expressed as ‰ relative to standard mean ocean water, SMOW) were determined using a Finnigan Thermoquest Delta plus XP IRMS. I used air as a primary standard (Dole et al. 1954) with a known $\delta^{18}O$ value of 23.5‰ (± 0.14‰ standard deviation, $n = 128$). The saturated artificial seawater used as procedural standard gave the expected $\delta^{18}O$ value of 24.2‰ (± 0.17‰ standard deviation for $\delta^{18}O$, $n = 113$) as well as accurate dissolved oxygen and nitrogen concentrations, whereby the saturation concentrations were calculated according to Weiss (1970) using known temperature and salinity. To investigate the precision of this analyses, I collected replicate samples at various depths throughout the study period ($n = 41$), and average differences for oxygen concentrations and $\delta^{18}O$ values were small at 0.08 mg L^{-1} (± 0.12 standard deviation) and 0.05‰ (± 0.04 standard deviation), respectively.

Because headspace injections were not carried out using high precision syringes, inaccurate injection volumes (± 0.1 mL) sometimes affected the oxygen concentration measurements. Nevertheless, based on the fact that dissolved nitrogen gas is generally inactive and should be close to 100% saturation in water samples, the parallel measurement of oxygen and nitrogen concentrations from the same sample allowed us to calculate the magnitude of over-

or under-estimation of nitrogen gas concentrations due to injection errors in the samples (Chapter 2). This adjustment of oxygen concentrations based on nitrogen saturation levels was made because the correction significantly improved the data so that the laboratory oxygen concentration estimates better matched the field Hydrolab measurements (which were routinely calibrated against Winkler titrations during all cruises). Thus, after these corrections, the r^2 value of calculated O_2 concentrations versus measured Hydrolab values for the 2002 and 2003 shelfwide cruise samples increased overall from 0.97 and 0.91 to 0.99 and 0.93, respectively, while for seasonal sampling along transect C, the r^2 value increased from 0.95 to 0.99.

To obtain a fractionation factor for water column respiration that was representative for this system, I incubated surface water that was collected during three cruises along transect C (October 2002, March and July 2003). The average system-specific fractionation factor for water column respiration was -22.0 ±0.7‰ (Chapter 2).

Modeling Approach

To evaluate oxygen dynamics recorded in the combined measurements of oxygen concentrations and $\delta^{18}O$ values, I developed a finite difference model (Chapter 2) with sequential steps for mixing, fractionation, and air-sea gas exchange (Fry 2006). The mixing pertains to new oxygen added from photosynthesis or gas invasion, and the fractionation pertains to oxygen removed by respiration or gas evasion. Isotope mixing can be understood as a weighted average, while isotopic fractionation for respiration can be described by logarithmic distillation equations (Mariotti et al. 1981). The eight sequential equations used in each time step (1 hour) of the model were as follows:

1. Oxygen Gain during Photosynthesis: $S_{S1} = S_{INITIAL} + C_P$
2. Isotope Mixing during Photosynthesis: $\delta_{S1}S_{S1} = \delta_{INITIAL}S_{INITIAL} + \delta_P C_P$

3. Oxygen Gain during Invasion: $S_{S2} = S_{S1} + C_I$

4. Isotope Mixing during Invasion: $\delta_{S2}S_{S2} = \delta_{S1}S_{S1} + \delta_I C_I$

5. Oxygen Loss during Respiration: $S_{S3} = S_{S2} - C_R$

6. Isotope Fractionation during Respiration: $\delta_{S3} = \delta_{S2} + \varepsilon_R \ln((S_{S2} - C_R)/S_{S3})$

7. Oxygen Loss during Evasion: $S_{S4} = S_{S3} - C_E$

8. Isotope Fractionation during Evasion: $\delta_{S4} = \delta_{S3} + \varepsilon_E \ln((S_3 - C_E)/S_4)$

where δ is the $\delta^{18}O$ value, S is % saturation of oxygen, ε_R and ε_E are the fractionation factors (negative in sign, Mariotti et al. 1981) associated with respiration and evasion, C is the change in oxygen saturation associated with photosynthesis, respiration, or air-sea gas transfer, and subscripts are as follows: P = new oxygen added from photosynthesis, I = new oxygen added by invasion, R = oxygen removed by respiration, E = oxygen removed by evasion. To complete the parameterization of these models, I selected the following values: $\delta^{18}O$ value of -2‰ for new photosynthetic oxygen (based on average salinity of 30, assuming mixing of Mississippi River water with a value of -7‰ (Kendall, personal communication) with full strength salinity water of 0‰), $\delta^{18}O$ value of 24.2‰ for invading atmospheric oxygen (Benson & Krause 1984, Knox et al. 1992), ε_R = -22‰ for respiration in surface waters (average value from three incubation experiments, see above), ε_R = 0‰ for respiration in sediments (Brandes & Devol 1997), and ε_E = -3.5‰ (derived from data presented in Knox et al. 1992).

Model runs typically started from initial conditions of 100% oxygen saturation and 24.2‰ $\delta^{18}O$ set by equilibration with the atmosphere. The equations were propagated over 100-10000 time intervals (hours) using incremental changes in concentration for photosynthesis, (C_P), respiration, (C_R), and air-sea gas exchange (C_I and C_E), and resulting curves were fit to experimental data (shown in Figures 3.5 and 3.12 below).

These finite difference models were used to estimate P/R ratios (hereafter, P/R) in surface waters, and respiration dynamics in bottom waters. To estimate P/R for individual samples of surface water, I started from a fixed point of air-equilibrated seawater (100% saturation, 24.2‰ $\delta^{18}O$). The respiration rate was held constant at 0.07 mg O_2 L^{-1} h^{-1}, which was the average decrease in O_2 concentration during three consecutive nights (PAR = 0) during the July 2001 shelfwide cruise (Chapter 2). Air-sea gas exchange is dependent on oxygen saturation levels and wind speed (Stigebrandt 1991), which was 3.4 and 4.0 m sec^{-1} during the shelfwide cruises in July 2002 and 2003, respectively. Average wind speeds during seasonal surveys along transect C (September 2002 to June 2003) ranged from 2.9 m sec^{-1} in June 2003 to 7.8 m sec^{-1} in February 2003. Wind speed readings for all cruises were taken from station BURL1 (NOAA National data Buoy Center) just to the west of the Mississippi River Southwest Pass.

I found little evidence for benthic photosynthesis or gas exchange with the upper water column for bottom waters in the sampling area (Chapter 2), and I refocused this model to estimate fractionations associated with respiration only, assuming benthic photosynthesis and gas exchange to be zero. This respiration-only formulation of the model generated curves from a starting point of air-equilibrated seawater (100% saturation, 24.2‰ $\delta^{18}O$) that intersected individual data points depending on the fractionation factor used during respiration (ε_R in equation 6 above). Estimates of the individual ε_R fractionation factors were used to partition the sources of respiration, with sediment respiration expected to occur with no fractionation, and respiration in bottom waters expected to occur with a fractionation of -22‰. Thus, the estimated ε_R values were intermediate between 0‰ ($\varepsilon_{benthic}$) and -22‰ ($\varepsilon_{water\ column}$) with values closer to 0‰ indicating stronger sediment respiration, according to the formula:

$$\%\ \text{benthic respiration} = 100 * (\varepsilon_{observed} - \varepsilon_{water\ column}) / (\varepsilon_{benthic} - \varepsilon_{water\ column})$$

RESULTS

Seasonal Trends

Surface Waters

Oxygen patterns in surface waters in monthly intervals between July 2001 and July 2003 were highly variable (Figure 3.2). Generally, wind speeds were higher in the fall and winter, when cold fronts were frequent. Even though summer conditions were typically calm, hurricanes and tropical storms in October 2002 and early July 2003 disrupted this pattern.

Surface salinity (as a proxy for nutrient availability) was mostly lower at onshore stations than at offshore stations, and during fall and winter there was an overall increase of salinity. Additionally, during high wind events (e.g. October 2002), I also found an increase in salinity, whereby the addition of high salinity water could have been either from offshore or bottom waters or both.

Particulate organic carbon (POC) concentrations were always higher at inshore stations compared to offshore stations (Figure 3.2). Seasonally across transect C, I found the maximum POC concentrations in March and July of both years. Overall, POC seemed to be a good indicator for algal concentrations as C:N ratios were mostly between 6 and 8, close to the Redfield ratio of 6.6. This was further confirmed by correlation analysis between POC and Chl *a* concentrations (Rabalais, unpubl. data), because r^2 values for seasonal sampling and shelfwide cruises in 2001, 2002 and 2003 were 0.81, 0.83, and 0.61, respectively.

Oxygen saturation and $\delta^{18}O$ values for transect C between July 2001 and July 2003 were well correlated ($r^2 = 0.82$). Lowest $\delta^{18}O$ values (and highest saturation levels) were frequently found in spring and summer when POC concentrations were high.

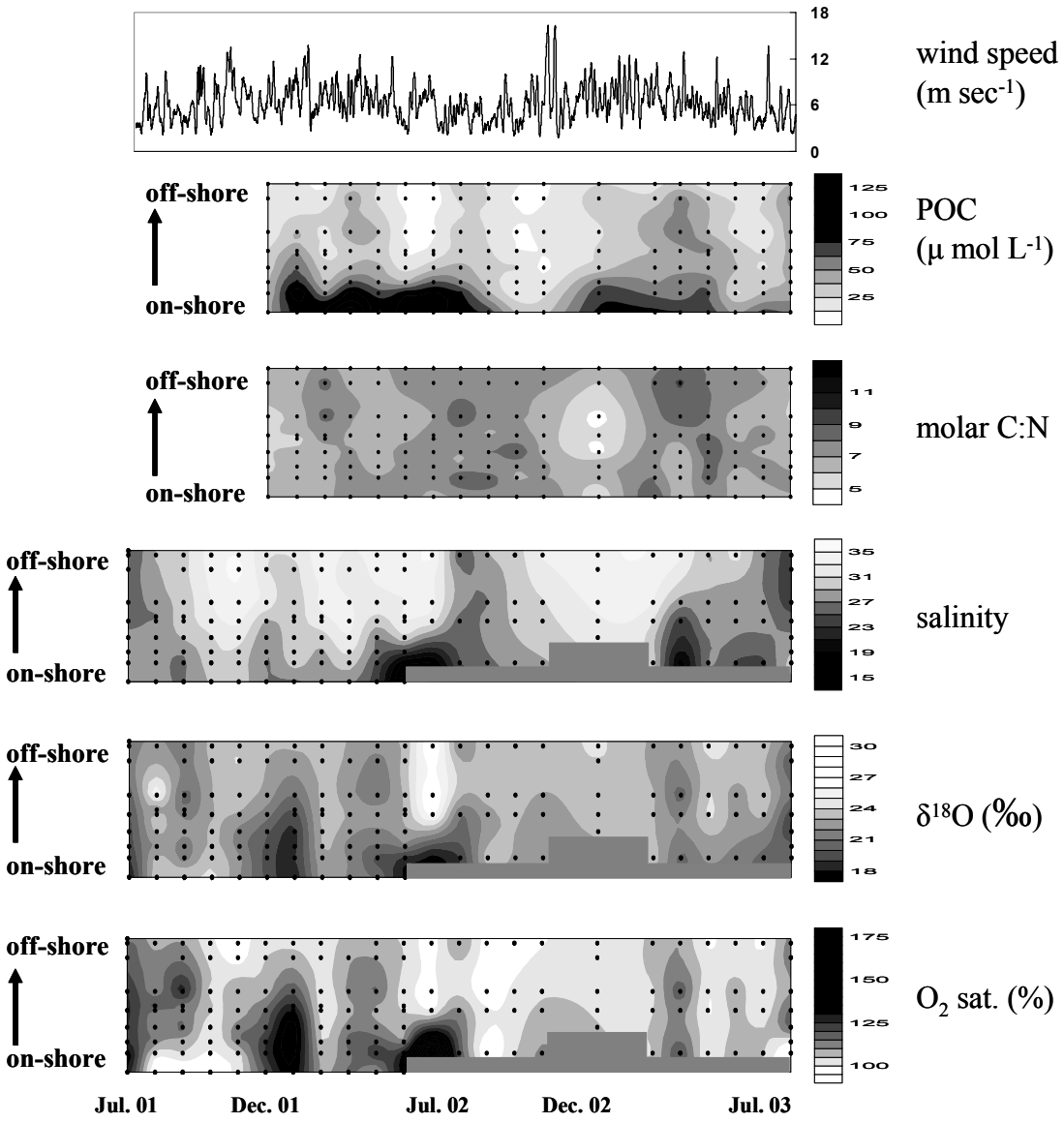

Figure 3.2 Wind speed (m sec^{-1}), POC concentration (µmol L^{-1}), salinity, oxygen saturation (%) and $\delta^{18}O$ (‰) for surface samples for transect C, August 2001 to June 2002.

Stepwise multiple linear regression identified POC as the single most important predictor for $\delta^{18}O$ values along transect C ($r^2 = 0.45$, Tab. 3.1). Additional significant parameters ($p < 0.05$) were C:N and salinity, whereby C:N and salinity were positively correlated with $\delta^{18}O$ (adj. $r^2 = 0.58$). Hence, a large addition of photosynthetic oxygen to the ambient oxygen pool (low

$\delta^{18}O$) was correlated with high POC (inferred algal concentration), low C:N (higher algal component, less detritus or sediment), and low salinity (as proxy for nutrients). The remaining independent variables (surface temperature, pH, and particulate organic nitrogen (PON)), were not included into the stepwise regression models ($p > 0.05$). PON by itself was significantly correlated with $\delta^{18}O$ but was not included into the regression because POC was a slightly better predictor of $\delta^{18}O$ values, and after inclusion of POC into the regression, PON did not have a significantly contribution to the regression models.

Additional information about physical and biological factors that were responsible for the observed oxygen dynamics was obtained from the P/R calculations for surface waters along transect C between July 2002 and July 2003. P/R values generally varied from 0.9 to 1.1, but higher values (up to 2.0) were observed in July and September of 2002 and in March and July of 2003. At these times, oxygen saturations frequently exceeded 110%. In contrast, P/R values slightly below 0.9 were found in August 2002 and in April 2003 when oxygen levels were at or slightly below saturation. Stepwise multiple linear regression was used to test which environmental variables, beyond oxygen concentrations and $\delta^{18}O$ as input parameters for P/R calculations, affected P/R. This analysis showed that higher POC and lower C:N were significantly correlated ($p < 0.05$) with P/R, even though the adjusted $r^2 = 0.15$ was fairly low (Table 3.1).

Bottom Waters

In bottom waters along transect C, strong oxygen depletion (< 20% saturation) was observed in summer months of 2002 and 2003. Oxygen depletion was associated with high $\delta^{18}O$ values, which often exceeded 40‰ (Figure 3.3). During the remainder of the year, oxygen saturations were mostly above 80% and $\delta^{18}O$ values were below 30‰, closer to equilibrium with

the atmosphere. The relationship between oxygen concentration and $\delta^{18}O$ in bottom waters was much stronger for winter months (October through March, $r^2 = 0.97$) than for summer months (April through September, $r^2 = 0.77$; Figure 3.4). Furthermore, net fractionation of bottom water respiration was much lower in the summer (-5.6‰) than in the winter (-12.8‰). Assuming that the fractionation factor of water column respiration was -22‰ (see Methods section), benthic respiration was responsible for 42 and 75% of the total oxygen uptake during winter and summer months, respectively.

Table 3.1 Results for stepwise multiple linear regressions for $\delta^{18}O$ and P/R as dependent variables for seasonal sampling and the shelfwide cruises in July 2002 and 2003. Independent variables were POC, PON, C:N, salinity, temperature, and pH. Variable selection (forward) and variable retention were both at $p < 0.05$

Seasonal transects (July 2001 to July 2002)	
$\delta^{18}O = 18 - 0.05$ POC $+ 0.53$ C:N $+ 0.12$ salinity	adj. $r^2 = 0.58$
P/R = 2 + 0.006 POC – 0.15 C:N	adj. $r^2 = 0.15$
Shelfwide cruise 2002	
$\delta^{18}O = 28 - 0.03$ POC $+ 0.65$ C:N	adj. $r^2 = 0.72$
P/R = -20 - 0.23 C:N + 2.3 pH	adj. $r^2 = 0.23$
Shelfwide cruise 2003	
$\delta^{18}O = 25 - 0.08$ POC $+ 0.28$ C:N	adj. $r^2 = 0.70$
P/R = -10 - 0.01 C:N + 0.1 pH	adj. $r^2 = 0.26$

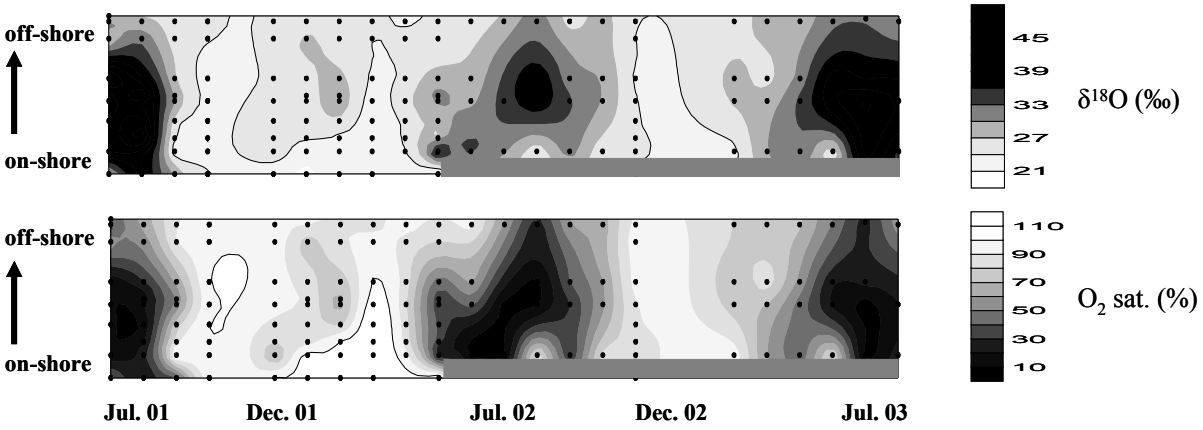

Figure 3.3 Oxygen saturation (%) and $\delta^{18}O$ (‰) for bottom samples for transect C, July 2001 to June 2003. The black reference lines represent air-equilibrated values.

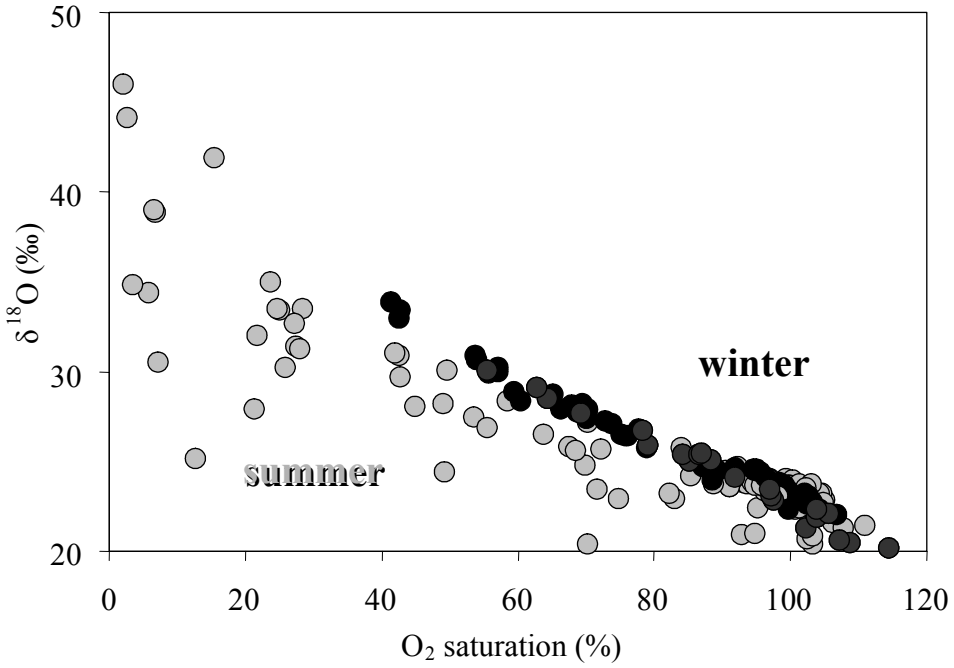

Figure 3.4 Relationship between oxygen saturation (%) and $\delta^{18}O$ (‰) for bottom water samples collected during winter months (October to March, black circles) and summer months (April to September, grey circles) for transect C between July 2001 and July 2003.

Depth Profiles

The analysis of vertical profiles of oxygen saturation and $\delta^{18}O$ along transect C between July 2002 and July 2003 indicated that surface waters were fairly homogeneous down to a water depth of 5 to 10 m (Figures 3.5 and 3.6). During summer, oxygen gradients were strong, ranging from 125% saturation ($\delta^{18}O < 20‰$) near the surface to almost zero ($\delta^{18}O > 40‰$) in bottom waters. In winter months, vertical oxygen gradients were generally weak, and in December 2002 the water column was well mixed. Although low oxygen saturations sometimes extended higher into the water column, oxygen saturations below 20% ($\delta^{18}O > 30‰$) were always restricted to within 5 m of the bottom.

Shelfwide Summer Cruises 2002 and 2003

Surface Waters

In July 2002, the spatial patterns of surface salinity, POC concentration, and $\delta^{18}O$ values were very similar (Figure 3.7, O_2 saturation is not shown here as it was highly correlated with $\delta^{18}O$, $r^2 = 0.82$). The lowest salinities were found to the west of the Mississippi and Atchafalaya Rivers. Low salinities were also observed on a number of stations located across the Louisiana shelf between the Mississippi and the Atchafalaya Rivers. The good correspondence between spatial patters of salinity, POC, and $\delta^{18}O$ values indicates the close coupling between the riverine nutrient inputs, nutrient enhanced primary productivity and biomass of phytoplankton on the Louisiana shelf. Stepwise multiple linear regression identified POC as the most important predictor for $\delta^{18}O$ ($r^2 = 0.66$, Table 3.1). C:N was the only other significant variable ($p < 0.05$) included into the regression (adj. $r^2 = 0.72$); low C:N indicated higher primary production (lower $\delta^{18}O$). PON and salinity were also significant as individual parameters, but inferior to POC and were not a significant contribution to the stepwise multiple regression after POC was included.

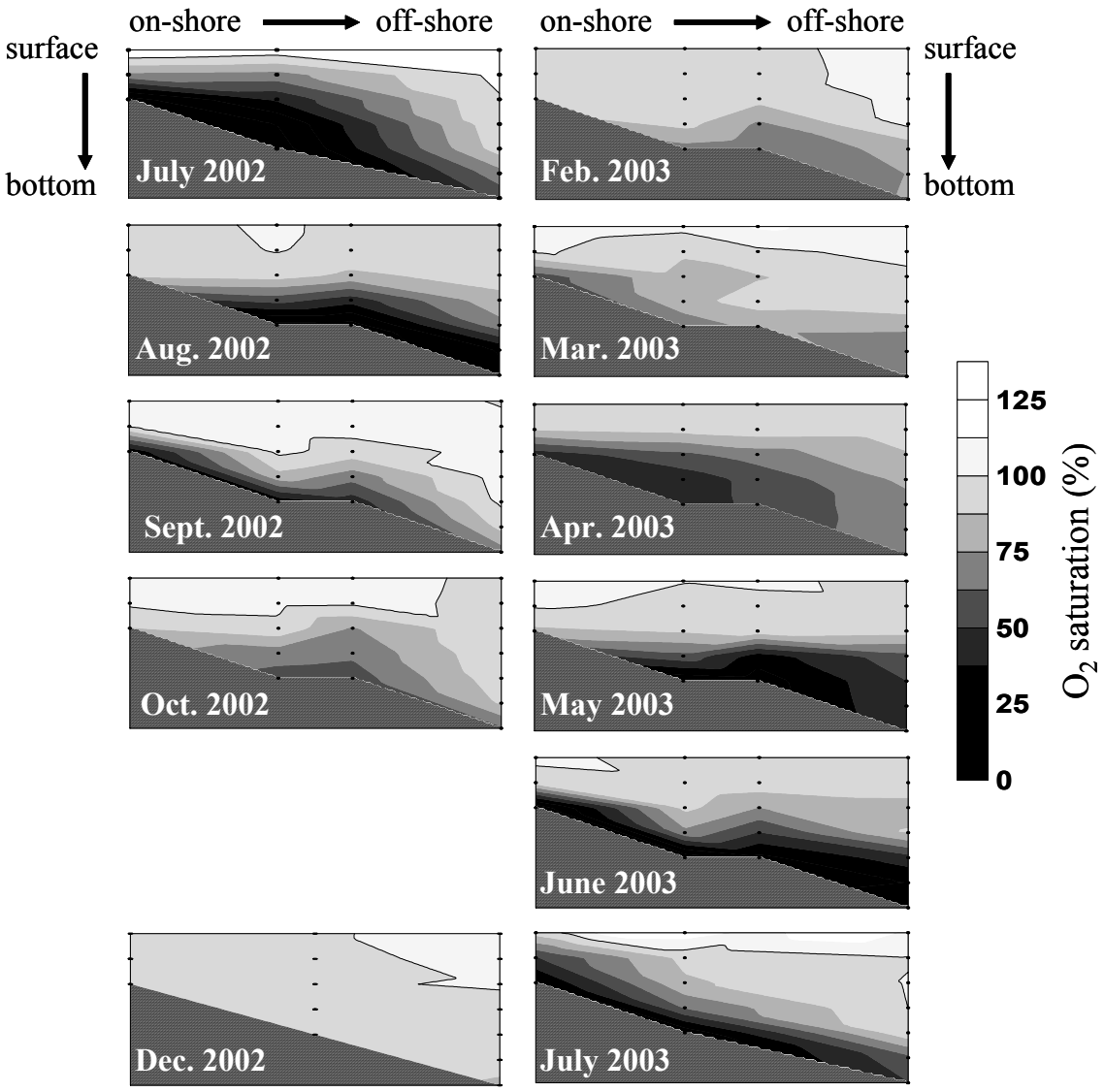

Figure 3.5 Depth profiles (5 m intervals) for oxygen saturation (%) for transect C between July 2002 and July 2003. The black reference lines represent air-equilibrated values.

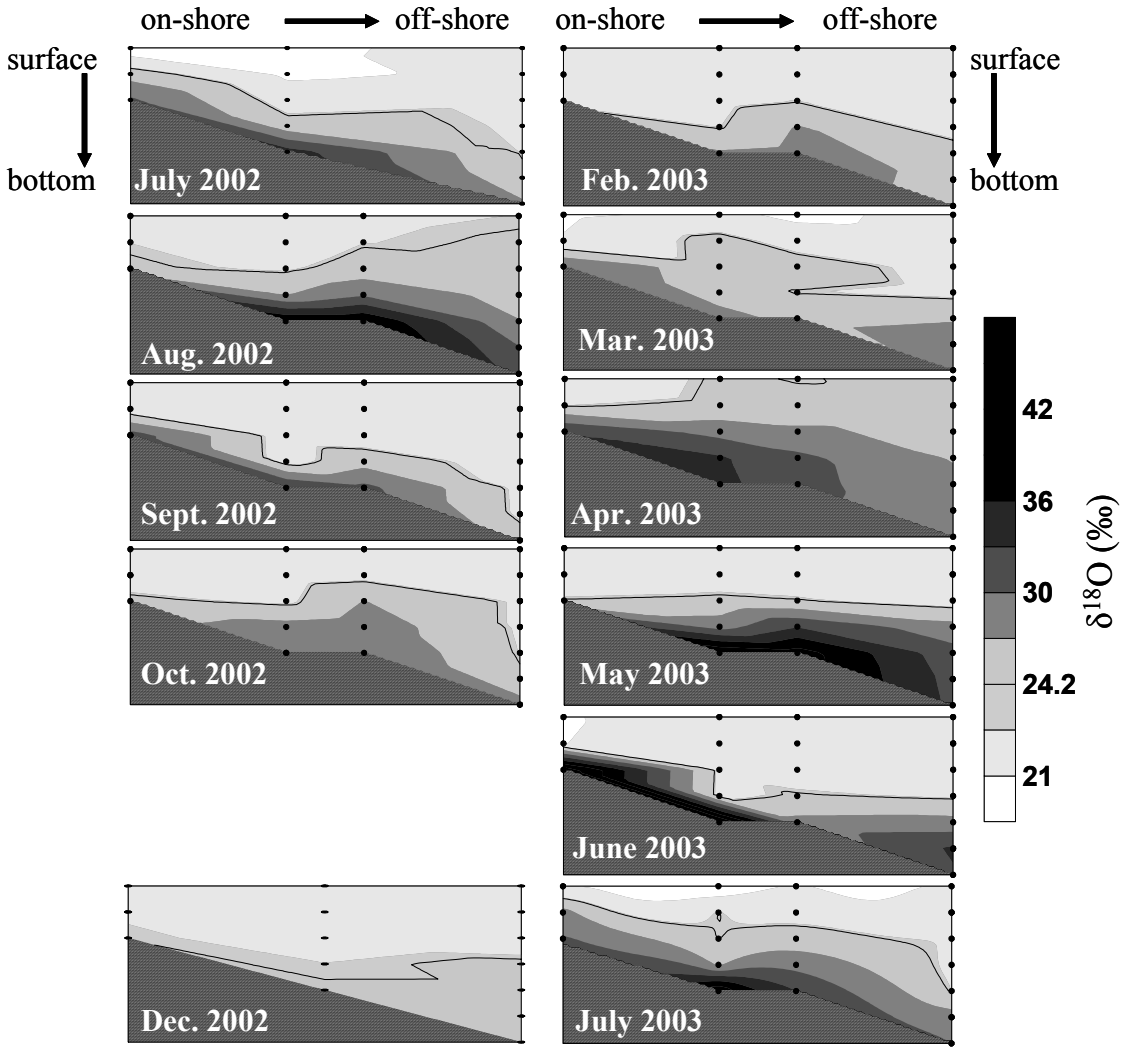

Figure 3.6 Depth profiles (5 m intervals) for $\delta^{18}O$ (‰) for transect C between July 2002 and July 2003. The black reference lines represent air-equilibrated values.

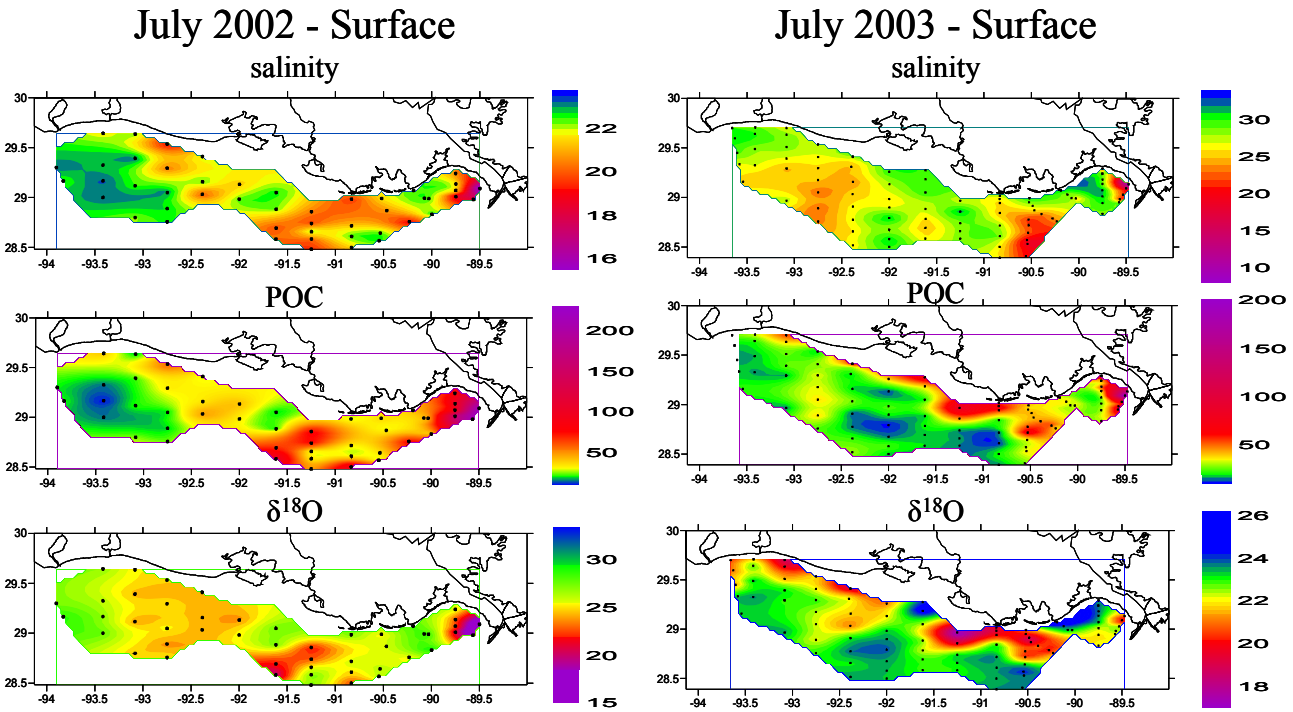

Figure 3.7 Surface salinity, POC (μmol L^{-1}), and $\delta^{18}O$ (‰) for surface samples collected during the shelfwide cruises in July 2002 and 2003. Black circles show the sampling grid.

In July 2003, spatial patterns of POC and $\delta^{18}O$ were similar with maxima close to the Mississippi River delta and across extended onshore areas (Figure 3.7). POC was again the most important predictor of $\delta^{18}O$ (r^2 of 0.60), while $\delta^{18}O$ and O_2 % had an r^2 of 0.71. The spatial pattern of salinity, however, was noticeably different with lowest salinities near the Mississippi River delta but also across large offshore areas east and west of the Atchafalaya River. Consequently, while C:N was selected again as second most important parameter in the stepwise regression (adj. $r^2 = 0.70$), salinity was not significant as an individual parameter ($p > 0.05$) (Table 3.1). Contrary to July 2002, low salinity in July 2003 was not a good proxy for nutrient availability.

In July 2002, P/R values in surface waters exceeded 1.0, except at the most western portion of the study area (Figure 3.8). Consistent with the observed patterns of POC and $\delta^{18}O$,

the highest values of P/R were found just to the west of the Mississippi and Atchafalaya Rivers. The median P/R value for the 2002 shelfwide cruise was 1.11, and the 10th and 90th percentile were 1.00 and 1.34 respectively (Table 3.2). Stepwise multiple regression identified C:N (negative factor) and pH (positive factor) to be significantly correlated with surface P/R ($p < 0.05$; adj. $r^2 = 0.23$, Table 3.1). Depth-stratified sampling also allowed us to calculate P/R for subsurface samples collected from the mixed layer (5 - 10 m). P/R at the depth of 5 m were 0.91, 0.99, and 1.08 for 10th percentile, median, and 90th percentile, respectively. At the depth of 10 m, 10th percentile, median, and 90th percentile of P/R were 0.71, 0.93, and 1.03, respectively. Assuming similar conditions as in 2001 (fractionation factor of respiration of -22‰ and a respiration rate of 0.07 mg O_2 L^{-1} hr^{-1}, Chapter 2), a P/R of 1.11 (median) would translate into net primary production (NPP) of 0.06 g C m^{-3} day^{-1} and P/R of 1.34 (90th percentile) would result in NPP of 0.18 g C m^{-3} day^{-1}.

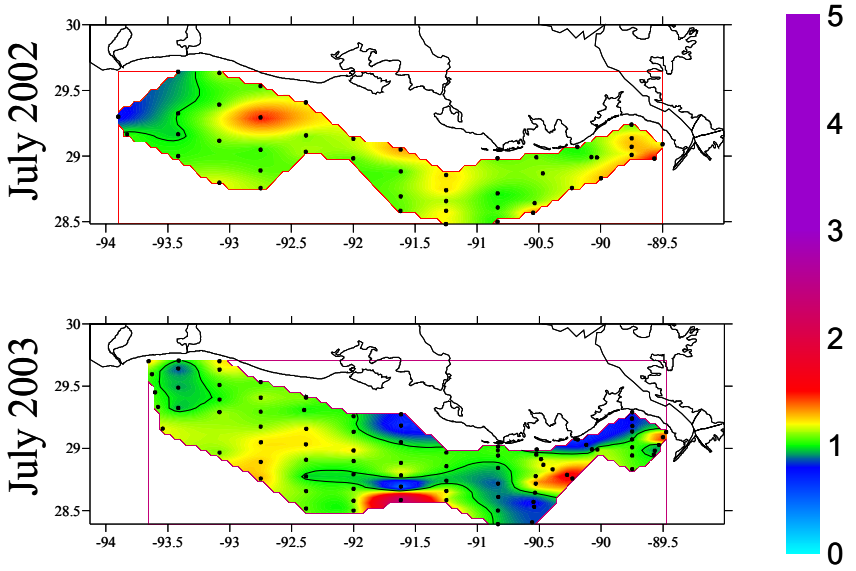

Figure 3.8 P/R for surface samples collected during the shelfwide cruises in July 2002 and 2003. Black circles show the sampling grid.

Table 3.2 Model results of P/R for fractionation factors (ε) of 18 and 22‰. Respiration rate was held constant at 0.07 mg O_2 L^{-1} h^{-1} for all scenarios.

Fractionation factor			**Fractionation factor**			**Fractionation factor**		
C transect	**18‰**	**22‰**						
10th %ile	0.75	0.87						
25th %tile	0.89	0.94						
Median	1.08	1.02						
75th %ile	1.37	1.12						
90th %tile	2.96	1.5						
July 2002 surface	**18‰**	**22‰**	**July 2002 5 m**	**18‰**	**22‰**	**July 2002 10 m**	**18‰**	**22‰**
10th %tile	1.01	1.00	10th %tile	0.83	0.91	10th %ile	0.49	0.71
25th %tile	1.10	1.03	25th %tile	0.90	0.96	25th %tile	0.69	0.84
Median	1.27	1.11	Median	0.96	0.99	Median	0.83	0.93
75th %ile	1.44	1.17	75th %ile	1.05	1.03	75th %ile	0.91	0.97
90th %tile	1.78	1.34	90th %tile	1.14	1.08	90th %tile	1.06	1.03
July 2003 surface	**18‰**	**22‰**	**July 2003 5 m**	**18‰**	**22‰**	**July 2003 10 m**	**18‰**	**22‰**
10th %ile	0.77	0.88	10th %ile	0.69	0.84	10th %ile	0.66	0.82
25th %tile	0.90	0.96	25th %tile	0.77	0.89	25th %tile	0.68	0.84
Median	1.11	1.04	Median	0.90	0.95	Median	0.85	0.93
75th %ile	1.38	1.18	75th %ile	1.10	1.04	75th %ile	0.93	0.97
90th %tile	2.02	1.35	90th %tile	1.33	1.16	90th %tile	1.00	1.00

In July 2003, P/R values were below 1.0 at a number of stations, even though the majority of the study area still had P/R values above 1.0. The spatial pattern of P/R was somewhat irregular but mostly followed oxygen dynamics for most of the area. The median P/R value for the 2003 shelfwide cruise was 1.04, and the 10^{th} and 90^{th} percentile were 0.88 and 1.35 respectively (Table 3.2). Similar to 2002, stepwise multiple regression identified C:N (negative) and pH (positive) to be significantly correlated with surface P/R ($p < 0.05$; adj. $r^2 = 0.26$). Subsurface P/R at a water depth of 5 m were 0.84, 0.95, and 1.16 for 10^{th} percentile, median, and 90^{th} percentile, respectively (Table 3.1). At a water depth of 10 m, 10^{th} percentile, median, and 90^{th} percentile of P/R were 0.82, 0.93, and 1.00, respectively. With respect to NPP, median and 90^{th} percentile of P/R would result in values of 0.06 and 0.18 g C m^{-3} day^{-1}, respectively.

Bottom Waters

In July 2002, the largest areal extent of hypoxia on record was measured (22,000 km^2, Rabalais and Turner 2006, Turner et al. 2006). Oxygen concentrations in bottom waters were below 2 mg O_2 L^{-1} over most of the study area, and $\delta^{18}O$ values were mostly above 30‰ (Figure 3.9). Only a limited number of onshore and offshore stations had higher oxygen concentration. In July 2003, the areal extent of hypoxia was much smaller than in 2002. Hypoxia was limited to three regions with water depth of less than 20 m, namely, the vicinity of the birdfoot delta and two areas centered approximately 100 km to the east of the Mississippi and the Atchafalaya Rivers, respectively. The net fractionation factor for respiration in bottom waters was much smaller in July 2002 (-4.1‰) than in July 2003 (-8.7‰), indicating that benthic respiration in bottom waters was responsible for 81% of the total oxygen demand, compared to only 60% in 2003. The spatial patterns of benthic versus water column respiration for 2002 showed that at onshore stations within water depths of 20 m the contribution of benthic respiration was higher

than at offshore stations (Figure 3.9). An exception to this pattern was the central area at which oxygen concentration in bottom waters at offshore stations were fairly high. In July 2003, most offshore stations in the mid- to western part of the continental shelf had large contributions of benthic respiration.

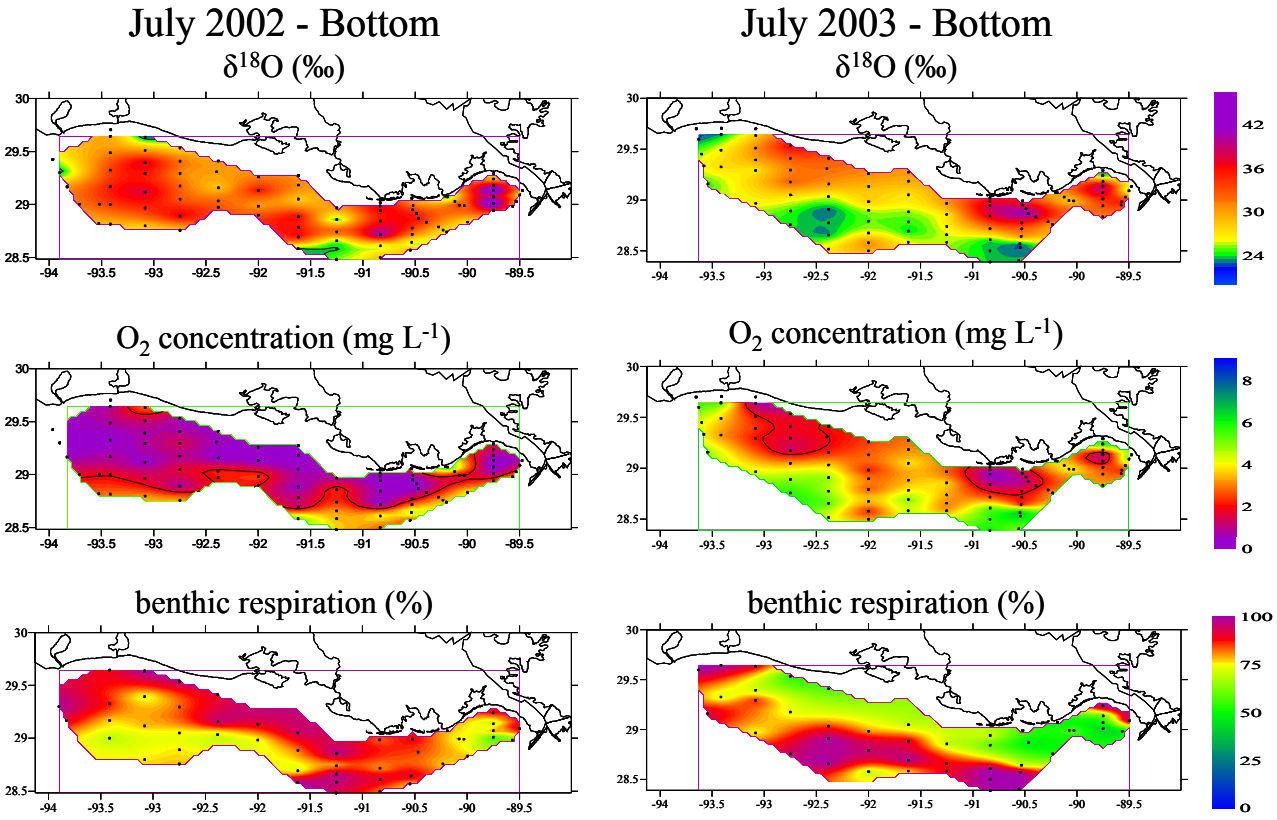

Figure 3.9 Oxygen saturation (%), $\delta^{18}O$ (‰), and spatial distribution of benthic respiration for bottom samples collected during the shelfwide cruises in July 2002 and 2003. Values for benthic respiration were obtained from a mixing model (see Methods), with 100% water column respiration consistent with a -22‰ respiratory fractionation and 100% benthic respiration consistent with 0‰ fractionation. Black circles show the sampling grid.

DISCUSSION

Seasonal and Inter-annual Variability of $\delta^{18}O$ in Surface Waters

For both seasonal (transect C) and inter-annual analyses (shelfwide cruises 2002 and 2003), POC was the single most important parameter for $\delta^{18}O$ values of these simple linear regressions, explaining about half to two-thirds of the total variability. The intercepts (at POC = 0) of these simple linear regressions were not significantly different from 24.2‰, the $\delta^{18}O$ value that represents a purely physical system (Dole et al. 1954). This regression result emphasized that in the absence of algae, continental shelf waters were in equilibrium with the atmosphere with no contributions from primary production or respiration. After POC, the second parameter entering the stepwise regressions was C:N for all surface water analyses. Hence, low $\delta^{18}O$ values due to the addition of photosynthetic oxygen were associated with high POC concentrations and low C:N ratios, where lower C:N denotes a larger algal contribution to POC (Wang et al. 2004, Wissel et al. 2005). For seasonal surveys, salinity was significantly correlated with $\delta^{18}O$ as well. Because there is no known direct effect of salinity on $\delta^{18}O$, this is probably due to the fact that higher nutrient concentrations are typically associated with lower salinity.

Calculated P/R values provided additional information about surface productivity in the northern Gulf of Mexico. As P/R was derived from oxygen concentrations and $\delta^{18}O$, it was not surprising that spatial and temporal pattern of P/R were similar to those of oxygen dynamics, which was statistically not explored any further due to autocorrelation of the parameters. With respect to additional environmental parameters, P/R was significantly correlated to POC (positive) and C:N (negative) for seasonal sampling along transect C, verifying the regression results for $\delta^{18}O$ dynamics (see above). Accordingly, when P/R was larger than 1.1, oxygen dynamics suggested high productivity, e.g., July 2002, and March and July 2003. P/R values

below 0.9 were associated with lower oxygen saturation and higher $\delta^{18}O$ values (August 2002 and April 2003).

The absolute values of P/R and productivity are to some extent dependent on the fractionation factor (ε) during respiration (Chapter 2). While spatial patterns are not affected, lower ε-values will result in higher P/R and productivity estimates when P/R is larger than 1, and in lower estimates when P/R is smaller 1. Even though my three independent estimates for ε were very close to -22‰, I explored the effects of ε-values of -18 and -25‰, because these values have been used in previous studies (Kroopnick 1975, Quay et al. 1995, Luz et al. 2002, Hendricks et al. 2004, Chapter 2). The ε -values of -25‰ did not seem reasonable for either seasonal transects or summer cruises in this study, because the actual values for most stations were outside of possible solutions for the P/R model for ε = -25‰. In contrast, the P/R model performed well for the lower fractionation factor of -18‰. For surface samples, P/R and productivity were moderately higher than reported for ε = -22‰, while for subsurface samples values were slightly lower (Table 3.2). At this point the P/R model generates estimates for P/R and productivity (Chapter 2), which will have to be validated in future parallel in-situ incubations using light-dark bottles or metabolic tracers such as ^{14}C or ^{18}O (Grande et al.1989, Lohrenz et al. 1999).

Generally, regression models for both $\delta^{18}O$ and P/R indicated that seasonal dynamics of surface oxygen across the Louisiana continental shelf could be largely explained by biological activity, which was likely controlled by nutrient inputs from the Mississippi and Atchafalaya Rivers (Turner et al. 2006). As indicated previously, seasonal temperature changes were not an important factor for oxygen dynamics during the duration of this study. Overall, the effects of

physical factors were less visible, except during strong physical disturbances, such as the passages of cold fronts in the winter and tropical storms and hurricanes during summertime.

Seasonal Trends in Bottom Waters

Seasonality in oxygen cycling in bottom waters along transect C was much stronger than in surface waters. Although biological and chemical oxygen demands are higher in the summer due to increased temperatures (Rowe et al. 2002), probably more important for the onset of hypoxia was the stratification of the water column during this time (Rabalais and Turner 2001). Nevertheless, even in winter months moderate oxygen depletion was possible as shown by low oxygen saturation (67%) and high $\delta^{18}O$ values (35‰) in February 2002. During this time, wind speeds were neither unusually low nor was the water column stratification stronger than during adjacent months (Rabalais, unpubl. data). Instead, the exceptionally high surface phytoplankton biomass in the preceding month should have resulted in a large flux of sedimenting organic particles to bottom waters. Similar time-lags were observed between high productivity in surface waters during spring of 2002 and 2003 and the beginning of oxygen depletion in bottom waters in early summer of 2002 and 2003 and are consistent with modeling results of Justić et al. (1993).

In addition to the strong contrast in oxygen dynamics between summer and winter months, I also found very distinct patterns for benthic versus water-column respiration among seasons. Despite considerable overlap in oxygen saturations, the contributions of benthic respiration in bottom waters in the summer were noticeably larger and more variable than during winter. Therefore, it appears that larger contributions of benthic respiration are generally associated with a strongly stratified water column.

Depth-stratified Sampling

A previous study analyzed oxygen dynamics in surface and bottom waters across the Louisiana continental shelf between July 2001 and June 2002 (Chapter 2), assuming that surface and bottom samples would represent upper and lower water column, respectively during summer stratification. Because vertical gradients in this area are known to be strong (Wiseman et al. 1997), I wanted to evaluate how well the previous simplified sampling design would represent oxygen dynamics throughout the water column. This study indicated that surface waters were fairly homogeneous to a depth of 5 to 10 m, especially in summer months. Similar conclusions were also derived by Lohrenz et al. (1999), who reported mixing depths of about 10 m for a number of summertime surveys across the Louisiana continental shelf. Nevertheless, P/R estimates showed that P/R was larger than 1 only in surface waters. At a depth of 5 m, production and respiration were roughly the same, and at 10 m depth, P/R was slightly less than 1, indicating that respiration was exceeding primary production. Consequently, extrapolating primary production estimates from surface samples over a mixed layer of about 10 m would overestimate productivity of the study area. Respiration was likely high throughout the water column because of the large concentration of organic material, and decreasing primary production with increasing depth due to light adsorption and shading likely caused P/R to drop below 1 within 10 m of the surface.

With respect to oxygen dynamics in bottom waters, I observed that hypoxic conditions usually did not extend more than 5 m up into the water column. This was not surprising for the summer survey in 2003 when hypoxia was not well established due to the preceding tropical storm Bill. During the summer survey in 2002 the areal extent of hypoxia was large, and oxygen re-supply from the upper water column was probably small due to intense stratification, but

hypoxia still did not extend more than 5 m up into the water column. It appears that respiration was less intense in the overlaying water column than near the sediment surface, where both benthic and water-column respiration were active. In support of this assumption, much higher respiration rates (based on ATP measurements) in bottom waters relative to the overlaying water column were previously documented by Dortch et al. (1994) in this area. The shallow water column of less than 40 m reduces the residence time of sedimenting organic material in the water column, and therefore, most material accumulates on the sediment surface (Rabalais and Turner 2001). This would also explain the overwhelming contribution of benthic respiration in bottom waters during summer months. However, Rabalais and Turner (2001) and Rabalais et al. (2002b) showed that at times hypoxia can extend well up into the water column, encompassing as much as 50 to 80% of the water column below a shallow pycnocline. Encountering such a scenario in future surveys would allow the calculation of benthic to total respiration under hypoxic conditions in the water column versus bottom waters.

Depth stratified sampling illustrated that focusing on surface and bottom water samples (e.g. Chapter 2) is an oversimplification of the oxygen dynamics across the Louisiana continental shelf. Nevertheless, for studies that focus on exploring extent and dynamics of hypoxia, it might be sufficient to rely on bottom water samples because hypoxia usually does not extend beyond 5 m above the sediments. In contrast, productivity and P/R estimates for the upper water layer should be conducted in a depth-integrated fashion to obtain better delineation of water column processes.

2002 vs. 2003 Summer Shelfwide Cruises

Surface Waters

The two summer comparison showed median P/R values were higher in July 2002 (1.11) than in July 2003 (1.04), which corresponded to net primary production (NPP) rates of 0.06 and 0.02 mg C m^{-3} day^{-1}, respectively. In subsurface samples (5 and 10 m), I detected a similar trend of higher P/R in 2002. Surface P/R and NPP for the 2001 shelfwide cruise (1.12 and 0.06 mg C m^{-3} day^{-1}, respectively; Chapter 2) were almost identical to the 2002 survey. The magnitude of riverine nutrient flux was comparable in 2001, 2002, and 2003 (Turner et al. 2006), but in 2003 the study area was affected by tropical storm Bill (Figure 3.2). Thus, it is likely that this major disturbance was responsible for the reduced surface productivity.

With respect to spatial patterns, the P/R values in both the 2002 and 2003 summer surveys closely followed POC concentrations. There was a striking difference with respect to the relationship between salinity, POC, and oxygen in the two years. In 2002, spatial patterns of salinity (proxy for nutrients flux), POC (algae), and oxygen (productivity) were similar. During 2003, only POC and oxygen dynamics were correlated, while salinity showed a very different spatial pattern. It appears that the physical disturbance of the water column due to tropical storm Bill was followed by a short-term un-coupling of freshwater supply from the Mississippi River and algal productivity across the continental shelf. Prior to the tropical storm, the water column was stratified whereby bottom waters were characterized not only by high salinity but also by high nutrient concentrations. Intense mixing might have brought nutrient-rich, high-salinity waters from the lower water column to the surface and stimulated enhanced primary production. This temporal co-occurrence of full-strength-salinity and nutrient–rich water would have negated the otherwise good correspondence of low salinity and high nutrients for a brief period.

Bottom Waters

The predicted bottom-water areas of hypoxia for the shelfwide cruises in July 2002 and July 2003 were very similar, because both years had comparable nutrient loads that were related to Mississippi River discharge (Turner et al. 2006). Yet, while in 2002 the largest hypoxic area on record was observed (22,000 km^2, Rabalais and Turner 2006), in 2003 only about 5,000 km^2 had bottom water oxygen concentrations of less than 2 mg L^{-1} (Rabalais et al. 2006). The passage of tropical storm Bill in early July 2003, just weeks before the survey, stirred up the water column and re-oxygenated bottom waters that previously were hypoxic. At the time of the survey, however, stratification was re-established locally and respiration in bottom waters was sufficient to deplete oxygen concentrations below 2 mg L^{-1}. This was evident in three small areas across the shelf, namely in the vicinity of the birdfoot delta, and the two areas approximately 100 km to the east of the Mississippi and the Atchafalaya Rivers. With respect to the long term record, these three areas have been hypoxic over 75% in summer for the period of 1985 to 2005 (Rabalais et al. 2007). Surface primary production that was newly produced after the passage of tropical storm Bill was probably not responsible for this oxygen depletion, as 2-weeks time would not have allowed for organic material to have reached the sediment and caused severe oxygen depletion. More likely, the sediment concentrations of organic material in these three areas were already high due to intense surface production during the months preceding tropical storm Bill.

Beside the much smaller areal extent of hypoxia in July 2003, the contribution of benthic respiration was reduced as well. During the shelfwide cruises in July 2001 and 2002 benthic respiration was 73 and 81%, respectively, compared to only 60% in July 2003, when stratification of the water column was disrupted shortly before sampling. This pattern was in

good agreement with the results from seasonal surveys, where benthic contributions to respiration in bottom waters were high in summer months, but low during winter when the water column was mixed more frequently. The general pattern of increased importance of benthic respiration during summer months is further supported by Stutes et al. (2006), who measured increased sediment respiration due to shading by both artificial screens and high algal biomass in overlaying waters in a eutrophied shallow estuary in Alabama. Furthermore, Rowe et al. (2002) reported higher sediment respiration rates during summer than during winter across the Louisiana continental shelf, which was attributed to a temperature effect (Q_{10} of about 2).

The spatial patterns of benthic versus water-column respiration were different between the two years. In 2002, benthic respiration was highest in hypoxic areas with water depths of up to 20 m. Deeper stations that were hypoxic might have had lower relative contributions of benthic respiration because sedimenting particles were exposed longer to water-column respiration before reaching the sediments. The same pattern was also previously described by Dortch et al. (1994), who measured absolute benthic and water-column respiration by the enzymatic respiratory electron-transport-system activity (ETS) method across the Louisiana continental shelf and found that at deeper stations water column respiration was more important than at shallower stations. The second group of stations that had high relative contributions of benthic respiration was located in deeper "blue" waters where bottom waters were not hypoxic. Because of the reduced primary production in surface waters and longer residence time of organic material in the water column, water column respiration was probably less intense than at shallower stations. Under these circumstances, even moderate benthic respiration could have had a stronger relative impact on total respiration in bottom waters.

In contrast to the 2002 shelfwide cruise, there was no significant relationship between the magnitude of benthic respiration and the depth of the water column during July 2003. Instead, I found that areas with high POC concentrations in surface waters also had higher contributions of water-column respiration. This indicated that recent primary production started to settle, which resulted in increased respiration rates in the water column. The relative contribution of benthic respiration was lower than usual, possibly due to resuspension of organic material into the water column or its removal during tropical storm Bill.

This model which calculated the relative contributions of water-column versus benthic respiration was based on the assumptions of a constant fractionation factor for water-column respiration and the absence of oxygen sources. Hence, the partition of total respiration could have been influenced by a smaller or larger fractionation factor (ε) for water column respiration (e.g. -18‰ or -25‰ instead of -22‰), mixing with water masses of higher oxygen concentration and $\delta^{18}O$ (offshore or surface water), and addition of oxygen with low $\delta^{18}O$ due to benthic photosynthesis. As discussed in Chapter 2, mixing with different water masses was unlikely in my study, and different fractionation factors for water-column respiration would result only in minor changes to the relative contributions of the two respiration types, while leaving spatial patterns unaffected. To estimate the potential impact of benthic primary production, in Chapter 2 light penetration into bottom waters based on Secchi disk data was investigated (R. E. Turner, unpublished). Results have shown that at stations where the depth of the water column was less than 2 to 3x the Secchi depth, benthic photosynthesis was likely to be insignificant with respect to separating benthic and water-column respiration. In July 2002, 3x Secchi depths were generally much shallower than station depths (Figure 3.10). On the other hand in July 2003, water transparency was higher so that 2x Secchi depths reached or even exceeded the depths of

the water column at about 30% of all stations. Therefore, the potential for benthic photosynthesis was much larger in 2003 than in 2002. As outlined earlier, benthic photosynthesis could have important implications for bottom oxygen dynamics. Yet, it appears that despite increased light penetration in July 2003, benthic photosynthesis was insignificant. Otherwise I should have observed higher contributions of "mimicked" benthic respiration under these conditions. Since the opposite was actually observed, benthic photosynthesis seemed to be of minor importance in this system and the analysis of respiration dynamics in bottom waters was likely fairly robust. Furthermore, if benthic photosynthesis were important, the addition of low $\delta^{18}O$ from benthic primary production should have skewed the results towards higher proportions of benthic respiration at stations with deep Secchi depths. Yet, I did not detect a significant relationship between Secchi depths and the contributions of benthic respiration ($p > 0.2$).

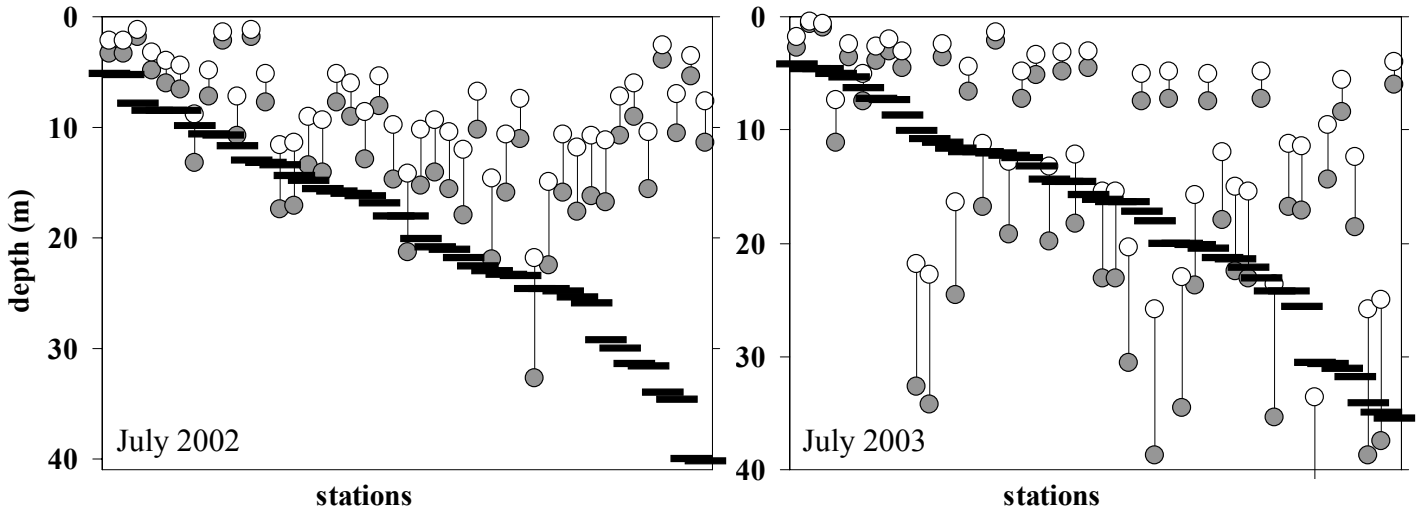

Figure 3.10 Relationship between 2x Secchi depth (open circles) and 3x Secchi depth (close circles) versus station depth (m, black bars) for the shelfwide cruises in July 2002 and 2003.

In conclusion, this study allowed me to contrast the effects of a tropical storm (2003) on productivity and respiration patterns across the Louisiana continental shelf with the usual calm

summer conditions (2001 and 2002). Multivariate regression analyses were applied to quantify the importance of biological and physical parameters that were responsible for the observed seasonal and interannual patterns. Except during periods following the passage of cold fronts and tropical storms, nutrient supply (salinity-inferred) and algal biomass (POC, C:N) explained most of the variability in surface productivity. In contrast, bottom waters showed a strong seasonality, as oxygen depletion and the relative importance of benthic respiration were much more intense during summer stratification; and only strong physical mixing due to a tropical storm could change this pattern.

REFERENCES

Bender ML, Grande K (1987) Production, respiration and the isotopic geochemistry O_2 in the upper water column. Global Biogeochem Cycles 1:49-59

Benson BB, Krause D (1984) The concentration and isotopic fractionation of oxygen dissolved in fresh water and seawater in equilibrium with the atmosphere. Limnol Oceanogr 29:620-632

Boesch DF (2002) Challenges and opportunities for science in reducing nutrient over-enrichment of coastal ecosystems. Estuaries 25:886-900

Brandes JA, Devol AH (1997) Isotopic fractionation of oxygen and nitrogen in coastal marine sediments. Geochim Cosmochim Acta 61:1793-1802

Dole M, Lane GA, Rudd DP, Zaukelies DA (1954) Isotopic composition of atmospheric oxygen and nitrogen. Geochim Cosmochim 6:65-78

Dortch Q, Turner RE, Rowe GT (1994) Respiration rates and hypoxia on the Louisiana shelf. Estuaries 17:862-872

Dunn DD (1996) Trends in nutrient inflows to the Gulf of Mexico from streams draining the conterminous United States 1972 – 1993. U.S. Geological Survey, Water Resources Investigation Report 96-4113, USGS Austin, Texas

Fry B (2006) Stable Isotope Ecology. Springer, New York.

Grande KD, Williams PJ, Marra J, Purdie DA, Heinemann K, Eppley RW, Bender ML (1989) Primary production in the North Pacific gyre: a comparison of rates determined by the ^{14}C, O_2 concentration and ^{18}O methods. Deep-Sea Res 36:1621-1634

Guy RD, Berry JA, Fogel ML, Hoering TC (1989) Differential fractionation of oxygen isotopes by cyanide-resistant and cyanide-sensitive respiration in plants. Planta 177:483-491

Guy RD, Fogel ML, Berry JA (1993) Photosynthetic fractionation of the stable isotopes of oxygen and carbon. Plant Physiol 101:47-47

Hendricks MB, Bender ML, Barnett BA (2004) Net and gross O_2 production in the Southern Ocean from measurements of biological O_2 saturation and its triple isotope composition. Deep-Sea Res 51:1541-1561

Justić D, Rabalais NN, Turner RE (2002) Modeling the impacts of decadal changes in riverine nutrient fluxes on coastal eutrophication near the Mississippi River Delta. Ecol Model 152:33-46

Justić D, Rabalais NN, Turner RE, Wiseman WJ Jr (1993) Seasonal coupling between riverborne nutrients, net productivity and hypoxia. Mar Poll Bull 26(4):184-189

Kampbell DH, Wilson JT, Vandergrift SA (1989) Dissolve oxygen and methane in water by a GC headspace equilibration technique. Intern J Environ Anal Chem 36:249-257

Knox M, Quay PD, Wilbur D (1992) Kinetic isotope fractionation during air-water gas transfer of O_2, N_2, Ch_4, and H_2. J Geophys Res 97:20335-20343

Kroopnick PM (1975) Respiration, photosynthesis, and oxygen isotope fractionation in oceanic surface water. Limnol Oceanogr 20:988-992

Lohrenz SE, Dagg MJ, Whitledge TE (1990) Enhanced primary production in the plume/oceanic interface of the Mississippi River. Cont Shelf Res 10:639-664

Lohrenz SE, Fahnenstiel GL, Redalje DG, Lang GA, Dagg MJ, Whitledge TE, Dortch Q (1999) Nutrients, irradiance, and mixing as factors regulating primary production in coastal waters impacted by the Mississippi River plume. Cont Shelf Res 19:1113-1141

Luz B, Barkan E, Sagi Y, Yacobi Y (2002) Evaluation of community respiratory mechanisms with oxygen isotopes: A case study in Lake Kinneret. Limnol Oceanogr 47:33-42

Mariotti A, Germon JC, Hubert P, Kaiser P, Letolle R, Tardieux A, Tardieux P (1981) Experimental determination of nitrogen kinetic isotope fractionation: Some principles; illustration for the denitrification and nitrification processes. Plant and Soil 62:413-430

Miyajima T, Yamada T, Hanba YT (1995) Determining the stable isotope ratio of total dissolved inorganic carbon in lake water by GC/C/IRMS. Limnol Oceanogr 40:994-1000

Ostrom NE, Carrick HJ, Twiss MR (2005) Evaluation of primary production in Lake Erie by multiple proxies. Oecologia 145:669-669

Quay PD, Wilbur DO, Richey JE, Devol AH, Benner R, Forsberg BR (1995) The ^{18}O:^{16}O of dissolved oxygen in rivers and lakes in the Amazon basin: Determining the ratio of respiration to photosynthesis rates in freshwaters. Limnol Oceanogr 40:718-729

Quiñones-Rivera ZJ, Wissel B, Justic D, Fry B (2007) Partitioning oxygen sources and sinks in a stratified, eutrophic coastal ecosystem using stable oxygen isotopes. Mar Ecol Progr Ser 342:69-83

Rabalais NN, Turner RE (2006) Oxygen depletion in the Gulf of Mexico adjacent to the Mississippi River. Pages 225-245 in L. N. Neretin, ed., *Past and Present Marine Water Column Anoxia*. NATO Science Series: IV-Earth and Environmental Sciences, Kluwer

Rabalais NN, Turner RE (2001) Hypoxia in the northern Gulf of Mexico: Description, causes and change. In: Rabalais NN, Turner RE (eds) Coastal Hypoxia: consequences for living resources and ecosystems. Coastal and Estuarine Studies 58, American Geophysical Union, Washington D.C., p 1-36

Rabalais NN, Turner RE, Scavia D (2002a) Beyond science into policy: Gulf of Mexico hypoxia and the Mississippi River. BioScience 52:129-142

Rabalais NN, Turner RE, Wiseman WJ Jr (2002b) Hypoxia in the Gulf of Mexico, a.k.a. "The Dead Zone." Annual Review of Ecology and Systematics 33: 235-263

Rabalais NN, Turner RE, Sen Gupta BK, Boesch DF, Chapman P, Murrell MC (2007) Characterization and Long-Term Trends of Hypoxia in the Northern Gulf of Mexico: Does the Science Support the Action Plan? Estuaries and Coasts 30: 753-772

Rabalais NN, Turner RE, Wiseman WJ Jr, Boesch DF (1991) A brief summary of hypoxia on the northern Gulf of Mexico continental shelf: 1985-1988. In: Tyson RV, Pearson TH (eds) Modern and ancient continental shelf anoxia. Geological Society Special Publication No. 58, London, p 35-47

Roberts BJ, Russ ME, Ostrom NE (2000) Rapid and precise determination of the $\delta^{18}O$ of dissolved and gaseous di-oxygen via gas chromatograph-isotope ratio mass spectrometry. Environ Sci Tech 34:2337-2341

Rowe GT, Cruz-Kaegi ME, Morse JW, Boland GS, Escobar-Briones EG (2002) Sediment community metabolism associated with continental shelf hypoxia, northern Gulf of Mexico. Estuaries 25:1097-1106

Scavia D, Justic D, Bierman VJ (2004) Reducing hypoxia in the Gulf of Mexico: advice from three models. Estuaries 27:419-425

Sklar FH, Turner RE (1981) Characteristics of phytoplankton production off Barataria Bay in an area influenced by the Mississippi River. Contrib Mar Sci 24:93-106

Stigebrandt A (1991) Computations of oxygen fluxes through the sea-surface and the net production of organic matter with application to the Baltic and adjacent seas. Limnol Oceanogr 36:444-454

Stutes AL, Cebrian J, Corcoran AA (2006) Effects of nutrients and shading on sediment primary production and metabolism in eutrophic estuaries. Mar. Ecol. Prog. Ser. 312:29-43

Turner RE, Rabalais NN (1991) Changes in the Mississippi River water quality this century – Implications for coastal food webs. BioScience 41:140-147

Turner RE, Qureshi N, Rabalais NN, Dortch Q, Justic D, Shaw RF, Cope J (1998) Fluctuating silicate:nitrate ratios and coastal plankton food webs. Proc Natl Acad Sci USA 95:13048-13051

Turner RE, Rabalais NN, and Justić D (2006) Predicting summer hypoxia in the northern Gulf of Mexico: riverine N, P, and Si loading. Mar Poll Bull 52:139-148

Wang X, Chen FC, Gardner GB (2004) Sources and transport of dissolved and particulate organic carbon in Mississippi River estuary and adjacent coastal waters of the northern Gulf of Mexico. Mar Chem 89:241-256

Weiss R (1970) The solubility of nitrogen, oxygen and argon in water and seawater. Deep-Sea Res 17:721-735

Wetzel RG (2001) Limnology - lake and river ecosystems. Academic Press.

Wiseman WJ Jr, Rabalais NN, Turner RE, Dinnel SP, MacNaughton A (1997) Seasonal and interannual variability within the Louisiana coastal current: stratification and hypoxia. J Mar Syst 12:237-248

Wissel B, Gace A, Fry B (2005) Tracing River Influences on Phytoplankton Dynamics in Two Louisiana Estuaries. Ecology 86:2251-2762

Wissel B, Quiñones-Rivera ZJ, Fry B (accepted) Combined Analyses of O_2 and CO_2 for Studying the Coupling of Photosynthesis and Respiration in Aquatic Systems. Oecologia

CHAPTER 4
DEVELOPMENT OF PRODUCTIVITY MODELS FOR THE NORTHERN GULF OF MEXICO BASED ON OXYGEN CONCENTRATIONS AND STABLE OXYGEN ISOTOPES

INTRODUCTION

A key parameter in characterizing aquatic ecosystems is the measurement of primary production, where low and high productivity are representative of oligotrophic and eutrophic conditions, respectively (Wetzel 2001). The measurement of productivity can be expressed as change in algal biomass or chlorophyll over time, incorporation of CO_2 as source for photosynthesis, or the generation of oxygen as the photosynthetic end product. Because these individual approaches focus of different processes during photosynthesis they do not generate identical results. Yet, conversions among methods are possible and are usually based on elemental stoichiometry of metabolic processes. For example, typical conversions are empirical or experimental C:Chl *a* ratio in algal biomass (Garnier et al. 1989), oxygen generation vs. production of organic C during photosynthesis (Justić et al. 1997), and CO_2 uptake vs. O_2 generation, which is also known as the respiratory quotient (Robinson et al. 1999). In addition to primary production, a second important ecosystem parameter is the ratio of primary production to respiration (P/R), which indicates not only if a system is autotrophic (P/R > 1) or heterotrophic (P/R < 1) but also shows the degree to which autotrophy or heterotrophy has been achieved (del Giorgio & Williams 2005).

Due to its simplicity, oxygen concentration measurements have been used in calculations of primary production and P/R ratios for decades since Odum (1956) measured primary production (PP) and respiration (R) in streams based on diurnal fluctuations of dissolved oxygen concentrations. This approach is now considered a standard technique across many aquatic

systems (Wetzel 2001, Mulholland et al. 2005). While concentration measurements of oxygen have helped to understand system metabolism in a number of cases, this approach is limited in its ability to separate effects of biological (P and R) and physical processes (e.g. mixing and exchange with the atmosphere) that are driving oxygen dynamics. Consequently, concentration measurements are now often complemented with the analyses of stable oxygen isotopes, because they correspond to biological and physical processes in aquatic systems. In equilibrium with the atmosphere, dissolved oxygen has a stable isotope value of 24.2‰ (Benson & Krause 1984, Knox et al. 1992), but photosynthesis and respiration can lead to significantly lower and higher $\delta^{18}O$ values, respectively. Decreasing $\delta^{18}O$ values in response to photosynthesis are due to the addition of isotopically depleted (light) oxygen that is derived from ambient water to the existing DO pool (Guy et al. 1986, 1993), whereby $\delta^{18}O$ of the source water can range from 0‰ (seawater) to as low as -25‰ for freshwater at high latitudes (IAEA 2006). In contrast, respiration preferentially removes light oxygen with a large fractionation factor (ε) of -15 to -25‰ (Kroopnick 1975, Quay et al. 1995, Luz et al. 2002, Hendricks et al. 2004, Chapter 2), which results in increased $\delta^{18}O$ values of the residual DO pool.

The combined use of oxygen concentrations and stable isotope values to estimate primary production and P/R in aquatic systems is appealing because it does not utilize time-consuming incubations that are necessary for methods that rely on CO_2 incorporation or oxygen concentration measurements alone (Grande et al. 1989). Therefore, productivity estimates can be achieved for large study areas within a fairly short time. The underlying mechanisms for calculating productivity and P/R were first described by Bender and Grande (1987). This work was significant as it has laid out and parameterized the individual processes influencing both oxygen concentrations and stable isotope values during photosynthesis and respiration.

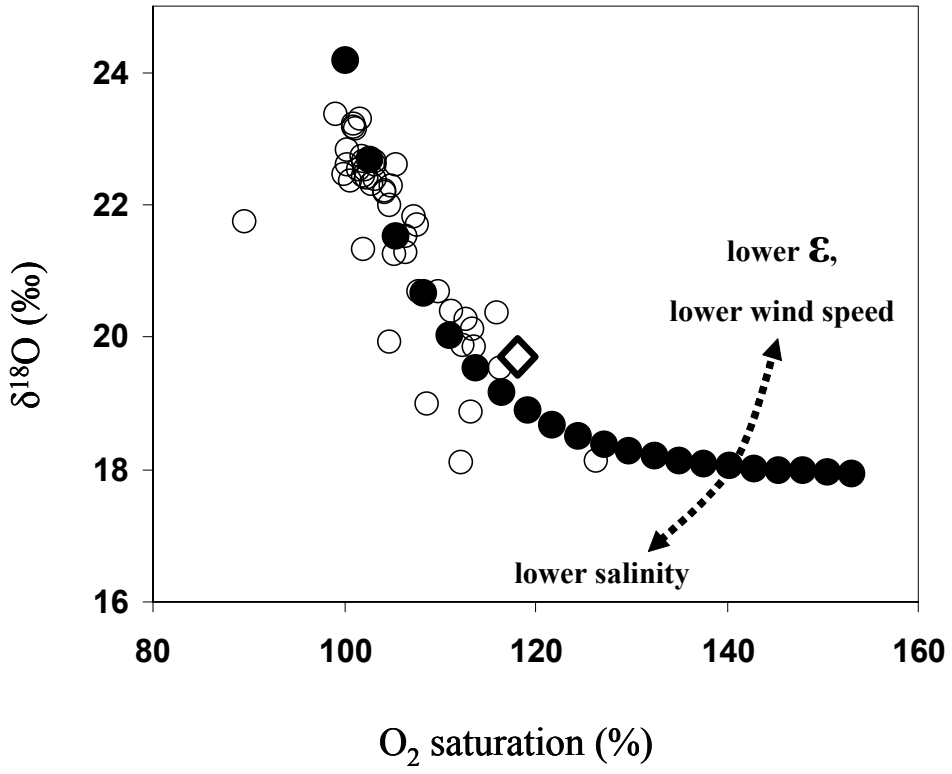

Figure 4.1 Conceptual model illustrating the effects of fractionation factor for water column respiration (ε), wind speed, and salinity ($\delta^{18}O$ of water) on the evolution of the line generated by the finite difference model. Open circles indicate values for surface samples that were collected during the July 2002 shelfwide cruise. Black circles represent the evolution of oxygen saturation versus $\delta^{18}O$-values based on the median P/R value 1.11. Input parameters for this model scenario were as follows: ε = -22‰; $\delta^{18}O$ of water = -2‰; average wind speed = 3.4 m sec^{-1}; respiration rate = 0.07 mg L^{-1} h^{-1}. Spacing along the O_2 vs. $\delta^{18}O$ line is shown in 24 h time intervals to demonstrate that initial changes are more intense. The arrows point out in which direction the curve will be inflected depending on decreasing values for water column respiration (ε), wind speed, and salinity ($\delta^{18}O$ of water), whereby an upward inflection would result in lower P/R values for individual data points.

Unfortunately, the algorithms were limited to describing closed system dynamics because equations for mixing or gas exchange with the atmosphere were not included. In contrast, a second P/R model that was developed by Quay et al. (1995) for the Amazon River and adjacent lakes did, at least partially, consider gas exchange with the atmosphere, but it is limited to steady-state conditions that are often not applicable to productive systems where diurnal changes in both oxygen concentrations and stable isotope values can be large. The Quay et al. (1995)

model performed well for the unproductive and oxygen undersaturated waters of the Amazon River, but applications to other systems revealed some problems, especially once the fractionation factor during respiration of ε = -18‰ (Chapter 2) is increased, the model does not generate reasonable results anymore. Yet, this did not prevent researchers from applying the model to a number of systems, whereby ε was assumed to be -18‰ (Russ et al. 2004, Ostrom et al. 2005, Parker et al. 2005). .

For the Louisiana continental shelf and other systems, larger fractionation factors between -20 and -25‰ have been measured (Luz et al. 2002, Hendricks et al. 2004, Chapter 2), which made it necessary to develop a more suited model. The Quay et al. (1995) model was not appropriate to characterize productivity patterns across the productive Louisiana continental shelf, not only because of apparent diurnal oxygen patterns that violate steady-state assumptions, but also because three independent measurements identified a system-specific ε-value of -22‰ for water column respiration (Chapter 2). Therefore, the original approach by Bender and Grande (1987) was expanded by including algorithms for gas-exchange with the atmosphere. The main objective of this study was to test the sensitivity of the newly developed model to changes in input parameters across the range that is commonly observed for surface and bottom water dynamics across the Louisiana continental shelf.

METHODS

Model Development and Parameterization

To evaluate oxygen dynamics recorded in the combined measurements of oxygen concentrations and $\delta^{18}O$ values, I developed a finite difference model equivalent to that used by Bender and Grande (1987), with sequential steps for mixing, fractionation, and air-sea gas exchange (Chapter 2). Mixing pertains to new oxygen added from photosynthesis or gas

invasion, and fractionation pertains to oxygen removed by respiration or gas evasion. Isotope mixing can be understood as a weighted average, while isotopic fractionation for respiration can be described by logarithmic distillation equations (Mariotti et al. 1981). The eight sequential equations used in each time step (1 hour) of the model were as follows:

1. Oxygen Gain during Photosynthesis: $S_{S1} = S_{INITIAL} + C_P$
2. Isotope Mixing during photosynthesis: $\delta_{S1}S_{S1} = \delta_{INITIAL}S_{INITIAL} + \delta_P C_P$
3. Oxygen Gain during Invasion: $S_{S2} = S_{S1} + C_I$
4. Isotope Mixing during Invasion: $\delta_{S2}S_{S2} = \delta_{S1}S_{S1} + \delta_I C_I$
5. Oxygen Loss during Respiration: $S_{S3} = S_{S2} - C_R$
6. Isotope Fractionation during Respiration: $\delta_{S3} = \delta_{S2} + \varepsilon_R \ln((S_{S2} - C_R)/S_{S3})$
7. Oxygen Loss during Evasion: $S_{S4} = S_{S3} - C_E$
8. Isotope Fractionation during Evasion: $\delta_{S4} = \delta_{S3} + \varepsilon_E \ln((S_{S3} - C_E)/S_4)$

where δ is the $\delta^{18}O$ value, S is % saturation of oxygen, ε_R and ε_E are the fractionation factors (negative in sign, Mariotti et al. 1981) associated with respiration and evasion, respectively. C is the change in oxygen saturation associated with photosynthesis, respiration, or air-sea gas transfer. Subscripts are as follows: P = new oxygen added from photosynthesis, I = new oxygen added by invasion, R = oxygen removed by respiration, E = oxygen removed by evasion. In practice, these equations are linked in a row of calculations in a spreadsheet, then the last values of a row are used as initial values for the next row, i.e., S_4 and δ_{S4} from the end of one row become the initial values (S_1 and δ_{S1}) of the next row, so that one row represents a complete cycle of photosynthesis + invasion + respiration + evasion accumulated a 1-hour time interval. To complete the parameterization of these models, I selected the following values: $\delta^{18}O$ value of -2‰ for new photosynthetic oxygen (based on average salinity of 30, assuming mixing of

Mississippi River water with a value of -7‰ (Kendall, personal communication) with full strength salinity water of 0‰), $\delta^{18}O$ value of 24.2‰ for invading atmospheric oxygen (Benson & Krause 1984, Knox et al. 1992), ε_R = -22‰ for respiration in surface waters (average value from three independent incubation experiments), ε_R = 0‰ for respiration in sediments (Brandes & Devol 1997), and ε_E = -3.5‰ (derived from data presented in Knox et al. 1992).

Application to Surface Waters

Model runs started from initial conditions of 100% oxygen saturation and 24.2‰ $\delta^{18}O$ set by equilibration with the atmosphere ($S_{INITIAL}$; $\delta_{INITIAL}$). Keeping all input parameters constant, the equations were propagated over 100-10000 time intervals until a steady state was achieved. Consequently, a curve was generated (black circles in Fig. 4.1) due to the incremental changes in oxygen concentrations and $\delta^{18}O$ values. I used this finite difference model to estimate P/R ratios (hereafter, P/R) for individual data points (samples) in surface waters. For all subsequent calculations, the respiration rate was held constant at 0.07 mg O_2 L^{-1} h^{-1}, which was the average decrease in O_2 concentration during three consecutive nights (PAR = 0) during the July 2001 shelfwide cruise (nevertheless, variations in respiration rate over a large range from 0.01 to 1.5 mg O_2 L^{-1} h^{-1}did not affect the calculated P/R values). Air-sea gas exchange was modeled based on oxygen saturation levels and the average wind speed during individual cruises (Stigebrandt 1991, Justić et al. 1995). Subsequently for each surface water sample, the photosynthetic rate was adjusted until the generated P/R-curve would intersect with the sample data point and the specific P/R could be extracted. For example, to generate a P/R line that intersects with the data point depicted by a black diamond (Fig. 4.1) the photosynthetic rate needed to be adjusted to 0.14 mg O_2 L^{-1} h^{-1}, whereby the respiration rate and wind speed were kept constant at 0.07 mg O_2 L^{-1} h^{-1} and 4 m sec^{-1}, respectively; the extracted P/R value was 2.0.

Parameters that can alter the evolution of the generated O_2-$\delta^{18}O$ curves (and thereby P/R) are 1) the fractionation factor for water column respiration (ε), whereby lower ε-values would move the curve upwards and generate lower P/R values for a given data point, 2) wind speed, whereby lower wind speed would also move the curve upward, and 3) salinity, which affects the $\delta^{18}O$ of the water and thereby the $\delta^{18}O$ of newly produced oxygen during photosynthesis (Figure 4.1). Lower salinity would shift the curve downwards and generate higher P/R values. The remaining parameters of this model, absolute rates of production and respiration, do not affect the shape of the generated curves of the calculation of P/R. To test the sensitivity of the model relative to changes in ε, $\delta^{18}O$ of the water, or wind speed, I re-parameterized the model using 1) alternative fractionation factors of -15 and -18 and -25‰ from the literature (Kroopnick 1975, Bender & Grande 1987, Guy et al. 1989, Quay et al. 1993, 1995, Luz et al. 2002, Hendricks et al. 2004; ε = -25‰ was removed from the analysis because the model could not generate reasonable solutions), 2) alternative values for $\delta^{18}O$ of the water of -1.5 and -2.5‰ to represent the range of observed salinities during summer conditions, and 3) alternative wind speeds of 4 and 6 m sec^{-1}, representing mid to lower average wind speeds during summer conditions. For all scenarios, I calculated the median as central value and the 10^{th}, 25^{th}, 75^{th}, and 90^{th} percentiles (Table 4.1). As data set, I used the samples from the July 2002 shelfwide cruise, representing calm and stratified summer conditions. The spatial patterns of selected scenarios are shown in Figure 4.2. All spatial diagrams were developed using Surfer Version 8.02 (Golden Software, Inc.). The spatial interpolation between individual sampling points was performed using the kriging technique. In the interpolations, I used standard features of the software to account for variable spacing between stations and transects.

To represent the effects of the full range of seasonal dynamics on P/R, I generated O_2-$\delta^{18}O$ curves for low, median and high P/R values for ε-values of -15, -18, and -22‰, $\delta^{18}O$ water of -1, -2, and -3‰, and wind speeds of 4, 6, and 20 m sec^{-1} (Figure 4.3 - 4.5).

Application to Bottom Waters

I found little evidence for benthic photosynthesis or gas exchange with the upper water column for bottom waters in the sampling area (Chapters 2 and 3), and I focused this model to estimate fractionations associated with respiration only, assuming benthic photosynthesis and gas exchange to be zero. This respiration-only formulation of the model generated curves from a starting point of air-equilibrated seawater (100% saturation, 24.2‰ $\delta^{18}O$ representing $S_{INITIAL}$ and $\delta_{INITIAL}$, respectively) that intersected individual data points depending on the fractionation factor used during respiration (ε_R in equation 6 above). Estimates of the individual ε_R fractionation factors were used to partition the sources of respiration, with sediment respiration expected to occur with no fractionation, and respiration in bottom waters expected to occur with a fractionation of -22‰. Thus, the estimated ε_R values were intermediate between 0‰ ($\varepsilon_{benthic}$) and -22‰ ($\varepsilon_{water\ column}$) with values closer to 0‰ indicating stronger sediment respiration, according to the formula:

$$\%\ \text{benthic respiration} = 100 * (\varepsilon_{observed} - \varepsilon_{water\ column}) / (\varepsilon_{benthic} - \varepsilon_{water\ column})$$

To test the sensitivity of the model, I used a range of alternative fractionation factors (ε) of -15, -18, and -25‰ (Figure 4.6) that were previously described in the literature (Kroopnick 1975, Bender & Grande 1987, Guy et al. 1989, Quay et al. 1993, 1995, Luz et al. 2002, Hendricks et al. 2004). Subsequently, I investigated the potential impact of benthic primary production (BPP, Figure 4.6) or gas exchange with the upper water column (mixing, Figure 4.6) on bottom water oxygen dynamics, by included equations 1 through 4 (photosynthesis and

invasion/evasion was not included as bottom waters were always undersaturated) into the model for bottom waters. In each time step, I allowed 0%, 10, 20, or 30% of the respired oxygen to be added back into bottom waters by either benthic photosynthesis (BPP) or gas exchange with the upper water column (mixing), whereby the $\delta^{18}O$ values for these two oxygen sources were respectively -2 and 21‰ (average $\delta^{18}O$ value of surface waters during summer stratification). I then re-calculated the $\delta^{18}O$ vs. O_2 saturation curves for these scenarios and compared them to the original model that was based on respiration only. For all scenarios, I calculated the median as central value and the 10^{th}, 25^{th}, 75^{th}, and 90^{th} percentiles (Table 4.5). As a data set, I used the samples from the July 2002 shelfwide cruise (see chapter 3), representing calm and stratified summer conditions. The spatial patterns of selected scenarios are shown in Figure 4.7. The spatial interpolation between individual sampling points was performed using the kriging technique (Surfer Version 8.02, Golden Software, Inc.). In the interpolations, I used standard features of the software to account for variable spacing between stations and transects.

RESULTS

Surface Model (Summer Conditions)

Sensitivity analysis of calculated P/R values to changes in various model parameters for the July 2002 shelfwide cruise revealed that fractionation factor had the strongest influence (Table 4.1). At low P/R values (10^{th} percentile), the differences among P/R for the tested ε-values was minor, but median P/R values increased from 1.11 to 1.27 to 1.37 for ε-values of -22, -18, and -15‰, respectively. At the high end of calculated P/R (90^{th} percentile), the differences were even more striking, increasing from 1.34 to 2.02. This was also clearly reflected in the spatial presentation of P/R over the Louisiana continental shelf (Figure 4.2, top two panels), which illustrated the much increased P/R values for ε = -15‰ relative to the average conditions

(ε = -22‰). Despite the large absolute differences, the spatial pattern remained the same. This finding is strongly supported by the regression coefficients among P/R for the three tested fractionation factors (Table 4.2), because r^2 values were high, ranging from 0.85 to 0.97. The absolute differences in P/R are expressed by the slopes of these regressions, which were quite similar (1.3) for ε-values of -15 and -18‰, but differed strongly among fractionation factors of -22‰ and lower values (2.4 and 3.0).

Table 4.1 Results of P/R values based on different scenarios using the finite difference model for surface samples that were collected during the July 2002 shelfwide cruise. Median, 10th, 25th, 75th, and 90th percentiles are shown for different fractionation factors, $\delta^{18}O$ of water, and wind speed. The ranges of these parameters encompass values that have been documented during calm summertime condition across the Louisiana continental shelf.

	Fractionation factor (ε)			δ $H_2{}^{18}O$ (‰)			Wind speed (m sec^{-1})		
	-15‰	-18‰	-22‰	-1.5	-2.0	-2.5	3.4	4	6
10%ile	1.01	1.01	1.00	1.01	1.00	1.01	1.00	1.01	1.01
25%ile	1.12	1.09	1.03	1.03	1.03	1.04	1.03	1.04	1.05
median	1.37	1.27	1.11	1.08	1.11	1.12	1.11	1.12	1.13
75%ile	1.68	1.47	1.17	1.13	1.17	1.21	1.17	1.21	1.29
90%tile	2.02	1.79	1.34	1.25	1.34	1.35	1.34	1.38	1.43

Table 4.2 Correlations of P/R values that were calculated based on different fractionation factors (Table 4.1). Higher slopes indicate higher P/R values for P/R larger 1.0, and lower P/R values for P/R smaller 1.0. At P/R of 1, all scenarios are aligned.

Fractionation factor (ε)		-18‰	-22‰
slope	-15‰	1.3	3.0
r^2		0.85	0.87
slope	-18‰	-	2.4
r^2		-	0.97

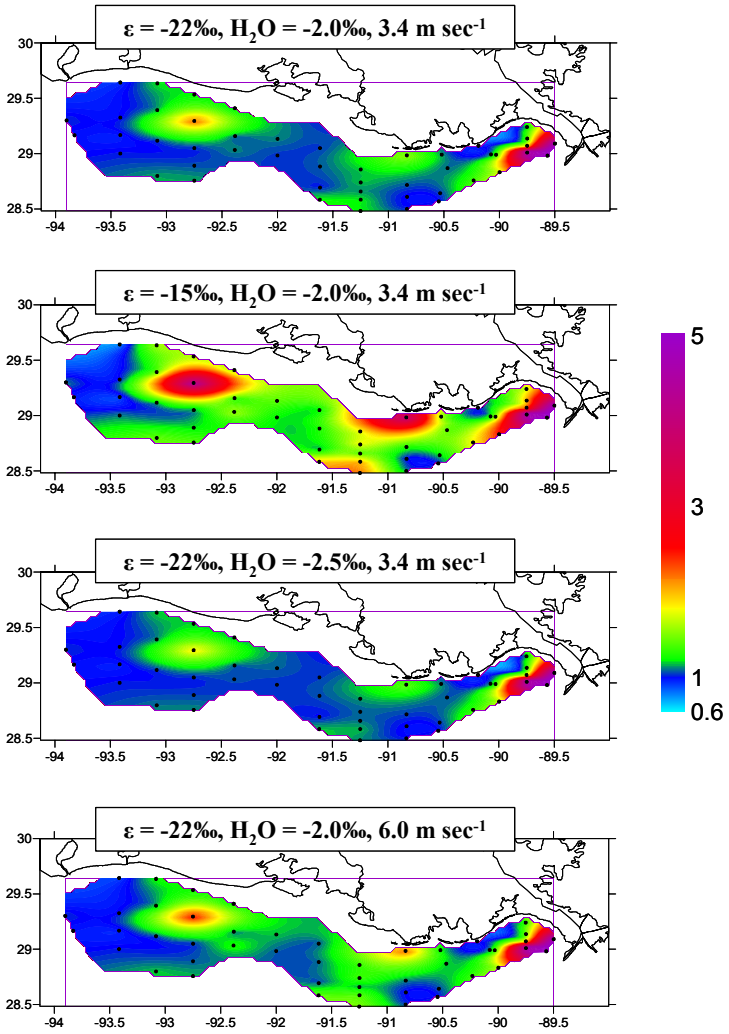

Figure 4.2 Spatial patterns of P/R for four of the 9 tested scenarios (Table 4.1). The top panel represents P/R values for average conditions that were encountered during the July 2002 shelfwide cruise (chapter 3). The second panel represents the results for the smallest fractionation factor (ε) of -15‰. The third panel illustrates the effect of a lower $\delta^{18}O$ of water (lower salinity), and the bottom panel shows how increased wind speed would effect P/R calculations. The model results were most sensitive to changes in fractionation factor, while wind speed and salinity only caused minor changes. The spatial patterns of P/R were not affected by any of the tested parameters.

Lower or higher salinities would have resulted in deviations from the average $\delta^{18}O$ value of ambient water (-2.0‰) as the source of newly generated oxygen during photosynthesis. Due to the fairly narrow salinity range during time of sampling across the study area, $\delta^{18}O$ values of water would not have varied by much, which was reflected by the small changes in P/R (Table 4.1). At the low end of calculated P/R (10^{th} and 25^{th} percentile) values were almost identical and

even at the high end (90th percentile) P/R only increased from 1.25 to 1.35 when a $\delta^{18}O$ value of -1.5‰ was used instead of -2.5‰. The spatial representation of different $\delta^{18}O$ values of water as input parameters confirmed this finding because both spatial patterns and absolute values were almost undistinguishable (Figure 4.2, top vs. third panel). Accordingly, the regression coefficients among the three scenarios were high (0.69 to 0.99) and the slopes were much more similar (0.63 to 0.86) than for the previous model scenarios based on different fractionation factors (Table 4.3).

The effect of wind speeds that can be encountered during typical summer conditions on P/R values was small as well. At the low end of calculated P/R values (10th and 25th percentile), wind speeds of 3.4, 4.0 and 6.0 m sec^{-1} only generated minute differences, and even at the high end (90th percentile) differences were small with a range of P/R from 1.34 to 1.43. There were no major differences in absolute values (Table 4.4), and spatial patterns were alike (Figure 4.2, top vs. bottom panes). In general, for calm summertime conditions, as encountered during the shelfwide cruise in July 2002, neither wind speed nor salinity-based variations in $\delta^{18}O$ values of water would have had a strong impact on the output of the P/R model. Nevertheless, variations in fractionation factor could strongly alter absolute values of calculated P/R but not its spatial pattern.

Table 4.3 Correlations of P/R values that were calculated based on different $\delta^{18}O$ values of water (Table 4.1). Higher slopes indicate higher P/R values for P/R larger 1.0, and lower P/R values for P/R smaller 1.0. At P/R of 1, all scenarios are aligned.

$\delta H_2{}^{18}O$ (‰)		-2.0‰	-2.5‰
slope	-1.5	0.74	0.63
r^2		0.99	0.69
slope	-2.0	-	0.86
r^2		-	0.98

Table 4.4 Correlations of P/R values that were calculated based on different wind speeds (Table 4.1). Higher slopes indicate higher P/R values for P/R larger 1.0, and lower P/R values for P/R smaller 1.0. At P/R of 1, all scenarios are aligned.

Wind speed (m sec^{-1})		4	6
slope	3.4	0.96	0.69
r^2		0.97	0.88
slope	4	-	0.74
r^2		-	0.95

Surface Model (Seasonal Conditions)

The range in fractionation factors should be the same for all seasons and therefore the range in calculated P/R among seasons should not exceed the range that was identified during calm summertime conditions. The large range in possible P/R values for different fractionation factors that was encountered for summer conditions was also applicable to seasonal dynamics across the Louisiana continental shelf. Figure 4.3 depicts the evolution for typical low, average, and high P/R values for the study area (0.9, 1.1, and 1.5 respectively) in relation to oxygen saturation and $\delta^{18}O$ values. Obviously, for P/R values closer to 1, the model is very sensitive in respect to fractionation factor, while at high P/R values the differences among model solution diminished.

For $\delta^{18}O$ values of water and wind speed, seasonal variability is larger than during summer condition as Mississippi River discharge patterns and mixing will affect salinity, and the passage of cold fronts in the fall and winter and tropical storms and hurricanes in the summer can increase wind speeds. Seasonally, salinity-based variations in $\delta^{18}O$ values of water can range from about -1 to -3‰ (Quiñones-Rivera, unpublished data). The implementation of these values into the model resulted in lower and higher P/R curves for oxygen saturation vs. $\delta^{18}O$, respectively (Figure 4.4). Consequently, the variability in P/R on a seasonal basis was larger

than during summer conditions, but effects were much smaller than for scenarios based on different fractionation factors. In contrast to summer conditions, increasing wind speeds could have had a strong effect on model outcomes (Figure 4.5), which were especially pronounced at tropical storm strength (20 m sec^{-1}). Under these conditions, oxygen saturation values would show only a minor response to P/R while $\delta^{18}O$ values maintain their response to P/R.

Bottom Model

The adjusted model for bottom waters to calculate relative contributions of benthic vs. water column respiration illustrated the effects of fractionation factors, benthic primary production, and mixing. With respect to fractionation factors during water column respiration, larger fractionations (e.g. -25‰) lead to higher $\delta^{18}O$ values at identical oxygen saturation levels (indicating the fraction of oxygen respired) than smaller fractionation factors (e.g. -15‰). Consequently, for a measured bottom water sample, a larger fractionation during water column respiration would mean a larger contribution of benthic respiration, because the sample point will be relatively closer to the $\delta^{18}O$ value of 24.2‰ that indicates zero fractionation during benthic respiration (Figure 4.6, top panel). This effect was more pronounced at very low saturation levels due to the exponential increase of the curves for $\delta^{18}O$ vs. oxygen saturation evolution. Nevertheless, the application of four scenarios (ε = -15, -18, -22, and -25‰) to bottom water samples that were collected during the July 2002 shelfwide cruise showed relatively small effects of fractionation factors of the relative importance of benthic vs. water column respiration (Table 4.5). For the 10^{th} percentile, median, and 90^{th} percentile the contribution of benthic respiration to total respiration differed by 18, 11, and 2%, respectively. Considering the large effect that fractionation factor had on P/R calculations for surface samples, these values should be considered small.

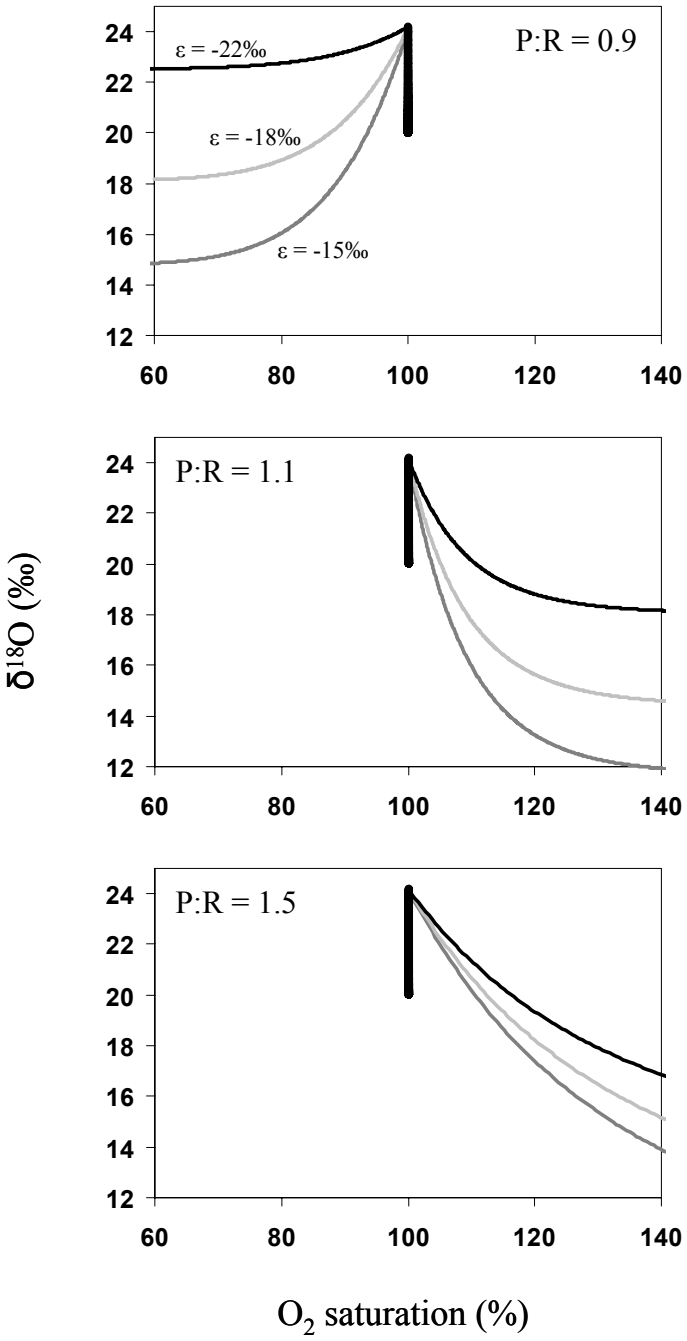

Figure 4.3 Evolution of O_2 vs. $\delta^{18}O$ lines generated by the finite difference model to calculate P/R in surface waters in response to different fractionation factors (ε = -15, -18, and -22‰). Top, middle, and bottom panels show the lines for P/R = 0.9, 1.1, and 1.5. The solid black line represents P/R of 1, a value at which all models align. Accordingly, P/R is identical within each scenario. For both P/R larger and smaller than 1, lower fractionation factors result in higher $\delta^{18}O$ at comparable oxygen saturation. Consequently, calculated P/R values for lower ε-values are more extreme than for higher fractionation factors, but the locations for P/R = 1 are identical for all scenarios.

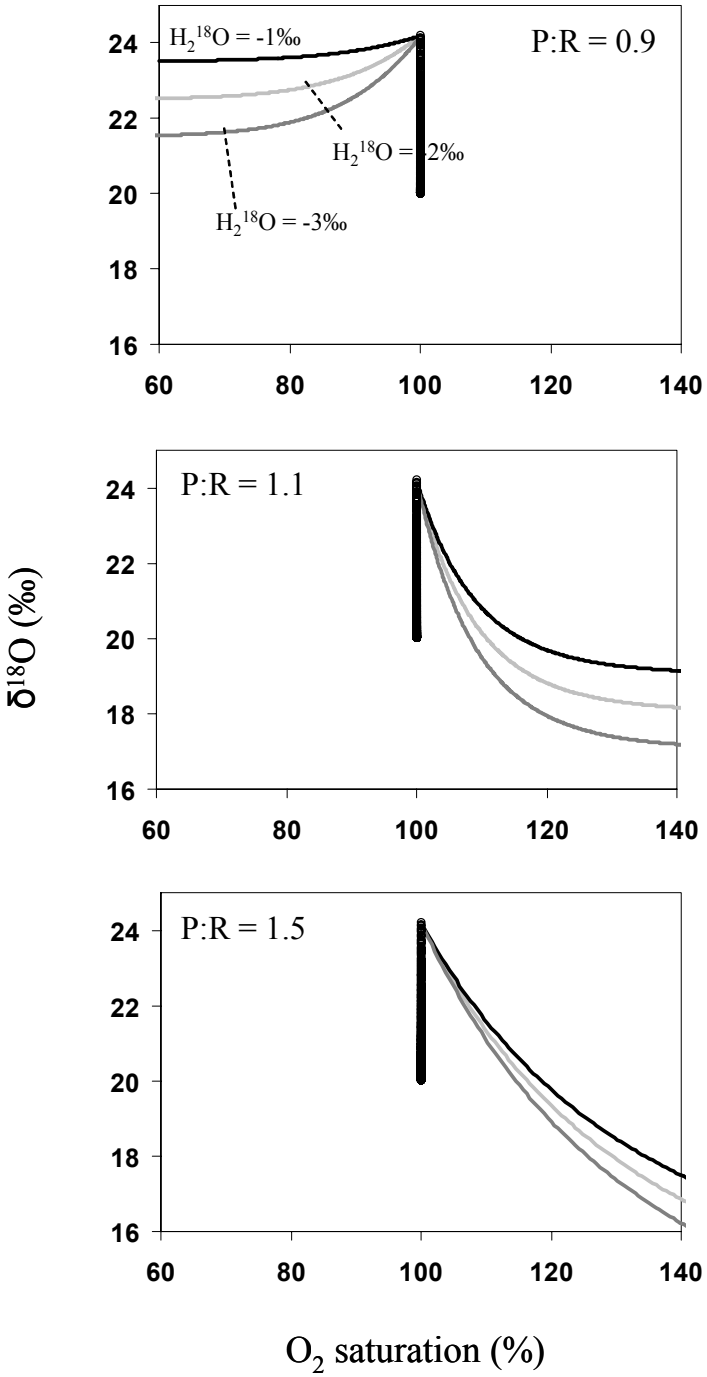

Figure 4.4 Same as Figure 4.3, but $\delta^{18}O$ of water is altered instead of fractionation factors. Actual values represent the seasonal range in salinity from about 20 to 34 psu that is commonly encountered across the sampling area. Higher values for ^{18}O of water represent higher salinities, which have a comparable effect as lower ε-values (Figure 4.3), but the magnitude of change is smaller.

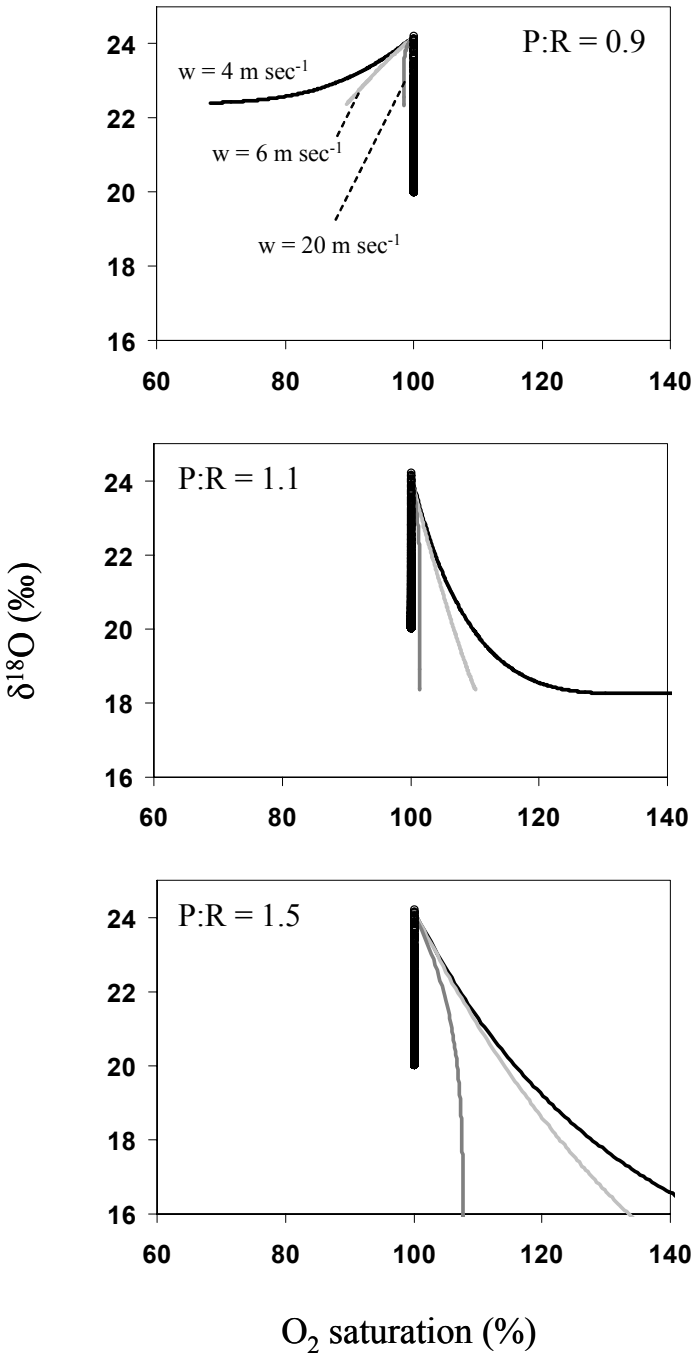

Figure 4.5 Same as Figure 4.3, but wind speed is altered instead of fractionation factors. Actual values of 4, 6, and 20 m sec^{-1} represent average summer, winter, and hurricane force winds that are commonly encountered across the sampling area. Increasing wind speed reduces over- or under-saturation as air-sea gas exchange rates are intensified, e.g. during hurricane force winds saturation levels are always close to 100%, while low wind speeds allow for more intense over- or under-saturation.

The addition of depleted oxygen ($\delta^{18}O$ value = 2‰) to bottom waters due to benthic primary production (BPP) would lower the $\delta^{18}O$ vs. oxygen evolution curves (Figure 4.6, middle panel). Consequently, a larger contribution of BPP would result in a relatively lower importance of benthic respiration. For the July 2002 shelfwide cruise data, an increase from 0 to 30% contribution of BPP to the ambient oxygen concentration would result in a reduction of the calculated contribution of benthic to total respiration from 81 to 72% (median). For smaller (10^{th} percentile) and higher contributions (90^{th} percentile) of benthic respiration these values would range from 69 to 54 and from 98 to 97%, respectively.

For bottom waters, the effect of mixing in surface water ($\delta^{18}O$ value = 21‰) had the lowest impact on the calculated contributions to benthic respiration. Four scenarios using 0, 10, 20, and 30% mixing resulted in very similar values that differed by only 0 to 2% (Table 4.5, Figure 4.6, bottom panel). Generally, the model application for bottom waters to calculate the relative importance of benthic respiration was more robust that for the calculation of P/R in surface waters. In comparison, especially the effect of different fractionation factors was reduced. This was also indicated by the very similar spatial patterns and absolute values that were generated by the model for all four scenarios depicted in Figure 4.7.

Table 4.5 Contribution of benthic to total respiration (%) based on scenarios using the finite difference model for bottom samples collected in July 2002. Median, 10^{th}, 25^{th}, 75^{th}, and 90^{th} percentiles are shown for different fractionation factors, BPP, and mixing.

	Fractionation factor (ε)				BPP				Mixing			
	-15‰	-18‰	-22‰	-25‰	0%	10%	20%	30%	0%	10%	20%	30%
10%ile	55	62	69	73	69	66	62	54	69	69	69	69
25%ile	64	70	75	78	75	73	68	62	75	76	74	75
median	73	77	81	84	81	79	75	72	81	81	80	81
75%ile	88	90	92	93	92	92	91	91	92	93	93	94
90%tile	97	97	98	98	98	97	97	97	98	98	98	98

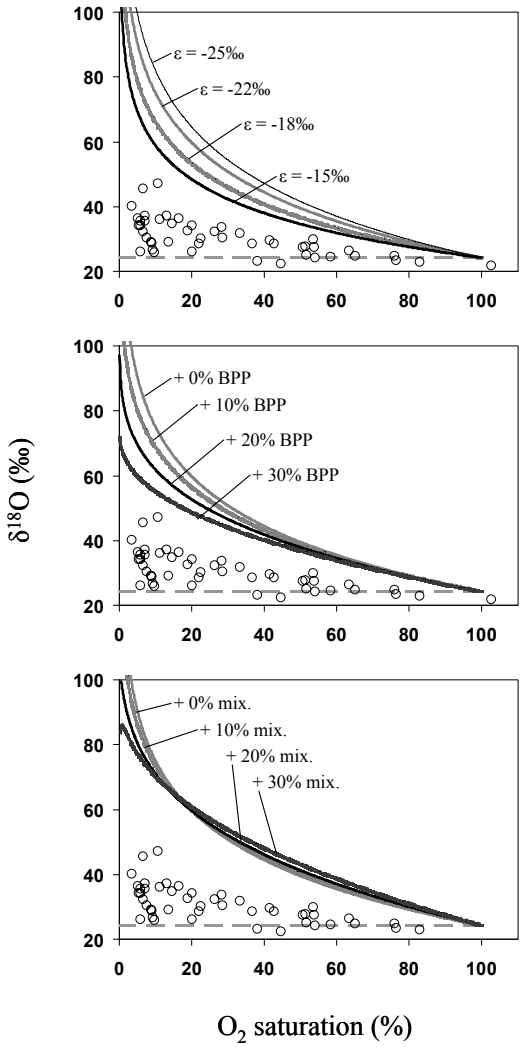

Figure 4.6 Evolution of O_2 vs. $\delta^{18}O$ lines generated by the finite difference model developed for this study to calculate the contribution of benthic vs. water-column respiration in bottom waters in response to different fractionation factors (ε = -15, -18, -22, and -22‰, top panel), addition of oxygen due to benthic primary production (BPP = 0, 10, 20, and 30%, middle panel), and addition of oxygen due addition of overlaying surface water (mixing = 0, 10, 20, and 30%, bottom panel). The different scenarios are represented by solid black and grey shaded lines. The dashed grey line represents 100% benthic respiration where oxygen is respired with fractionation. Open circles show values for bottom water samples during the July 2002 shelfwide cruise. Top panel: lower fractionation factors will shift the O_2 vs. $\delta^{18}O$ line lower, which would increase the relative contribution of water column respiration. Middle panel: increasing contribution of BPP will shift the O_2 vs. $\delta^{18}O$ line lower, which would increase the relative contribution of water column respiration. Bottom panel: the addition of oxygen from overlaying water does not have the consistent effect as seen above. A large contribution of mixing results in decreased water-column respiration at higher saturation levels, but in increased water column-respiration at low saturation levels, whereby the inflection point is around 15% saturation.

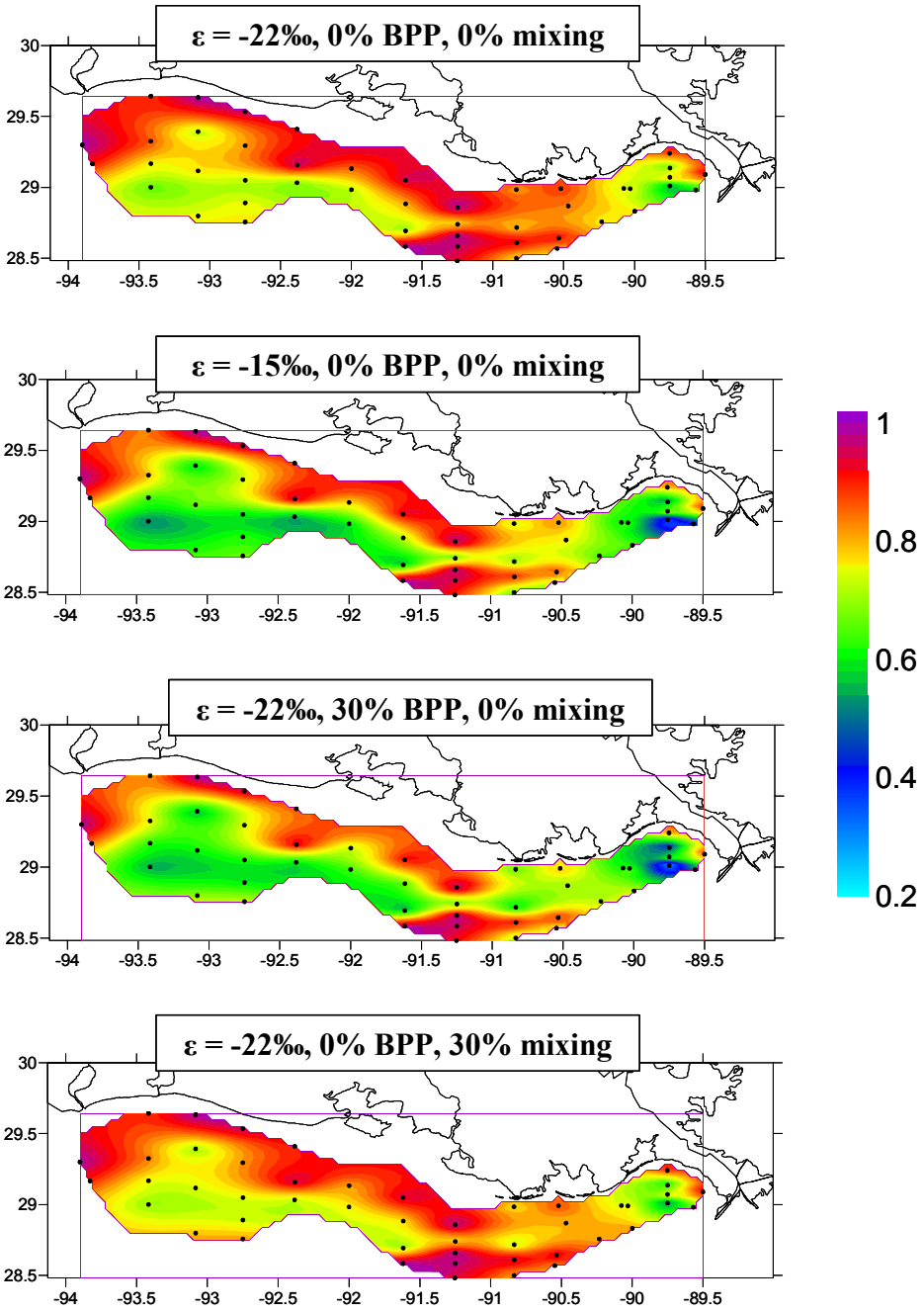

Figure 4.7 Spatial patterns of benthic vs. water-column respiration for four of the 12 tested scenarios (Table 4.5). The top panel represents the fraction of benthic respiration for average conditions that were encountered during the July 2002 shelfwide cruise (Chapter 3). The second panel represents the results for the smallest fractionation factor (ε) of -15‰. The third panel illustrates the effect of a 30% BPP, and the bottom panel shows how 30% mixing would affect the fraction of benthic respiration. The model results were most sensitive to changes in fractionation factor and BPP, while mixing only caused minor changes. The spatial patterns of benthic vs. water column respiration were not affected by any of the tested parameters.

DISCUSSION

Surface Model

The largest variability of the sensitivity of the surface model was observed for changes in the fractionation factor (ε) of water column respiration. Reducing ε-values from -22 to -18 or -15‰ would increase the calculated P/R values at identical oxygen saturation and $\delta^{18}O$ by a factor of 2.4 or 3.0, respectively. This large range of possible model outcomes makes it crucial to obtain a precise measurement of system-specific fractionation factors. Fortunately, three independent incubation experiments that were performed seasonally (September 2002, March 2003, and July 2003) indicated that variations in ε were small across the study area (-22.0‰ ±0.7‰). Furthermore, this analysis showed that the developed model performed well for fractionation factors larger than -18‰, which was one of the limitations of the Quay et al. (1995) model. Nevertheless, using a fractionation factor of -25‰, the model could not generate P/R values for a large number of data points (approximately 30%). This was not surprising as the system-specific ε-value was -22‰. With respect to alternative values for wind speed and $\delta^{18}O$ values of water that could be encountered during calm summer condition, the model was less sensitive because the range of P/R values was small for all tested scenarios. In conclusion, during calm summertime conditions, it is most critical to obtain an accurate fractionation factor, while small deviations of average wind speed or salinity based $\delta^{18}O$ values of water are less critical. Yet, deviations of salinity based $\delta^{18}O$ values of water and especially wind speed can have strong effects on a seasonal basis. Therefore, it is important to measure these parameters during and preceding to the sampling period and then implement season-specific values into the model to ensure more realistic estimates of P/R and productivity.

Bottom Model

Even though bottom water dynamics during stratification can be expressed as a closed system, gas exchange with the atmosphere, mixing with the upper water column or adjacent water masses, and benthic photosynthesis may be important. To test the sensitivity of the bottom model in response to these factors, different fractionation factors for water column respiration and various degrees of benthic primary production (BPP) and mixing were included into the model. The analyses showed that mixing had almost no effect, but decreasing fractionation factors and increasing BPP would lower the calculated relative contribution of benthic to total respiration. Yet, even an increase of ε by 10‰, or the addition of 30% BPP did not decrease the average (median) contribution of benthic respiration by more than 11%. This finding is important because while the fractionation factor can be easily measured using incubations, it would be much more challenging to measure the amount of BPP across a large sampling area. In shallow and / or very transparent systems, where light intensities at the sediment surface can be high, the model could be associated with a large error. Nevertheless, the model estimates of benthic respiration seem reasonable for the study area because the water column generally exceeds a water depth of 10 m and water transparency is low due to high concentrations of suspended algae and sediment (Chapter 2).

Future Considerations

Once adjusted for system-specific ε-values and seasonal aspects, the newly developed model performed well with respect to surface and bottom water dynamics across the Louisiana continental shelf. Nevertheless, the model outcome can only be seen as an approximation of P/R in surface waters and respiration dynamics in bottom waters. While the validity of absolute

values will have to be tested in future independent incubations, relative changes of spatial and seasonal patterns can be compared reliably.

Recently, two alternative models have been developed that use oxygen concentrations and stable isotope values to characterize productivity in aquatic systems (Tobias et al. 2007, Venkiteswaran et al. 2007). These models attempt to fit model parameters to measured diurnal oxygen patterns. Both studies successfully modeled productivity with a high degree of certainty in streams and lakes based on observed diurnal oxygen patterns. Both studies concluded that productivity estimates were most sensitive to the fractionation factor of respiration. Unfortunately, both methods relied on time consuming incubations that would prevent large scale studies as conducted across the Louisiana continental shelf. Furthermore in some instances, the study by Venkiteswaran et al. (2007) had to use very low, unrealistic ε-values (-2.0‰) to produce a good agreement between observed and modeled data.

The model presented here can be modified easily to include the diurnal changes of oxygen concentrations and stable isotope values. As for the original model (Quay et al. 1995), production and respiration will occur in hourly time steps during daylight, but during nighttime only respiration will be implemented. Similar to the original model (Quay et al. 1995), oxygen concentration vs. $\delta^{18}O$ evolution curves represent specific P/R values (Figure 4.8). The only difference between the two models is that for the diurnal model P/R follows a zig-zag pattern instead of a straight line for each P/R value, and the model usually reaches a steady state within 7 to 10 days without further mixing. The amplitudes (widths) of day-night changes in oxygen concentrations and $\delta^{18}O$ were dependent of the respiration rate that was used, and smaller respiration rates generated smaller amplitude. This model might also easily be further adjusted to test how different respiration rates or fractionation factors during day and night would affect

the model outcome. But until these values are examined and experimentally established, the original, simpler model seemed to be a good choice to estimate productivity and respiration dynamics in surface and bottom waters.

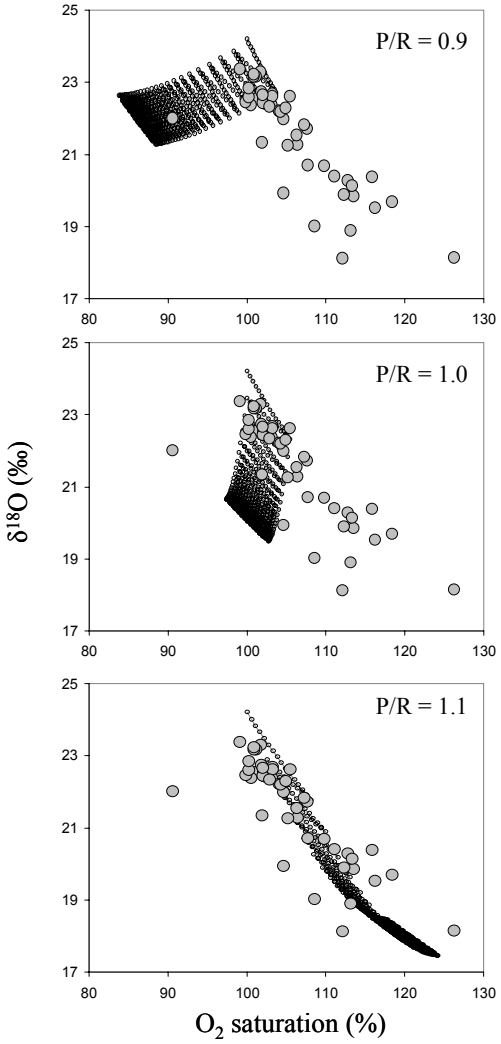

Figure 4.8 Evolution of O_2 vs. $\delta^{18}O$ lines generated by the extended finite difference model that was adjusted to include diurnal oxygen cycling to calculate P/R in surface waters. All other parameters represent average conditions as presented in figure 4.2 (top panel). Top, middle, and bottom panels show the lines for P/R = 0.9, 1.0, and 1.1. The current model assumed 14 hours daylight and 10 hours darkness, representing calm summertime conditions. Data points are for surface water samples that were collected during the July 2002 shelfwide cruise. The amplitude of diurnal variations decreases with the used respiration rate, whereby the current scenarios used a respiration rate of 0.07 mg L^{-1} h^{-1}. After 7 to 10 days, steady state conditions are reached, changes between consecutive days disappear, and oxygen saturation and $\delta^{18}O$ values cycle back and forth diurnally.

REFERENCES

Bender ML, Grande K (1987) Production, respiration and the isotopic geochemistry O_2 in the upper water column. Global Biogeochem Cycles 1:49-59

Benson BB, Krause D (1984) The concentration and isotopic fractionation of oxygen dissolved in fresh water in equilibrium with the atmosphere. Limnol Oceanogr 29:620-632

Brandes JA, Devol AH (1997) Isotopic fractionation of oxygen and nitrogen in coastal marine sediments. Geochim Cosmochim Acta 61:1793-1802

Del Giorgio PA, Williams PJ leB (2005) Respiration in aquatic ecosystems. Oxford University Press, New York

Garnier J, Blanc P, Benest D (1989) Estimating a carbon/chlorophyll ratio in nannoplankton (Créteil Lake, S-E Paris, France). Water Res Bull 25:751-754

Grande KD, Williams PJ, Marra J, Purdie DA, Heinemann K, Eppley RW, Bender ML (1989) Primary production in the North Pacific gyre: a comparison of rates determined by the ^{14}C, O_2 concentration and ^{18}O methods. Deep-Sea Res 36:1621-1634

Guy RD, Berry JA, Fogel ML, Hoering TC (1989) Differential fractionation of oxygen isotopes by cyanide-resistant and cyanide-sensitive respiration in plants. Planta 177:483-491

Guy RD, Fogel ML, Berry JA (1993) Photosynthetic fractionation of the stable isotopes of oxygen and carbon. Plant Physiol 101:47-47

Hendricks MB, Bender ML, Barnett BA (2004) Net and gross O_2 production in the Southern Ocean from measurements of biological O_2 saturation and its triple isotope composition. Deep-Sea Res 51:1541-1561

Justić D, Rabalais NN, Turner RE (1997) Impacts of climate change on net productivity of coastal waters: implication for carbon budgets and hypoxia. Clim Res 8:225-237

Knox M, Quay PD, Wilbur D (1992) Kinetic isotope fractionation during air-water gas transfer of O_2, N_2, Ch_4, and H_2. J Geophys Res 97:20335-20343

Kroopnick PM (1975) Respiration, photosynthesis, and oxygen isotope fractionation in oceanic surface water. Limnol Oceanogr 20:988-992

Luz B, Barkan E, Sagi Y, Yacobi Y (2002) Evaluation of community respiratory mechanisms with oxygen isotopes: A case study in Lake Kinneret. Limnol Oceanogr 47:33-42

Mariotti A, Germon JC, Hubert P, Kaiser P, Letolle R, Tardieux A, Tardieux P (1981) Experimental determination of nitrogen kinetic isotope fractionation: Some principles; illustration for the denitrification and nitrification processes. Plant and Soil 62:413-430

Mulholland PJ, Houser JN, Hayden MG (2005) Stream diurnal dissolved oxygen profiles as indicators of stream metabolism and disturbance effects: Fort Bennings as a case study. Ecol Indicators 5:243-252

Odum HT (1956) Primary production in flowing waters. Limnol Oceanogr 1:102-117

Ostrom NE, Carrick HJ, Twiss MR (2005) Evaluation of primary production in Lake Erie by multiple proxies. Oecologia 145:669-669

Parker SR, Poulson SR, Gammons CH, Degrandpre MD (2005) Biogiochemicals controls on diel cycling of stable isotopes of dissolved O2 and dissolved inorganic carbon in the Big Hole River, Montana. Environ Sci Technol 39:7134-7140

Quay PD, Emerson S, Wilbur DO, Stump C (1993) The $\delta^{18}O$ of dissolved O_2 in the surface waters of the Subarctic pacific: A tracer of biological productivity. J Geophys Res 98:8447-8458

Quay PD, Wilbur DO, Richey JE, Devol AH, Benner R, Forsberg BR (1995) The ^{18}O:^{16}O of dissolved oxygen in rivers and lakes in the Amazon basin: Determining the ratio of respiration to photosynthesis rates in freshwaters. Limnol Oceanogr 40:718-729

Quiñones-Rivera ZJ, Wissel B, Justic D, Fry B (2007) Partitioning oxygen sources and sinks in a stratified, eutrophic coastal ecosystem using stable oxygen isotopes. Mar Ecol Progr Ser 342:69-83

Robinson C, Archer SD, Williams PJ leB (1999) Microbial dynamics in coastal waters of East Antarctica: Plankton production and respiration. Mar Ecol Progr Ser 180:23-36

Russ ME, Ostrom NE, Gandhi H, Ostrom PH, Urban NR (2004) Temporal and spatial variation in R:P ratios in Lake Superior, an oligotrophic freshwater environment. J Geophis Res C 109:C10S12

Stigebrandt A (1991) Computations of oxygen fluxes through the sea-surface and the net production of organic matter with application to the Baltic and adjacent seas. Limnol Oceanogr 36:444-454

Tobias CR, Böhlke JK, Harvey JW (2007) The oxygen-18 isotope approach for measuring aquatic metabolism in high-productivity waters. Limnol Oceanogr 52:1439-1453

Venkiteswaran JJ, Wassenaar LI, Schiff SL (2007) Dynamics of dissolved oxygen isotopic ratios: a transient model to quantify primary production, community respiration, and air-water exchange in aquatic ecosystems. Oecologia 153:385-398

Wetzel RG (2001) Limnology - lake and river ecosystems. Academic Press

CHAPTER 5
SUMMARY

The occurrence and severity of hypoxic events in many estuarine and coastal areas have increased during the last five decades, particularly in those areas affected by riverine freshwater inflows. Negative effects of hypoxia include loss of species diversity, mass mortalities of benthic organisms and, rarely, local species extinctions (Officer et al. 1984, Benović et al. 1987, Justić 1991, Rabalais and Turner 2001). These negative impacts on benthic fauna are expected to decrease food resources for demersal prey that rely on benthic organisms, including commercially important species such as many fishes and penaeid shrimps (Justić et al. 1996). Because of the potential ecological and economic impacts of hypoxia, the Mississippi River Watershed/Gulf of Mexico Hypoxia Task Force set a goal in 2001 to reduce the five year running average of the areal extent of the hypoxic zone in the northern Gulf of Mexico to less than 5,000 km^2 by the year 2015 (Rabalais et al. 2002). The proposed action plan suggested that a 30% reduction in nitrogen load is needed to reach this goal, and the implementation should be based on voluntary, incentive-based strategies applied to individual watersheds (Mitsch et al. 2001, Rabalais et al. 2002). Initial modeling results have generally suggested that reductions in nitrogen may indeed decrease the areal extent and severity of hypoxia (Scavia et al. 2004; Turner et al. 2006). However, uncertainties with respect to the importance of physical and biological factors that can act as sinks and sources of oxygen can limit the accuracy of models that attempts to forecast timing and extent of hypoxia. To better understand the development of hypoxia in the Gulf or Mexico, it is important to partition oxygen dynamics among the primary physical and biological processes that regulate the supply and consumption of oxygen to these waters. This study describes a new, integrated monitoring and modeling approach to the study of hypoxia in

the Northern Gulf of Mexico. The use of oxygen isotopes, along with conventional oxygen concentrations measurements, has proven to be a novel way to assess oxygen dynamics as it can complement and crosscheck conventional oxygen measurements due to its large signal associated with oxygen isotopes, from 15‰ to above 40‰. Because biological and physical processes influence oxygen stable isotopes dynamics in different ways, it is possible to effectively and accurately describe their roles in the development of hypoxia. Based on literature values and system-specific incubations, I developed a model that calculates productivity and respiration for surface waters, and the relative contribution of sediment (benthic) and water-column respiration.

During the initial survey across the Louisiana continental shelf in July 2001, bottom and surface waters showed intense oxygen dynamics, with a wide range of oxygen saturations between 180% and almost 0% and corresponding $\delta^{18}O$ values from 15‰ to 50‰. Generally, in surface waters where O_2 concentration was above saturation, isotope values were lower than 24.2‰, while in bottom waters low oxygen concentration or hypoxic conditions corresponded to $\delta^{18}O$ values higher than 24.2‰. Seasonal analyses showed that in fall and winter, oxygen dynamics was largely controlled by physical mixing, but during summer stratification, oxygen dynamics were controlled predominantly by biological processes. Model estimates indicated that during the summer 2001 shelfwide cruise, stratified surface waters were very productive with an average median calculated production/respiration (P/R) ratio of 1.12 and average gross and net primary productivities of 0.54 and 0.06 g C m^{-3} day^{-1}, respectively. In bottom waters, summer oxygen depletion was predominantly due to benthic respiration, accounting for about 73% of the total oxygen loss.

To further understand oxygen dynamics in the Gulf of Mexico, oxygen concentration measurements and stable oxygen isotopes values were used to explore how physical (wind, salinity, water temperature, pH) and biological (concentrations and C/N ratios of particulate organic matter) parameters affect the seasonal variability of oxygen dynamics in this area during the three consecutive years (2001 to 2003). For surface waters, multiple linear regression identified POC, C/N, and salinity (as proxy for nutrient flux) as significant predictors of $\delta^{18}O$ values. This indicated that biological parameters were important for surface oxygen dynamics not only during summer but also during winter. Surprisingly, temperature as indicator of seasonality was not a significant factor. The effects of physical factors on oxygen dynamics in surface waters were less obvious, except during severe physical disturbances, such as tropical storms and hurricanes when the complete water column experienced mixing. In contrast, oxygen dynamics in bottom waters showed strong seasonal trends. During summer, high oxygen depletion and larger contributions of benthic respiration were observed, which corresponded well to the strong stratification of the water column during this time. Depth stratified sampling (5 m intervals) showed that for surface layers $\delta^{18}O$ values were consistently lower than 24.2‰, and similar values extended 5 to 10 m into the water column. Elevated $\delta^{18}O$ values (26 to 40‰) dominated bottom waters even at 30-m deep stations were oxygen depletion did not reach hypoxic conditions. These depleted $\delta^{18}O$ values extended vertically into the water column to depths up to 10 m above the sediment, and also expanded laterally to neighboring stations that were not hypoxic. In addition, stratified sampling showed that productivity in the mixed layer (5 to 10 m) was not homogeneous. Calculated production to respiration ratios (P/R) exceeded a value of 1.0 only in the surface layer, while at 5 m P/R was approximately 1.0 and at a depth of

10 m, P/R was generally smaller than 1.0. With respect to bottom waters, hypoxic conditions could only be detected within 5 m of the sediment surface for the periods examined.

With respect to seasonality, the relationship between oxygen concentration and $\delta^{18}O$ in bottom waters was much stronger for winter months (October through March, $r^2 = 0.97$) than for summer months (April through September, $r^2 = 0.77$). Furthermore, net fractionation of bottom water respiration along transect C was much lower in the summer (-5.6‰) than in the winter (-12.8‰). Assuming that the fractionation factor of water column respiration was -22‰, benthic respiration was responsible for 42 and 75% of the total oxygen uptake during winter and summer months, respectively. Despite considerable overlap in oxygen saturations, the contributions of benthic respiration in bottom waters in the summer were noticeably larger and more variable than during winter. Therefore, it appeared that larger contributions of benthic respiration were associated with a strongly stratified water column that was only apparent in the summer.

The combined use of oxygen concentrations and stable isotope values to estimate the patterns of productivity and respiration in aquatic systems is appealing because it does not rely on time-consuming incubations that are necessary for methods that rely on CO_2 incorporation or oxygen concentration measurements alone (Grande et al. 1989). Therefore, productivity estimates can be achieved for large study areas within a fairly short time. The underlying mechanisms for calculating productivity and P/R were first described by Bender and Grande (1987). This work was significant because it laid out and parameterized the individual processes influencing both oxygen concentrations and stable isotope values during photosynthesis and respiration. The major shortcoming of the previous model was that it disregarded gas exchange with the atmosphere, mixing and the effects of benthic primary production. Therefore, I extended the original approach of Bender and Grande (1987) by including algorithms for gas-

exchange with the atmosphere, mixing and benthic primary production (BPP). Subsequently, I needed to evaluate the quality of the newly developed model by testing the sensitivity of the model to changes in input parameters across a range that is commonly observed for surface and bottom water dynamics across the Louisiana continental shelf.

For surface waters, the developed model showed the largest variability in response to changes in the fractionation factor (ε) of water column respiration. Fortunately, independent system-specific incubations revealed that variations in ε were small across the study area (-22 ± 0.7‰). The model was less sensitive to the range of values for wind speed and $\delta^{18}O$ of water (as proxy for salinity) that could be encountered during calm summer condition, as the range of P/R values was small for all tested scenarios. Hence, it is most crucial to obtain an accurate fractionation factor during calm summertime conditions, while small deviations of average wind speed or salinity based $\delta^{18}O$ values of water are less critical. For bottom waters different model simulations showed that mixing had almost no effect, but decreasing fractionation factors and increasing BPP would lower the calculated relative contribution of benthic to total respiration. However, system-specific fractionation was fairly constant and even an increase of ε by 10‰, or a 30% addition of oxygen due to BPP did not decrease the average contribution of benthic respiration by more than 11%. Yet, an even larger contribution BPP could eventually interfere with the model solutions, which could certainly be the case in shallow and/or less turbid systems. Nonetheless, for the Northern Gulf of Mexico, the model estimates of benthic respiration seemed sensible because the water column generally exceeds a depth of 10 m and water transparency is low due to high concentrations of suspended algae and sediments (Chapter 2). Overall, the dual budget approach yielded reasonable new estimates of productivity dynamics in surface waters and of sediment oxygen demand in bottom waters.

REFERENCES

Bender ML, Grande K (1987) Production, respiration and the isotope geochemistry of O_2 in the upper water column. Global Biogeochem. Cycles 1:49-59

Benović T, Justic D, Bender A (1987) Enigmatic changes in the hydromedusan fauna of the northern Adriatic Sea. Nature 326:597-600

Grande KD, Williams PJ, Marra J, Purdie DA, Heinemann K, Eppley RW, Bender ML (1989) Primary production in the North Pacific gyre: a comparison of rates determined by the ^{14}C, O_2 concentration and ^{18}O methods. Deep-Sea Res 36:1621-1634

Justić D (1991) Hypoxic conditions in the northern Adriatic Sea: Historical development and ecological significance, p. 95-105. In R.V. Tyson and T.H. Pearson (eds.), Modern and ancient continental shelf anoxia. Geol. Soc. Spec. Publ. 58, London.

Justić D, Rabalais NN, Turner RE (1996) Effects of climate change on hypoxia in coastal waters: A doubled CO_2 scenario for the northern Gulf of Mexico. Limnol. Oceanogr. 41:992-1003

Mitsch WJ, Day JW, Gilliam JW, Groffman PM, Hey DL, Randall GW, Wang N (2001) Reducing nitrogen loading to the Gulf of Mexico from the Mississippi River Basin: Strategies to counter a persistent ecological problem. BioScience 51:373-388

Officer, CC, Biggs RB, Taft JL, Cronin LE, Tyler M, Boynton WR (1984) Chesapeake Bay anoxia: origin, development and significance. Science 223:22-27

Quiñones-Rivera ZJ, Wissel B, Justic D, Fry B (2007) Partitioning oxygen sources and sinks in a stratified, eutrophic coastal ecosystem using stable oxygen isotopes. Mar Ecol Progr Ser 342:69-83

Rabalais NN, Turner RE (2001) Hypoxia in the northern Gulf of Mexico: Description, causes and change. In: Rabalais NN, Turner RE (eds) Coastal Hypoxia: consequences for living resources and ecosystems. Coastal and Estuarine Studies 58, American Geophysical Union, Washington D.C., p 1-36

Rabalais NN, Turner RE, Scavia D (2002) Beyond science into policy: Gulf of Mexico hypoxia and the Mississippi River. BioScience 52:129-142

Scavia D, Justic D, Bierman VJ (2004) Reducing hypoxia in the Gulf of Mexico: advice from three models. Estuaries 27:419-425

Turner RE, Rabalais NN, Justić D (2006) Predicting summer hypoxia in the northern Gulf of Mexico: riverine N, P, and Si loading. Mar Poll Bull 52:139-148

APPENDIX I
DATA

Sample	Date	Time	PAR	Depth m	Transect	IRMS δ18O ‰	IRMS O2 mg/L	Hydrolab O2 mg/L	Hydrolab Temp C	Hydrolab Salinity ‰	IRMS O2 %
AA1	Jul-01	1:11 PM	1497	0	AA	16.0	10.3	9.6	30.7	14.0	149.3
AA2	Jul-01	2:25 PM	1528	0	AA	15.6	11.8	13.2	30.0	17.3	171.7
AA3	Jul-01	3:22 PM	1271	0	AA	14.3	9.7	9.8	30.8	26.3	151.0
AA4	Jul-01	4:31 PM	1122	0	AA	22.1	6.5	6.9	30.6	30.4	102.6
AA5	Jul-01	5:27 PM	1003	0	AA	21.5	6.6	7.0	30.7	29.8	104.3
A7	Jul-01	7:57 PM	148	0	A	21.5	6.5	7.0	30.5	29.7	102.8
A6	Jul-01	9:08 PM	1	0	A	22.0	6.6	7.1	30.4	30.2	103.6
A5	Jul-01	10:10 PM	1	0	A	21.1	7.0	7.9	30.5	28.6	109.0
A4	Jul-01	11:06 PM	1	0	A	20.7	7.2	8.0	30.5	28.1	111.9
A3	Jul-01	11:55 PM	1	0	A	16.5	10.8	11.8	31.5	20.8	164.5
A2	Jul-01	12:56 AM	1	0	A	15.1	12.1	12.5	31.3	21.1	184.6
A1	Jul-01	1:43 AM	1	0	A	19.2	7.4	9.4	30.5	22.0	112.3
B1	Jul-01	5:16 AM	1	0	B	22.1	6.2	7.0	29.9	29.3	95.8
B2	Jul-01	5:46 AM	1	0	B	20.5	6.8	7.3	30.2	29.2	106.0
B4	Jul-01	6:47 AM	3	0	B	20.4	7.2	7.8	30.4	27.9	112.0
B6	Jul-01	8:11 AM	163	0	B	20.4	7.5	8.4	30.5	25.8	115.4
B8	Jul-01	9:08 AM	567	0	B	20.5	7.6	8.5	30.6	24.9	117.1
B9	Jul-01	10:17 AM	566	0	B	21.8	6.6	7.3	30.4	25.0	101.4
C9B	Jul-01	12:20 PM	715	0	C	21.5	6.9	7.4	30.5	24.4	105.2
C9	Jul-01	1:32 PM	1502	0	C	21.3	6.8	7.9	30.7	24.5	104.8
C8	Jul-01	2:25 PM	1600	0	C	21.5	6.8	7.6	30.8	26.0	105.0
C7	Jul-01	3:39 PM	608	0	C	20.2	7.5	8.1	31.0	25.5	115.5
C6B	Jul-01	4:58 PM	834	0	C	19.7	7.5	8.1	31.4	26.4	117.5
C5	Jul-01	6:25 PM	49	0	C	19.5	7.4	8.0	31.1	27.5	116.8
C4	Jul-01	7:11 PM	6	0	C	19.4	7.1	7.9	31.1	27.7	111.1
C3	Jul-01	8:05 PM	1	0	C	18.8	7.0	8.8	30.5	27.2	108.8
C1	Jul-01	9:10 PM	1	0	C	17.7	7.6	8.2	30.9	28.9	120.1
DD1	Jul-01	11:44 PM	1	0	DD	22.2	6.7	7.6	30.3	26.6	103.6
DD2	Jul-01	12:38 AM	1	0	DD	21.3	7.0	7.3	30.2	25.5	106.5
DD3	Jul-01	1:43 AM	1	0	DD	21.8	6.7	7.0	30.3	26.5	103.2
DD4	Jul-01	2:49 AM	1	0	DD	21.9	6.6	6.9	30.1	28.6	102.0
DD5	Jul-01	3:34 AM	1	0	DD	22.1	6.4	6.9	30.0	29.0	100.1
DD6	Jul-01	4:58 AM	1	0	DD	22.3	6.6	7.1	29.8	26.6	101.3
D6	Jul-01	7:03 AM	22	0	D	22.3	6.6	6.9	29.8	29.2	102.4
D5	Jul-01	8:11 AM	26	0	D	23.5	6.3	6.9	29.7	28.7	97.0
D4	Jul-01	9:22 AM	790	0	D	22.5	6.5	7.0	30.0	28.9	101.3
D3	Jul-01	10:34 AM	1117	0	D	21.4	6.9	7.5	30.3	28.4	107.8
D2	Jul-01	12:06 PM	1372	0	D	21.3	6.9	7.3	30.5	28.7	107.6
D1	Jul-01	1:23 PM	1430	0	D	21.1	6.7	7.2	30.6	28.4	104.5
D0	Jul-01	1:53 PM	1420	0	D	17.4	7.5	7.3	30.3	28.1	116.9
E1	Jul-01	4:36 PM	155	0	E	19.5	7.2	9.9	30.8	24.8	111.1
E2	Jul-01	5:45 PM	120	0	E	17.6	8.0	9.2	30.7	25.4	123.9
E2A	Jul-01	6:52 PM	71	0	E	19.7	7.3	7.9	30.4	26.9	112.7
E3	Jul-01	8:04 PM	36	0	E	20.7	6.7	7.0	30.5	29.4	104.4
E4	Jul-01	9:16 PM	1	0	E						0.0
F6	Jul-01	11:58 PM	1	0	F	21.5	6.9	7.1	30.0	27.0	106.4
F5	Jul-01	1:15 AM	1	0	F	22.9	6.2	6.9	29.9	28.5	96.5
F4	Jul-01	2:14 AM	1	0	F	22.1	6.4	7.0	29.9	28.6	99.4
F3	Jul-01	3:10 AM	1	0	F	21.1	6.7	7.2	29.8	28.5	104.3
F2	Jul-01	4:29 AM	1	0	F	20.6	7.3	8.7	30.6	24.6	111.5
F1	Jul-01	5:37 AM	1	0	F	23.7	6.0	7.7	30.5	22.8	90.4
F0	Jul-01	6:33 AM	3	0	F		5.9	6.5	29.9	22.6	88.1
G1	Jul-01	9:14 AM	739	0	G	22.9	6.3	7.8	30.4	23.1	95.4
G2	Jul-01	10:29 AM	1014	0	G	23.7	6.2	8.1	30.4	25.9	95.5
G3	Jul-01	11:50 AM	1310	0	G	23.2	6.4	7.2	30.4	26.8	98.6
G4	Jul-01	12:53 PM	1451	0	G	21.2	6.8	7.3	30.5	26.7	105.1
G5	Jul-01	2:02 PM	1494	0	G	21.4	6.7	7.2	30.5	27.5	103.8
H5	Jul-01	5:05 PM	978	0	H	19.8	7.3	7.9	30.8	23.1	110.8
H4	Jul-01	6:26 PM	506	0	H	17.9	8.0	8.5	30.6	26.4	123.4
H3	Jul-01	7:37 PM	137	0	H	17.6	7.5	7.7	31.1	25.7	117.1
H2	Jul-01	8:57 PM	1	0	H		7.1	7.3	30.9	26.7	110.3

Sample	Date	Time	PAR	Depth m	Transect	IRMS δ18O ‰	IRMS O2 mg/L	Hydrolab O2 mg/L	Hydrolab Temp C	Hydrolab Salinity ‰	IRMS O2 %
I1	Jul-01	12:31 AM	1	0	I	20.4	6.5	6.8	30.5	25.6	100.5
I2	Jul-01	1:44 AM	1	0	I	19.8	7.1	7.2	30.6	26.8	109.5
I3	Jul-01	2:57 AM	1	0	I	20.4	6.8	7.1	30.6	25.7	104.7
I4	Jul-01	4:14 AM	1	0	I	20.4	6.9	7.1	30.3	26.6	106.2
I5	Jul-01	5:36 AM	1	0	I	20.5	7.0	7.3	30.4	26.9	108.6
J6	Jul-01	8:07 AM	215	0	J	22.1	6.6	6.6	30.4	27.6	101.7
J5	Jul-01	9:27 AM	775	0	J	21.4	6.5	6.7	30.6	27.9	100.9
J4	Jul-01	11:01 AM	1188	0	J	21.8	6.5	7.0	30.5	27.5	100.7
J3	Jul-01	12:03 PM	1429	0	J	21.5	6.3	6.5	30.9	27.5	97.9
J2	Jul-01	1:09 PM	538	0	J	20.4	6.6	6.9	31.0	27.6	104.1
J1	Jul-01	2:17 PM	1470	0	J	19.9	6.8	7.2	31.5	27.3	107.2
AA1	Jul-01	1:11 PM	1497	b	AA	36.6	0.4	0.7	27.8	32.1	5.7
AA2	Jul-01	2:25 PM	1528	b	AA						0.0
AA3	Jul-01	3:22 PM	1271	b	AA	26.1	1.9	1.6	28.1	24.6	28.1
AA4	Jul-01	4:31 PM	1122	b	AA	25.6	4.9	5.4	22.9	36.0	70.0
AA5	Jul-01	5:27 PM	1003	b	AA	26.4	4.0	4.5	21.4	36.3	55.5
A7	Jul-01	7:57 PM	148	b	A	32.8	2.3	2.9	21.1	37.6	32.4
A6	Jul-01	9:08 PM	1	b	A	30.3	2.8	3.2	22.6	36.0	39.4
A5	Jul-01	10:10 PM	1	b	A						0.0
A4	Jul-01	11:06 PM	1	b	A	24.9	4.0	4.6	27.7	35.6	61.8
A3	Jul-01	11:55 PM	1	b	A	38.6	0.3	0.7	27.5	34.4	5.3
A2	Jul-01	12:56 AM	1	b	A		0.7	1.0	27.5	34.4	10.3
A1	Jul-01	1:43 AM	1	b	A	32.8	1.5	1.4	29.1	30.3	23.6
B1	Jul-01	5:16 AM	1	b	B	34.2	0.6	1.2	28.7	32.9	9.7
B2	Jul-01	5:46 AM	1	b	B	25.2	3.0	3.6	28.5	33.5	46.5
B4	Jul-01	6:47 AM	3	b	B	41.9	0.4	1.0	27.5	34.8	6.7
B6	Jul-01	8:11 AM	163	b	B	36.0	0.3	0.7	26.9	34.7	5.0
B8	Jul-01	9:08 AM	567	b	B	34.3	1.3	1.9	24.7	35.9	19.6
B9	Jul-01	10:17 AM	566	b	B	26.5	3.6	4.4	22.5	35.9	51.7
C9B	Jul-01	12:20 PM	715	b	C	27.6	2.8	3.1	24.3	36.0	41.5
C9	Jul-01	1:32 PM	1502	b	C	33.8	1.6	2.0	25.3	35.5	23.3
C8	Jul-01	2:25 PM	1600	b	C	25.3	3.7	3.8	26.7	36.4	56.6
C7	Jul-01	3:39 PM	608	b	C	49.7	0.2	0.8	26.9	35.0	3.1
C6B	Jul-01	4:58 PM	834	b	C	37.9	0.3	0.7	27.0	35.3	5.0
C5	Jul-01	6:25 PM	49	b	C		0.2	0.8	27.2	34.8	3.0
C4	Jul-01	7:11 PM	6	b	C						0.0
C3	Jul-01	8:05 PM	1	b	C	43.3	0.2	0.7	27.7	36.3	3.6
C1	Jul-01	9:10 PM	1	b	C	27.9	2.2	2.9	29.0	33.3	34.6
DD1	Jul-01	11:44 PM	1	b	DD	29.8	2.1	0.8	26.9	36.1	31.8
DD2	Jul-01	12:38 AM	1	b	DD	27.0	3.1	3.3	27.4	36.2	47.9
DD3	Jul-01	1:43 AM	1	b	DD	26.5	3.4	4.1	27.4	35.6	52.7
DD4	Jul-01	2:49 AM	1	b	DD	28.2	2.0	2.8	25.2	35.4	30.2
DD5	Jul-01	3:34 AM	1	b	DD	29.3	1.9	2.6	24.5	35.8	27.4
DD6	Jul-01	4:58 AM	1	b	DD	26.0	4.0	4.8	21.4	38.8	56.1
D6	Jul-01	7:03 AM	22	b	D	25.6	4.1	4.9	21.3	36.4	57.0
D5	Jul-01	8:11 AM	26	b	D	29.4	2.6	3.6	23.0	36.3	38.0
D4	Jul-01	9:22 AM	790	b	D	25.8	3.3	4.1	26.9	35.2	50.8
D3	Jul-01	10:34 AM	1117	b	D	32.9	0.6	1.1	27.3	35.1	8.9
D2	Jul-01	12:06 PM	1372	b	D	27.9	2.2	2.7	28.3	34.7	33.6
D1	Jul-01	1:23 PM	1430	b	D	28.5	0.6	0.8	28.5	33.6	8.7
D0	Jul-01	1:53 PM	1420	b	D	21.2	2.7	3.0	29.3	31.5	42.6
E1	Jul-01	4:36 PM	155	b	E	22.9	2.9	3.0	29.7	30.6	45.7
E2	Jul-01	5:45 PM	120	b	E	25.0	1.2	1.6	28.4	34.0	18.3
E2A	Jul-01	6:52 PM	71	b	E	26.8	1.3	2.0	27.9	36.5	20.9
E3	Jul-01	8:04 PM	36	b	E	38.9	0.7	1.3	26.8	36.0	10.9
E4	Jul-01	9:16 PM	1	b	E	28.9	2.7	3.7	22.9	35.9	39.2
F6	Jul-01	11:58 PM	1	b	F						0.0
F5	Jul-01	1:15 AM	1	b	F						0.0
F4	Jul-01	2:14 AM	1	b	F	32.1	1.5	2.2	25.9	36.2	23.1
F3	Jul-01	3:10 AM	1	b	F	36.1	0.8	1.6	26.4	35.2	12.8
F2	Jul-01	4:29 AM	1	b	F	29.8	2.0	2.6	29.6	30.9	30.4
F1	Jul-01	5:37 AM	1	b	F	29.3	2.8	3.5	29.9	28.1	43.0
F0	Jul-01	6:33 AM	3	b	F	25.0	2.5	2.5	30.0	25.9	37.8
G1	Jul-01	9:14 AM	739	b	G	24.6	3.3	2.3	30.0	29.1	50.6
G2	Jul-01	10:29 AM	1014	b	G	24.6	1.4	0.8	28.0	33.7	21.8
G3	Jul-01	11:50 AM	1310	b	G	27.8	1.4	1.7	26.5	35.0	20.5

Sample	Date	Time	PAR	Depth m	Transect	IRMS δ18O ‰	IRMS O2 mg/L	Hydrolab O2 mg/L	Hydrolab Temp C	Hydrolab Salinity ‰	IRMS O2 %
G4	Jul-01	12:53 PM	1451	b	G	28.5	2.0	2.7	25.7	35.4	30.0
G5	Jul-01	2:02 PM	1494	b	G	25.3	3.5	4.6	24.4	36.0	51.6
H5	Jul-01	5:05 PM	978	b	H						
H4	Jul-01	6:26 PM	506	b	H	45.5	0.2	0.8	25.1	36.3	3.0
H3	Jul-01	7:37 PM	137	b	H		0.1	0.8	27.1	34.5	2.1
H2	Jul-01	8:57 PM	1	b	H	30.9	0.8	1.6	29.4	30.7	13.0
H1	Jul-01	9:56 PM	1	b	H	25.2	2.4	3.3	29.7	31.4	37.2
I1	Jul-01	12:31 AM	1	b	I	39.3	0.3	0.9	29.1	31.7	4.0
I2	Jul-01	1:44 AM	1	b	I	47.6	0.2	0.7	28.7	32.6	3.1
I3	Jul-01	2:57 AM	1	b	I		0.1	1.3	27.7	34.8	2.0
I4	Jul-01	4:14 AM	1	b	I	36.9	0.8	1.4	27.8	34.4	12.4
I5	Jul-01	5:36 AM	1	b	I	32.1	1.5	2.2	27.1	35.1	23.1
J6	Jul-01	8:07 AM	215	b	J	25.8	3.4	4.0	27.4	35.2	52.7
J5	Jul-01	9:27 AM	775	b	J	27.9	2.7	3.5	28.2	33.9	41.7
J4	Jul-01	11:01 AM	1188	b	J	42.1	0.3	1.0	28.3	33.4	5.0
J3	Jul-01	12:03 PM	1429	b	J	28.8	0.7	1.3	29.1	32.4	10.8
J2	Jul-01	1:09 PM	538	b	J	31.5	0.3	0.9	29.2	31.9	5.3
J1	Jul-01	2:17 PM	1470	b	J		0.9	1.1	29.6	30.1	13.6
C1-s	Aug-01			0	C	24.0	6.1	6.2	28.6	27.7	92.6
C1-b	Aug-01			b	C	40.0	0.8	1.2	28.8	31.9	13.1
C3-s	Aug-01			0	C	23.5	6.9	6.7	28.6	27.7	104.2
C3-b	Aug-01			b	C	39.1	1.5	1.8	28.9	33.2	23.4
C4-s	Aug-01			0	C	21.9	8.3	7.6	28.9	27.3	126.0
C4-b	Aug-01			b	C	51.3	0.6	1.2	28.8	33.6	9.0
C5-s	Aug-01			0	C	23.4	7.4	7.3	29.2	27.8	112.7
C5-b	Aug-01			b	C	45.1	0.6	0.7	28.7	33.7	9.7
C6b-s	Aug-01			0	C	24.0	7.5	7.3	29.1	27.4	113.5
C6b-6.5m	Aug-01			7	C	25.2	6.8	6.5	29.0	29.5	103.9
C6b-14m	Aug-01			14	C	30.4	3.5	3.2	29.0	33.1	55.2
C6b-b	Aug-01			b	C	49.3	0.5	0.6	28.7	33.6	7.8
C6-s	Aug-01			0	C	21.3	9.2	8.1	29.5	26.5	140.6
C6-b	Aug-01			b	C	41.5	1.0	1.4	28.8	33.6	15.7
C7-s	Aug-01			0	C	26.4	6.7	7.1	29.4	28.4	102.2
C7-b	Aug-01			b	C	39.0	1.6	1.9	28.8	33.6	24.4
C8-b	Aug-01			b	C	32.7	3.4	3.5	27.0	35.0	51.5
C8-s	Aug-01			b	C	22.7	7.9	7.0	29.3	29.5	121.5
C9-s	Aug-01			0	C	22.3	8.1	7.0	29.4	29.3	124.7
C9-mid	Aug-01			15	C	27.9	5.2	4.2	28.8	33.0	80.8
C9-b	Aug-01			b	C	27.5	5.2	4.2	25.2	35.6	77.6
F0-s	Sep-01			0	F	22.4	7.2	6.6	28.7	27.8	109.1
F0-b	Sep-01			b	F	22.7	6.9	6.6	28.7	27.8	104.4
F1-s	Sep-01			0	F	23.2	7.0	6.4	28.5	28.5	105.7
F1-b	Sep-01			b	F	23.4	6.8	6.5	28.5	28.5	102.9
F2-s	Sep-01			0	F	22.1	9.7	6.5	28.8	29.0	148.5
F2-b	Sep-01			b	F	22.8	7.8	6.6	28.8	28.9	118.6
F3-b	Sep-01			b	F	45.7	2.7	6.1	28.9	30.4	41.3
F3-mid	Sep-01			10	F	24.2	7.0	6.1	28.9	30.4	107.1
F3-b	Sep-01			b	F	29.6	3.9	3.6	29.1	32.2	61.2
F4-s	Sep-01			0	F	22.1	9.1	6.4	29.0	32.3	142.3
F4-b	Sep-01			b	F	24.6	6.4	5.5	29.1	32.9	99.5
F5-s	Sep-01			0	F	23.9	7.0	5.6	29.0	33.8	110.4
F5-b	Sep-01			b	F	23.0	7.8	6.3	29.0	34.1	123.0
F6-s	Sep-01			0	F	23.6	7.3	6.0	28.9	33.2	114.0
F6-b	Sep-01			b	F	27.8	3.6	3.4	27.4	35.4	55.1
C1-s	Sep-01			0	C	24.2	6.3	6.2	28.2	26.8	93.5
C1-s	Sep-01			0	C	23.3	7.0	6.2	28.2	26.8	104.8
C1-b	Sep-01			b	C	29.8	3.6	2.2	28.7	29.4	55.3
C3-s	Sep-01			0	C	21.2	8.4	7.1	28.3	26.6	125.0
C3-b	Sep-01			b	C	21.9	8.2	7.1	28.9	31.2	126.4
C4-s	Sep-01			0	C	21.3	8.2	7.1	28.4	26.9	123.4
C4-b	Sep-01			b	C	24.3	6.5	5.4	28.9	31.5	100.0
C5-s	Sep-01			0	C	22.2	8.2	7.8	28.5	29.4	124.7
C5-b	Sep-01			b	C	25.3	5.9	5.0	28.9	31.6	91.4
C6b-s	Sep-01			0	C	21.8	8.3	7.1	29.0	30.4	127.7
C6b-6.5m	Sep-01			7	C	21.5	8.5	7.0	29.0	30.8	130.8
C6b-14m	Sep-01			14	C	23.3	7.5	6.0	28.9	31.1	116.5

Sample	Date	Time	PAR	Depth m	Transect	IRMS δ18O ‰	IRMS O2 mg/L	Hydrolab O2 mg/L	Hydrolab Temp C	Hydrolab Salinity ‰	IRMS O2 %
C6b-b	Sep-01			b	C	29.7	3.7	3.2	29.1	32.6	58.6
C6-s	Sep-01			0	C	21.0	9.5	7.3	28.9	30.2	145.3
C6-b	Sep-01			b	C	30.6	3.5	3.2	29.1	32.7	54.3
C7-s	Sep-01			0	C	20.4	9.0	8.5	29.1	29.5	138.0
C7-b	Sep-01			b	C	26.9	5.3	4.0	29.1	32.3	82.7
C8-s	Sep-01			0	C	21.7	8.5	7.3	29.5	30.5	132.8
C8-b	Sep-01			b	C	25.5	6.3	5.9	29.0	32.4	98.8
C9-s	Sep-01			0	C	21.2	8.4	7.1	29.5	30.2	129.7
C9-mid	Sep-01			15	C	25.0	7.0	6.0	29.0	31.9	108.5
C9-b	Sep-01			b	C	25.3	6.7	5.8	29.0	32.7	104.1
C1-b (A)	Oct-01			b	C	24.3	7.6	7.4	20.9	29.3	101.2
C1-s (A)	Oct-01			0	C	24.3	7.8	7.3	20.9	29.3	104.1
C3-b (A)	Oct-01			b	C	23.9	7.8	7.1	22.9	30.1	108.1
C3-s (A)	Oct-01			0	C	23.8	7.7	7.1	23.0	30.1	107.6
C4-b (A)	Oct-01			b	C	23.5	7.8	7.0	23.5	30.8	109.1
C4-s (A)	Oct-01			0	C	23.1	8.1	7.3	23.3	30.5	113.9
C5-b (A)	Oct-01			b	C	23.7	7.6	6.9	24.6	32.9	109.9
C5-s (A)	Oct-01			0	C	23.3	7.9	7.2	23.4	30.6	110.7
C6b-17m (A)	Oct-01			14	C	23.6	7.7	6.7	24.6	33.1	111.9
C6b-6.5m (A)	Oct-01			7	C	23.3	7.8	7.2	24.3	32.4	111.9
C6b-b (A)	Oct-01			b	C	23.8	7.5	6.6	24.6	33.1	108.3
C6b-s (A)	Oct-01			0	C	22.9	8.1	7.3	24.3	32.3	117.1
C7-b (A)	Oct-01			b	C	23.3	7.7	6.9	24.7	33.0	112.7
C7-s (A)	Oct-01			0	C	23.1	8.0	7.1	24.7	32.9	115.7
C8-b (A)	Oct-01			b	C	24.3	7.5	6.5	25.6	34.4	112.1
C8-s (A)	Oct-01			0	C	23.2	7.5	7.0	25.1	33.7	110.6
C9-b (A)	Oct-01			b	C	24.7	6.9	6.1	26.0	35.1	104.1
C9-mid (A)	Oct-01			15	C	23.9	7.4	6.7	25.5	34.2	109.8
C9-s (A)	Oct-01			0	C	23.5	7.8	6.8	25.3	34.1	114.9
C1-b (B)	Oct-01			b	C	24.4	7.5	7.4	20.9	29.3	99.8
C1-s (B)	Oct-01			0	C	24.3	7.5	7.3	20.9	29.3	99.5
C3-b (B)	Oct-01			b	C	23.9	7.6	7.1	22.9	30.1	105.7
C3-s (B)	Oct-01			0	C	23.8	7.6	7.1	23.0	30.1	106.3
C4-b (B)	Oct-01			b	C	23.6	7.7	7.0	23.5	30.8	108.4
C4-s (B)	Oct-01			0	C	23.1	8.0	7.3	23.3	30.5	112.4
C5-b (B)	Oct-01			b	C	23.6	7.5	6.9	24.6	32.9	108.3
C5-s (B)	Oct-01			0	C	23.4	7.8	7.2	23.4	30.6	109.6
C6b-17m (B)	Oct-01			14	C	23.6	7.6	6.7	24.6	33.1	110.6
C6b-6.5m (B)	Oct-01			7	C	23.4	7.9	7.2	24.3	32.4	113.3
C6b-b (B)	Oct-01			b	C	23.7	7.6	6.6	24.6	33.1	110.2
C6b-s (B)	Oct-01			0	C	22.9	8.0	7.3	24.3	32.3	114.6
C7-b (B)	Oct-01			b	C	23.3	7.8	6.9	24.7	33.0	113.4
C7-s (B)	Oct-01			0	C	23.1	7.9	7.1	24.7	32.9	115.1
C8-b (B)	Oct-01			b	C	24.4	7.3	6.5	25.6	34.4	108.5
C8-s (B)	Oct-01			0	C	23.2	7.7	7.0	25.1	33.7	112.8
C9-b (B)	Oct-01			b	C	24.7	6.7	6.1	26.0	35.1	101.6
C9-mid (B)	Oct-01			15	C	23.9	7.2	6.7	25.5	34.2	106.9
C9-s (B)	Oct-01			0	C	23.6	7.7	6.8	25.3	34.1	114.4
F0-s	Nov-02			0	F	21.0	10.2	9.1	21.2	15.0	125.4
F0-b	Nov-02			b	F	21.4	9.2	8.2	20.8	25.8	119.4
F1-s	Nov-02			0	F	21.8	9.5	8.4	21.6	22.7	123.6
F1-b	Nov-02			b	F	22.7	8.7	7.4	21.6	29.8	117.3
F2-s	Nov-02			0	F	23.0	8.8	7.6	22.4	30.7	121.2
F2-b	Nov-02			b	F	22.7	8.5	7.5	22.0	30.8	115.9
F3-s	Nov-02			0	F	22.7	8.8	7.5	22.6	30.9	122.4
F3-mid	Nov-02			10	F	22.5	8.6	7.1	22.8	33.6	121.0
F3-b	Nov-02			b	F	24.6	7.3	6.1	23.3	34.8	104.7
F4-s	Nov-02			0	F	22.3	8.7	7.4	22.9	32.7	122.8
F4-b	Nov-02			b	F	23.6	7.9	6.2	23.6	30.8	111.8
F5-s	Nov-02			0	F	23.5	8.3	6.9	24.2	35.9	121.4
F5-b	Nov-02			b	F	23.9	8.1	6.5	23.9	35.9	118.1
F6-s	Nov-02			0	F	23.8	8.1	6.8	24.6	36.1	120.5
F6-b	Nov-02			b	F	24.0	8.0	6.5	24.5	36.0	118.6
C1-s	Nov-02			0	C	22.0	8.7	7.5	21.8	30.5	118.4
C1-b	Nov-02			b	C	22.8	7.5	6.6	22.4	32.1	104.1
C3-s	Nov-02			0	C	22.3	8.9	7.5	21.7	29.9	120.0

Sample	Date	Time	PAR	Depth m	Transect	IRMS δ18O ‰	IRMS O2 mg/L	Hydrolab O2 mg/L	Hydrolab Temp C	Hydrolab Salinity ‰	IRMS O2 %
C3-b	Nov-02			b	C	25.8	6.4	5.4	22.9	33.8	90.2
C4-s	Nov-02			0	C	21.3	9.8	8.5	21.9	30.4	133.2
C4-b	Nov-02			b	C	24.5	7.4	6.0	23.0	34.3	105.0
C5-s	Nov-02			0	C	21.4	9.8	8.2	22.3	32.0	136.1
C5-b	Nov-02			b	C	24.4	7.5	6.2	23.1	34.9	107.4
C6b-s	Nov-02			0	C	23.0	8.8	7.5	22.5	33.4	123.7
C6b-6.5m	Nov-02			7	C	23.2	8.5	7.4	22.5	33.5	119.4
C6b-14m	Nov-02			14	C	23.7	8.1	6.6	23.1	35.2	115.6
C6b-b	Nov-02			b	C	24.3	7.8	6.2	23.1	35.2	111.5
C7-s	Nov-02			0	C	23.5	8.0	7.0	30.0	34.6	128.9
C7-b	Nov-02			b	C	23.7	8.3	6.6	23.2	35.2	119.4
C8-s	Nov-02			0	C	24.1	8.2	6.7	23.5	35.5	118.1
C8-b	Nov-02			b	C	24.1	8.0	6.7	23.4	35.3	115.9
C9-s	Nov-02			0	C	23.8	8.2	6.9	23.3	35.0	118.2
C9-mid	Nov-02			15	C	23.8	8.3	6.8	23.5	35.1	119.4
C9-b	Nov-02			b	C	24.3	8.0	6.4	23.8	35.6	116.5
C1-b	Dec-01			b	C	20.8	8.2	7.8	20.6	27.4	107.3
C1-s	Dec-01			0	C	19.7	9.1	9.1	20.8	27.0	119.6
C3-b	Dec-01			b	C	27.9	4.8	4.6	22.5	33.2	67.6
C3-s	Dec-01			0	C	19.5	9.3	9.6	20.9	26.7	122.0
C4-b	Dec-01			b	C	25.9	5.8	5.9	22.9	34.1	82.0
C4-s	Dec-01			0	C	19.8	9.1	9.5	21.0	27.0	119.7
C5-b	Dec-01			b	C	25.6	6.2	6.1	23.2	34.8	88.4
C5-s	Dec-01			0	C	20.1	8.8	8.9	21.1	27.3	116.9
C6b-14m	Dec-01			14	C	24.5	7.0	6.3	23.5	35.4	101.4
C6b-6.5m	Dec-01			7	C	25.0	6.6	6.1	22.9	34.2	93.8
C6b-b	Dec-01			b	C	24.9	6.7	6.5	23.5	35.4	96.6
C6b-s	Dec-01			0	C	21.5	8.4	8.7	21.4	28.5	112.5
C7-b	Dec-01			b	C	24.5	6.8	6.6	23.5	35.4	97.8
C7-s	Dec-01			0	C	22.6	7.9	7.6	22.3	32.7	110.6
C8-b	Dec-01			b	C	24.8	6.8	6.6	23.7	35.7	98.6
C8-s	Dec-01			0	C	23.0	7.9	7.7	21.8	31.0	107.8
C9-b	Dec-01			b	C	24.6	7.1	6.5	23.7	35.8	103.5
C9-mid	Dec-01			15	C	25.2	6.7	6.5	23.5	34.9	96.0
C9-s	Dec-01			0	C	23.2	7.9	7.5	21.8	31.2	108.8
F0-b	Dec-01			b	F	24.5	7.5	7.3	19.6	28.9	97.3
F0-s	Dec-01			0	F	24.2	7.8	8.2	18.5	33.7	101.4
F1-b	Dec-01			b	F	23.8	7.6	7.3	20.0	31.7	101.1
F1-s	Dec-01			0	F	23.7	7.7	7.5	19.0	25.8	96.7
F2-b	Dec-01			b	F	23.8	6.7	7.2	21.1	33.1	91.7
F2-s	Dec-01			0	F	23.5	7.2	7.3	21.0	33.0	98.1
F3-b	Dec-01			b	F	24.2	6.6	6.8	22.2	35.3	93.1
F3-mid	Dec-01			10	F	23.8	7.2	7.0	21.9	34.5	99.9
F3-s	Dec-01			0	F	23.1	7.5	7.3	21.5	33.8	104.1
F4-b	Dec-01			b	F	24.2	6.8	6.8	22.8	35.9	97.9
F4-s	Dec-01			0	F	23.2	7.6	7.3	21.7	34.4	106.0
F5-b	Dec-01			b	F	23.5	7.2	6.8	23.2	36.3	103.5
F5-s	Dec-01			0	F	23.5	7.2	7.0	22.9	36.2	103.5
F6-b	Dec-01			b	F	24.0	6.7	6.7	23.5	36.4	97.1
F6-s	Dec-01			0	F	23.8	6.8	6.8	23.5	36.4	99.4
C1-s	Jan-02			0	C	18.1	10.6	11.4	15.7	26.4	125.2
C1-b	Jan-02			b	C	20.5	9.2	9.0	15.4	27.3	108.8
C3-s	Jan-02			0	C	19.0	10.0	11.0	17.0	30.2	123.9
C3-b	Jan-02			b	C	21.4	8.5	8.7	16.8	31.2	106.3
C4-s	Jan-02			0	C	18.6	9.6	11.1	17.3	30.6	119.7
C4-b	Jan-02			b	C	25.0	6.5	6.4	17.5	32.3	82.8
C5-s	Jan-02			0	C	18.6	10.2	11.1	17.2	30.4	127.5
C5-b	Jan-02			b	C	25.9	6.4	6.7	18.1	33.2	82.5
C6-s	Jan-02			0	C	20.0	9.7	10.2	16.8	30.1	119.7
C6-b	Jan-02			b	C	25.4	6.6	6.9	18.2	33.3	85.3
C6b-s	Jan-02			0	C	19.4	9.5	10.7	16.8	30.2	117.6
C6b-6.5m	Jan-02			7	C	21.8	9.1	9.1	16.9	31.9	114.3
C6b-14m	Jan-02			14	C	23.3	7.8	8.2	17.4	32.3	99.0
C6b-b	Jan-02			b	C	25.5	6.7	6.9	18.2	33.4	87.0
C7-s	Jan-02			0	C	20.9	8.7	9.7	16.7	29.4	107.6
C7-b	Jan-02			b	C	26.1	6.3	6.5	18.6	33.5	82.8

Sample	Date	Time	PAR	Depth m	Transect	IRMS δ18O ‰	IRMS O2 mg/L	Hydrolab O2 mg/L	Hydrolab Temp C	Hydrolab Salinity ‰	IRMS O2 %
C8-s	Jan-02			0	C	22.3	7.9	8.8	16.7	30.2	98.3
C8-b	Jan-02			b	C	27.9	4.8	5.3	20.5	35.9	66.6
C9-s	Jan-02			0	C	23.3	8.2	8.1	17.7	31.3	104.0
C9-mid	Jan-02			15	C	25.9	6.4	6.4	20.6	34.8	87.6
C9-b	Jan-02			b	C	24.6	7.0	6.8	20.1	36.1	96.1
C1-b	Feb-02			b	C	23.2	8.3	8.8	15.6	28.3	99.5
C1-s	Feb-02			0	C	22.6	8.7	9.1	15.6	27.7	103.8
C3-b	Feb-02			b	C	23.3	8.0	8.5	16.0	28.8	96.9
C3-s	Feb-02			0	C	22.7	8.5	8.9	16.0	28.0	101.6
C4-b	Feb-02			b	C	23.4	8.0	8.6	16.2	28.9	97.6
C4-s	Feb-02			0	C	23.2	8.3	8.7	16.2	28.5	100.7
C5-b	Feb-02			b	C	26.8	5.6	5.8	18.6	32.5	73.3
C5-s	Feb-02			0	C	23.2	8.2	8.4	16.7	29.7	101.4
C6-b	Feb-02			b	C	29.0	4.7	4.9	20.3	35.1	63.9
C6b-14m	Feb-02			14	C	28.5	4.8	4.9	20.1	34.7	65.6
C6b-6.5m	Feb-02			7	C	23.4	7.7	8.1	17.9	32.4	99.0
C6b-b	Feb-02			b	C	28.7	4.6	5.0	20.2	34.9	62.6
C6b-s	Feb-02			0	C	23.4	7.8	8.0	17.9	32.4	99.6
C6-s	Feb-02			0	C	23.3	7.7	8.0	17.9	32.6	99.1
C7-b	Feb-02			b	C	27.7	5.2	5.4	20.4	35.3	71.4
C7-s	Feb-02			0	C	23.3	7.7	7.8	18.3	33.6	99.5
C8-b	Feb-02			b	C	25.5	6.4	6.5	20.4	35.8	87.1
C8-s	Feb-02			0	C	23.5	7.6	7.7	18.6	33.9	99.3
C9-b	Feb-02			b	C	25.5	6.4	6.5	20.7	36.0	88.2
C9-mid	Feb-02			15	C	23.7	6.8	7.1	20.2	35.5	92.6
C9-s	Feb-02			0	C	23.3	7.6	7.8	18.8	34.3	100.2
F0-b	Feb-02			b	F	25.7	7.4	8.2	13.2	20.4	79.6
F0-s	Feb-02			0	F	24.9	8.5	9.3	12.1	13.7	85.9
F1-b	Feb-02			b	F	26.5	6.2	6.7	16.1	29.6	75.1
F1-s	Feb-02			0	F	24.4	8.8	9.8	12.3	13.1	89.6
F2-b	Feb-02			b	F	23.9	7.9	8.1	14.8	25.6	91.6
F2-s	Feb-02			0	F	22.8	9.1	10.3	13.3	18.0	97.3
F3-b	Feb-02			b	F	27.2	5.7	6.1	18.8	34.4	75.1
F3-mid	Feb-02			10	F	24.1	7.8	8.0	16.3	31.1	95.9
F3-s	Feb-02			0	F	22.0	8.6	9.7	14.8	25.8	99.7
F4-b	Feb-02			b	F	26.8	6.0	6.1	19.7	35.2	80.5
F4-s	Feb-02			0	F	22.3	8.9	9.4	15.2	27.5	105.2
F5-b	Feb-02			b	F	26.5	6.1	6.2	20.1	35.6	82.8
F5-s	Feb-02			0	F	23.3	8.1	8.3	16.9	31.5	101.5
F6-b	Feb-02			b	F	25.3	6.6	6.7	20.4	36.1	91.2
F6-s	Feb-02			0	F	23.4	7.4	9.4	19.2	35.2	98.4
C1-s	Mar-02			0	C	21.8	9.4	9.6	16.3	27.6	114.1
C1-b	Mar-02			b	C	21.9	9.0	9.1	16.0	27.7	107.6
C3-s	Mar-02			0	C	21.8	9.4	9.2	17.0	30.0	116.0
C3-b	Mar-02			b	C	21.6	8.8	8.8	16.9	30.2	109.4
C4-s	Mar-02			0	C	21.3	9.4	9.4	17.5	31.5	119.1
C4-b	Mar-02			b	C	21.7	9.2	8.8	17.1	31.7	115.3
C5-s	Mar-02			0	C	22.4	8.8	8.7	18.0	33.1	113.8
C5-b	Mar-02			b	C	22.5	8.7	8.7	17.8	33.1	111.3
C6b-s	Mar-02			0	C	22.9	8.4	8.3	18.4	33.7	108.8
C6b-6.5m	Mar-02			7	C	22.7	8.3	8.3	18.3	33.7	108.6
C6b-14m	Mar-02			14	C	23.0	7.6	8.2	18.2	33.7	98.9
C6b-b	Mar-02			b	C	22.9	8.3	8.2	18.2	33.7	108.4
C7-s	Mar-02			0	C	22.1	8.5	8.6	18.5	33.1	110.8
C7-b	Mar-02			b	C	23.7	7.6	7.7	18.6	34.0	99.6
C8-s	Mar-02			0	C	22.8	7.8	8.6	17.7	31.3	99.2
C8-b	Mar-02			b	C	24.1	7.6	7.4	18.7	34.2	99.3
C9-b	Mar-02			b	C	24.8	7.2	6.3	19.3	34.7	95.5
C1-s	Apr-02			0	C	21.1	9.0	8.1	22.5	23.8	118.9
C3-s	Apr-02			0	C	19.3	11.1	9.6	22.1	24.3	146.5
C3-b	Apr-02			b	C	24.0	7.9	7.0	21.2	27.8	104.7
C4-s	Apr-02			0	C	20.9	9.3	8.8	22.0	26.5	124.4
C4-b	Apr-02			b	C	24.8	6.8	6.3	21.6	31.3	92.7
C5-s	Apr-02			0	C	21.7	8.5	8.3	22.5	26.5	113.9
C5-b	Apr-02			b	C	24.6	6.8	6.0	21.9	34.9	94.9
C6b-s	Apr-02			0	C	22.8	8.3	8.0	21.8	29.9	112.6

Sample	Date	Time	PAR	Depth m	Transect	IRMS δ18O ‰	IRMS O2 mg/L	Hydrolab O2 mg/L	Hydrolab Temp C	Hydrolab Salinity ‰	IRMS O2 %
C6b-6.5m	Apr-02			7	C	21.3	8.6	8.1	22.2	32.3	119.4
C6b-14m	Apr-02			14	C	23.0	8.0	7.2	22.4	35.3	113.4
C6b-b	Apr-02			b	C	26.6	5.6	5.8	21.7	35.3	78.8
C7-s	Apr-02			0	C	21.0	8.4	8.4	22.2	32.1	115.9
C7-b	Apr-02			b	C	24.5	6.8	6.1	22.0	35.4	95.1
C8-s	Apr-02			0	C	21.6	8.3	7.9	22.2	33.7	116.4
C8-b	Apr-02			b	C	25.0	6.4	6.0	22.1	35.4	90.6
C9-s	Apr-02			0	C	22.3	7.9	7.7	22.1	34.0	110.6
C9-mid	Apr-02			15	C	23.3	7.6	7.1	23.1	35.5	108.8
C9-b	Apr-02			b	C	23.8	7.1	6.8	22.5	36.0	100.8
F0-s	Apr-02			0	F	24.5	7.0	6.5	21.1	21.3	88.7
F0-b	Apr-02			b	F	24.7	6.4	6.2	21.1	21.6	81.8
F1-s	Apr-02			0	F	22.9	7.5	7.8	21.3	23.9	97.1
F1-b	Apr-02			b	F	22.8	7.6	7.5	21.2	24.0	98.9
F2-s	Apr-02			0	F	23.1	7.7	7.6	21.8	24.6	100.8
F2-b	Apr-02			b	F	23.3	7.2	7.0	21.3	21.7	92.4
F3-s	Apr-02			0	F	23.0	7.3	7.4	22.3	29.3	99.5
F3-mid	Apr-02			10	F	24.7	6.7	6.6	21.4	31.8	90.6
F3-b	Apr-02			b	F	24.6	6.2	6.8	21.6	34.6	85.6
F4-s	Apr-02			0	F	21.4	7.9	8.1	22.4	30.7	108.8
F5-s	Apr-02			0	F	23.4	7.2	7.1	23.1	35.7	103.2
F5-b	Apr-02			b	F	24.0	7.0	6.9	22.2	35.8	99.6
F6-s	Apr-02			0	F	23.6	7.1	7.0	23.9	36.0	103.8
C1-s	May-02			0	C	17.8	10.1	9.6	28.8	13.6	141.8
C1-b	May-02			b	C	17.7	10.3	8.2	28.2	15.0	143.6
C3-s	May-02			0	C	18.1	10.2	9.3	28.9	16.1	144.9
C3-b	May-02			b	C	40.7	0.8	0.9	24.1	35.4	12.2
C4-s	May-02			0	C	21.9	8.5	7.5	27.7	24.0	124.5
C4-b	May-02			b	C	26.3	7.5	2.5	24.8	35.1	110.0
C5-s	May-02			0	C	22.8	8.2	7.1	27.7	31.0	124.7
C5-b	May-02			b	C	27.9	3.7	2.6	24.3	35.3	54.3
C6-s	May-02			0	C	23.1	8.1	6.9	26.7	33.4	121.8
C6-b	May-02			b	C	30.6	3.0	2.2	23.8	35.3	44.2
C6b-s	May-02			0	C	23.2	8.2	7.0	26.8	33.2	123.4
C6b-6.5	May-02			7	C	23.3	7.8	6.9	26.6	34.2	118.2
C6b-14	May-02			14	C	24.1	6.5	5.9	25.9	34.6	97.6
C6b-b	May-02			b	C	31.5	2.6	2.3	23.8	35.3	37.5
C7-s	May-02			0	C	23.2	7.7	6.9	26.4	32.7	115.4
C7-b	May-02			b	C	28.4	3.4	3.0	23.4	35.6	48.8
C8-s	May-02			0	C	23.4	8.2	6.9	26.8	34.1	124.3
C8-b	May-02			b	C	24.3	6.8	5.5	23.4	35.8	98.9
C9-s	May-02			0	C	23.2	7.9	6.9	26.5	34.1	119.5
C9-m	May-02			15	C	23.4	7.2	6.2	23.5	35.1	103.4
C9-b	May-02			b	C	24.7	6.9	6.0	23.4	36.0	99.4
C3-s	Jun-02			0	C	17.2	12.7	12.3	30.3	16.2	184.8
C3-5m	Jun-02			5	C	26.3	6.7	6.3	26.7	22.3	94.6
C3-b	Jun-02			b	C	33.8	0.7	0.4	25.4	34.2	9.7
C6b-s	Jun-02			0	C	26.8	6.7	6.3	27.8	32.1	102.6
C6b-5m	Jun-02			5	C	26.4	5.2	6.5	27.5	34.5	79.8
C6b-10m	Jun-02			10	C	26.1	4.2	5.6	26.2	35.6	63.6
C6b-15m	Jun-02			15	C	28.8	4.4	3.9	25.6	35.9	66.4
C6b-b	Jun-02			b	C	29.1	3.1	2.9	25.6	35.9	47.2
C7-s	Jun-02			0	C	27.2	6.8	6.4	27.7	33.7	103.8
C7-5m	Jun-02			5	C	27.4	7.0	6.4	27.4	34.8	107.9
C7-10m	Jun-02			10	C	27.5	6.9	6.4	27.4	35.1	106.7
C7-15m	Jun-02			15	C	27.0	6.9	6.5	27.2	35.4	105.5
C7-b	Jun-02			b	C	27.7	4.3	4.2	26.0	35.8	64.7
C9-s	Jun-02			0	C	27.3	6.7	6.3	27.1	35.5	103.6
C9-5m	Jun-02			5	C	27.2	6.5	6.3	27.1	35.5	100.0
C9-10m	Jun-02			10	C	27.6	6.8	6.3	27.3	35.6	104.8
C9-15m	Jun-02			15	C	27.3	6.7	6.3	27.3	35.6	103.5
C9-20m	Jun-02			20	C	27.9	6.8	6.4	27.1	35.7	104.8
C9-25m	Jun-02			25	C	25.8	6.7	6.1	26.3	36.0	102.3
C9-b	Jun-02			b	C	25.3	6.8	6.2	26.1	36.1	103.1
F2-s	Jun-02			0	F	23.8	7.3	7.7	28.8	21.2	106.1
F2-5m	Jun-02			5	F	24.0	7.0	6.6	28.3	21.7	101.2

Sample	Date	Time	PAR	Depth m	Transect	IRMS δ18O ‰	IRMS O2 mg/L	Hydrolab O2 mg/L	Hydrolab Temp C	Hydrolab Salinity ‰	IRMS O2 %
F2-b	Jun-02			b	F	24.7	6.5	6.6	28.2	22.0	93.9
F3-s	Jun-02			0	F	26.0	6.7	6.6	28.6	31.7	104.0
F3-5m	Jun-02			5	F	26.5	6.7	6.7	28.2	31.9	102.9
F3-10m	Jun-02			10	F	27.3	6.7	6.5	27.8	34.9	103.5
F3-15m	Jun-02			15	F	27.4	6.6	6.4	27.3	35.4	101.2
F3-b	Jun-02			b	F	27.2	6.6	5.7	27.0	35.6	101.9
F5-s	Jun-02			0	F	27.5	6.6	6.4	28.2	35.5	103.3
F5-5m	Jun-02			5	F	27.4	6.8	6.5	28.0	35.5	105.2
F5-10m	Jun-02			10	F	27.7	6.7	6.5	27.8	35.5	104.3
F5-15m	Jun-02			15	F	27.5	6.7	6.5	27.6	35.5	103.3
F5-20m	Jun-02			20	F	26.7	6.8	6.6	26.9	35.6	103.9
F5-25m	Jun-02			25	F	25.5	6.9	6.8	26.8	35.8	105.4
F5-b	Jun-02			b	F	25.6	7.0	6.8	26.8	35.8	107.8
F6-s	Jun-02			0	F	27.8	6.6	6.5	28.0	35.4	103.7
F6-5m	Jun-02			5	F	27.8	6.7	6.5	27.9	35.5	104.2
F6-10m	Jun-02			10	F	27.8	6.7	6.6	27.3	35.4	102.7
F6-15m	Jun-02			15	F	27.5	6.9	6.6	26.8	35.8	105.1
F6-20m	Jun-02			20	F	27.5	6.9	6.7	26.7	35.8	105.9
F6-25m	Jun-02			25	F	27.6	7.0	6.7	26.6	35.9	106.1
F6-30m	Jun-02			30	F	27.4	7.0	6.8	26.0	35.8	106.5
F6-35m	Jun-02			35	F	25.4	7.5	7.0	25.6	35.9	112.6
F6-b	Jun-02			b	F	25.0	7.5	7.0	25.6	35.9	113.4
AA2-s	Jul-02	0.60	1104	0	AA	14.7	10.1		32.7	14.7	151.4
AA2-5m	Jul-02			5	AA	23.3	5.9	6.8	30.5	28.9	91.8
AA2-b	Jul-02			b	AA	26.3	1.3	0.5	28.0	33.2	20.0
AA4-s	Jul-02	0.69	200	0	AA	18.1	8.2		33.7	16.4	126.3
AA4-5m	Jul-02			5	AA	20.8	7.0	7.3	30.7	27.5	109.2
AA4-10m	Jul-02			10	AA	26.2	5.3	5.6	29.1	34.0	83.9
AA4-15m	Jul-02			15	AA	24.7	5.9	6.0	29.1	34.7	93.0
AA4-20m	Jul-02			20	AA	33.0	1.1	1.2	27.4	34.6	17.6
AA4-25m	Jul-02			25	AA	35.9	1.6	1.7	26.5	35.0	23.6
AA4-b	Jul-02			b	AA	30.0	3.7	4.0	23.7	35.4	53.5
A2-s	Jul-02	1.03	1	0	A	18.1	7.3	7.9	32.5	20.5	112.1
A2-5m	Jul-02			5	A	21.2	5.5	5.4	30.1	30.7	87.1
A2-b	Jul-02			b	A	28.5	1.4	0.8	28.2	33.1	21.9
A4-s	Jul-02	0.97	1	0	A	21.8	6.9	7.2	32.1	23.0	107.2
A4-5m	Jul-02			5	A	22.4	5.7	6.9	30.6	28.4	89.6
A4-10m	Jul-02			10	A	28.1	4.4	4.7	28.9	33.6	68.7
A4-15m	Jul-02			15	A		0.6	0.7	27.3	34.5	9.1
A4-b	Jul-02			b	A	45.5	0.2	0.4	27.0	34.8	3.1
A5-s	Jul-02	0.92	1	0	A	21.7	6.9	7.3	31.9	22.8	107.6
A5-5m	Jul-02			5	A	21.2	6.6	5.7	29.5	31.9	104.1
A5-10m	Jul-02			10	A	23.8	6.1	6.2	29.2	34.4	96.3
A5-15m	Jul-02			15	A	24.3	6.1	6.3	28.9	34.9	95.9
A5-20m	Jul-02			20	A	24.6	5.2	5.5	28.1	35.0	81.7
A5-25m	Jul-02			25	A	27.5	2.6	1.9	26.9	35.2	40.0
A5-b	Jul-02			b	A	35.5	0.4	0.4	25.6	35.4	5.8
A6-s	Jul-02	0.78	1	0	A	20.7	6.9	7.5	32.2	25.9	109.7
A6-5m	Jul-02			5	A	20.4	7.0	7.3	30.9	27.1	109.6
A6-10m	Jul-02			10	A	24.2	6.0	6.2	29.1	34.7	95.2
A6-15m	Jul-02			15	A	24.5	6.0	6.2	28.9	34.8	95.0
A6-20m	Jul-02			20	A	24.2	6.0	6.1	28.3	34.9	93.3
A6-25m	Jul-02			25	A	27.8	2.5	3.3	27.2	35.2	39.2
A6-30m	Jul-02			30	A	33.6	1.6	2.0	26.6	35.3	24.7
A6-35m	Jul-02			35	A	35.4	1.3	0.9	23.4	35.5	18.5
A6-b	Jul-02			b	A	47.3	0.7	0.9	23.2	35.5	10.7
MR-3PSU	Jul-02			0	MR	23.8	11.7			3.0	82.0
MR-5PSU	Jul-02			0	MR	23.9	10.9			5.0	77.5
MR-4	Jul-02			0	MR	19.1	13.8			15.0	104.5
MR-5	Jul-02			0	MR	20.2	13.1			25.0	106.3
B2-s	Jul-02	1.24	36	0	B	22.4	6.3	6.8	31.7	28.1	100.5
B2-5m	Jul-02			5	B	22.2	6.3	6.8	31.7	28.2	100.6
B2-b	Jul-02			b	B	22.0	6.5	6.7	31.6	28.4	102.6
B6-s	Jul-02	1.32	118	0	B	22.6	6.4	6.8	31.1	28.3	101.4
B6-15m	Jul-02			15	B	21.4	6.3	6.9	31.1	28.5	99.3
B6-5m	Jul-02			5	B	32.4	5.9	6.3	29.7	32.6	92.5

Sample	Date	Time	PAR	Depth m	Transect	IRMS δ18O ‰	IRMS O2 mg/L	Hydrolab O2 mg/L	Hydrolab Temp C	Hydrolab Salinity ‰	IRMS O2 %
B6-10m	Jul-02			10	B	26.0	4.5	4.9	28.3	34.9	69.9
B6-b	Jul-02			b	B	34.3	1.3	1.3	27.4	34.9	20.0
B8-s	Jul-02	1.36	660	0	B	22.7	6.5	6.7	30.9	28.8	103.2
B8-5m	Jul-02			5	B	22.5	6.3	6.7	31.0	29.0	99.1
B8-10m	Jul-02			10	B	22.2	6.6	6.9	30.1	32.0	104.6
B8-15m	Jul-02			15	B	23.2	6.1	6.2	29.2	34.4	96.4
B8-20m	Jul-02			20	B	23.8	6.0	6.1	28.1	35.1	94.3
B8-25m	Jul-02			25	B	26.1	2.9	3.6	27.1	35.2	43.8
B8-b	Jul-02			b	B	30.6	1.9	2.2	26.8	35.2	28.4
B9-s	Jul-02	1.51	1334	0	B	22.6	6.7	6.9	30.8	29.3	105.4
B9-5m	Jul-02			5	B	22.3	6.6	6.9	30.7	29.3	104.7
B9-10m	Jul-02			10	B	23.3	6.2	6.4	29.6	33.8	98.1
B9-15m	Jul-02			15	B	24.1	5.9	6.3	29.3	34.7	94.0
B9-20m	Jul-02			20	B	24.1	5.2	5.7	28.1	35.0	80.5
B9-25m	Jul-02			25	B	24.8	5.1	5.6	27.5	35.1	78.7
B9-30m	Jul-02			30	B	25.2	4.8	5.0	26.1	35.4	71.8
B9-35m	Jul-02			35	B	26.5	4.4	4.8	24.4	35.5	64.8
B9-b	Jul-02			b	B	26.6	4.4	4.6	23.7	35.5	63.4
C3-s	Jul-02	1.82	1	0	C	18.9	7.2	7.6	31.7	25.2	113.2
C3-5m	Jul-02			5	C	25.7	4.6	4.6	30.1	30.7	72.2
C3-b	Jul-02			b	C	30.5	0.5	0.4	28.3	34.0	7.4
C6b-s	Jul-02	1.70	86	0	C	20.7	6.8	7.2	31.8	25.9	107.7
C6b-5m	Jul-02			5	C	20.4	4.5	6.7	31.3	26.6	70.3
C6b-10m	Jul-02			10	C		2.6	2.2	28.1	34.2	39.8
C6b-15m	Jul-02			15	C	25.1	0.8	0.4	27.7	34.9	12.7
C6b-b	Jul-02			b	C	34.4	0.4	0.4	27.7	35.0	5.8
C9-s	Jul-02	1.55	1305	0	C	21.5	6.8	7.2	32.1	25.0	106.3
C9-5m	Jul-02			5	C	21.6	6.5	6.8	31.4	27.0	102.8
C9-10m	Jul-02			10	C	23.5	6.3	6.4	28.9	34.6	99.1
C9-15m	Jul-02			15	C	23.8	6.2	6.2	28.6	34.8	96.9
C9-20m	Jul-02			20	C	24.0	6.0	6.2	28.0	34.9	93.4
C9-25m	Jul-02			25	C	24.8	4.5	6.0	27.5	35.0	69.9
C9-b	Jul-02			b	C	27.5	3.5	3.9	26.6	35.2	53.6
DD3-s	Jul-02	2.06	1	0	DD	22.6	6.5	6.8	31.3	26.2	102.1
DD3-5m	Jul-02			5	DD	22.1	6.5	6.3	31.0	28.0	101.6
DD3-10m	Jul-02			10	DD	22.6	6.1	1.7	28.6	33.6	94.8
DD3-15m	Jul-02			15	DD	24.6	5.0	5.3	28.4	34.8	78.7
DD3-b	Jul-02			b	DD	24.7	4.9	5.1	28.3	34.9	75.9
DD4-s	Jul-02	2.12	1	0	DD	22.6	6.4	6.7	31.5	26.3	100.3
DD4-5m	Jul-02			5	DD	22.0	6.2	6.6	31.5	27.0	98.4
DD4-10m	Jul-02			10	DD	23.1	6.0	6.2	29.3	34.4	95.5
DD4-15m	Jul-02			15	DD	23.1	6.1	6.3	28.9	34.7	96.7
DD4-20m	Jul-02			20	DD	23.7	6.0	6.2	28.3	35.0	94.3
DD4-25m	Jul-02			25	DD	25.0	4.0	5.1	27.2	35.1	61.5
DD4-b	Jul-02			b	DD	28.5	2.4	2.8	26.4	35.3	36.5
D1-s	Jul-02	2.48	1340	0	D	21.3	6.5	6.9	32.7	22.3	101.9
D1-5m	Jul-02			5	D	21.8	3.9	1.2	30.4	28.5	61.2
D1-b	Jul-02			b	D	36.4	0.3	0.4	28.8	32.7	5.0
D3-s	Jul-02	2.34	711	0	D	22.5	6.5	6.7	31.1	24.7	99.9
D3-5m	Jul-02			5	D	21.8	5.9	6.3	31.0	26.2	91.3
D3-10m	Jul-02			10	D	21.9	1.2	1.4	28.5	33.7	18.0
D3-b	Jul-02			b	D	40.2	0.2	0.4	27.0	34.8	3.4
D4-s	Jul-02	2.29	203	0	D	21.3	6.7	7.1	31.2	25.9	105.2
D4-5m	Jul-02			5	D	23.1	5.7	6.0	30.1	29.9	88.7
D4-10m	Jul-02			10	D	22.7	4.7	4.6	29.3	32.0	73.4
D4-15m	Jul-02			15	D	24.7	4.3	4.7	28.5	34.5	66.6
D4-b	Jul-02			b	D	24.9	4.2	4.5	28.3	34.7	64.9
D5-s	Jul-02	2.23	28	0	D	19.7	7.5	7.8	31.5	27.4	118.4
D5-5m	Jul-02			5	D	19.5	7.2	7.8	31.5	27.9	114.0
D5-10m	Jul-02			10	D	20.6	5.9	5.9	29.9	31.2	92.5
D5-15m	Jul-02			15	D	23.0	4.7	6.2	29.2	34.3	74.4
D5-20m	Jul-02			20	D	23.3	5.7	5.6	28.2	34.8	89.4
D5-25m	Jul-02			25	D	25.2	3.6	4.3	27.1	35.1	54.9
D5-b	Jul-02			b	D	28.6	2.7	3.0	26.4	35.2	40.3
E2-s	Jul-02	2.67	721	0	E	20.4	7.2	7.6	32.0	21.7	111.1
E2-5m	Jul-02			5	E	19.8	5.9	5.8	30.6	25.5	90.6

Sample	Date	Time	PAR	Depth m	Transect	IRMS δ18O ‰	IRMS O2 mg/L	Hydrolab O2 mg/L	Hydrolab Temp C	Hydrolab Salinity ‰	IRMS O2 %
E2-b	Jul-02			b	E	23.2	2.4	0.5	28.9	32.8	38.1
E2a-s	Jul-02	2.72	388	0	E	19.9	7.4	7.6	31.5	22.8	113.5
E2a-5m	Jul-02			5	E	21.5	6.3	6.4	31.0	27.8	98.1
E2a-10m	Jul-02			10	E	31.5	1.3	2.9	29.0	34.1	19.9
E2a-b	Jul-02			b	E	32.7	1.2	1.2	28.8	34.3	18.8
E3-s	Jul-02	2.76	139	0	E	22.2	6.6	7.0	32.1	25.4	104.1
E3-5m	Jul-02			5	E	21.8	6.0	7.0	31.6	27.4	94.9
E3-10m	Jul-02			10	E	24.3	4.6	6.4	30.3	32.1	73.1
E3-15m	Jul-02			15	E	22.5	6.3	4.9	28.8	34.5	98.7
E3-b	Jul-02			b	E	24.3	3.5	0.6	27.4	34.9	53.9
E4-s	Jul-02	2.80	1	0	E	20.1	5.1	7.6	32.1	27.4	80.9
E4-5m	Jul-02			5	E	22.7	7.2	6.6	30.8	30.9	114.9
E4-10m	Jul-02			10	E	23.9	6.4	6.4	30.0	32.7	101.6
E4-15m	Jul-02			15	E	23.9	6.4	6.4	29.3	34.6	101.5
E4-20m	Jul-02			20	E	23.9	6.4	6.2	28.8	34.7	100.1
E4-25m	Jul-02			25	E	24.1	5.4	4.3	27.8	34.9	84.4
E4-b	Jul-02			b	E	24.7	3.9	0.7	26.1	35.2	58.4
E5-s	Jul-02	2.86	1	0	E	19.5	7.3	7.8	32.1	27.5	116.3
E5-5m	Jul-02			5	E	22.1	6.3	6.4	30.2	31.4	98.8
E5-10m	Jul-02			10	E	23.8	6.4	6.5	30.0	34.5	102.5
E5-15m	Jul-02			15	E	23.9	6.5	6.5	29.5	34.7	102.6
E5-20m	Jul-02			20	E	23.7	6.4	6.5	29.2	34.8	101.0
E5-25m	Jul-02			25	E	23.8	6.5	6.6	28.9	34.8	103.0
E5-30m	Jul-02			30	E	23.4	6.7	6.8	27.4	34.9	103.2
E5-35m	Jul-02			35	E	25.6	3.1	3.4	25.9	35.3	47.0
E5-b	Jul-02			b	E	25.3	3.5	3.8	24.5	35.4	51.6
F2-s	Jul-02	3.20	1	0	F	20.3	7.4	7.9	31.7	19.3	112.7
F2-5m	Jul-02			5	F	27.2	0.7	0.8	29.0	31.2	10.7
F2-b	Jul-02			b	F	26.7	0.6	0.5	28.3	33.2	9.2
F3-s	Jul-02	3.13	1	0	F	19.9	6.9	7.4	31.1	21.8	104.7
F3-5m	Jul-02			5	F	19.1	5.6	4.2	29.2	31.6	87.9
F3-10m	Jul-02			10	F	22.9	5.3	5.2	28.6	34.4	83.5
F3-15m	Jul-02			15	F	25.8	1.3	0.5	27.7	34.8	20.7
F3-b	Jul-02			b	F	35.6	0.4	0.5	27.7	34.8	6.9
F5-s	Jul-02	3.04	1	0	F	22.3	6.6	6.7	31.0	27.4	102.8
F5-5m	Jul-02			5	F	21.7	6.4	6.5	30.5	30.4	100.9
F5-10m	Jul-02			10	F	21.8	5.0	6.5	29.9	33.1	80.1
F5-15m	Jul-02			15	F	23.7	6.4	6.4	29.4	33.8	100.7
F5-20m	Jul-02			20	F	24.4	4.3	5.7	28.2	34.8	66.4
F5-25m	Jul-02			25	F	35.4	1.1	1.3	27.6	34.9	17.1
F5-b	Jul-02			b	F	36.3	1.1	1.3	27.5	35.0	16.4
F6-s	Jul-02	2.98	1	0	F	22.7	6.5	6.6	31.0	27.6	102.0
F6-5m	Jul-02			5	F	21.7	6.4	6.5	30.7	29.6	100.1
F6-10m	Jul-02			10	F	22.9	6.3	6.4	29.8	32.7	99.5
F6-15m	Jul-02			15	F	23.3	4.3	5.9	29.2	33.6	68.0
F6-20m	Jul-02			20	F	27.2	3.1	3.3	27.8	34.9	47.6
F6-25m	Jul-02			25	F	29.2	2.5	2.6	27.3	35.1	38.6
F6-30m	Jul-02			30	F	25.5	3.9	4.1	26.9	35.2	59.1
F6-35m	Jul-02			35	F	23.0	5.5	6.1	24.7	35.4	81.3
F6-b	Jul-02			b	F	23.6	5.2	5.4	24.3	35.4	76.3
G2-s	Jul-02	3.46	1253	0	G	21.3	6.9	7.2	31.3	23.6	106.4
G2-5m	Jul-02			5	G	19.6	5.3	6.0	30.9	25.1	81.8
G2-b	Jul-02			b	G	34.3	0.3	0.5	28.2	34.3	5.3
G3-s	Jul-02	3.52	1382	0	G	22.4	6.6	6.8	30.7	25.2	102.3
G3-5m	Jul-02			5	G	21.3	6.6	6.8	30.6	26.5	102.7
G3-10m	Jul-02			10	G	25.6	3.5	3.5	28.9	31.8	54.7
G3-15m	Jul-02			15	G	24.7	5.7	6.1	28.6	34.4	89.3
G3-b	Jul-02			b	G	29.7	2.7	2.6	27.5	34.9	41.3
H1-s	Jul-02	3.89	1	0	H	19.9	7.3	7.7	31.1	24.1	112.3
H1-5m	Jul-02			5	H	17.5	5.9	5.8	30.1	25.7	90.9
H1-b	Jul-02			b	H	28.9	0.6	0.8	28.9	31.2	8.8
H3-s	Jul-02	3.78	10	0	H	22.4	6.6	6.9	31.4	24.4	103.1
H3-5m	Jul-02			5	H	20.2	6.3	6.9	31.1	24.4	97.3
H3-10m	Jul-02			10	H		1.1	1.8	28.4	33.7	17.1
H3-b	Jul-02			b	H	26.2	0.4	0.6	28.0	34.4	5.8
H4-s	Jul-02	3.72	348	0	H	22.0	6.8	7.1	31.3	24.2	104.7

Sample	Date	Time	PAR	Depth m	Transect	IRMS δ18O ‰	IRMS O2 mg/L	Hydrolab O2 mg/L	Hydrolab Temp C	Hydrolab Salinity ‰	IRMS O2 %
H4-5m	Jul-02			5	H	21.7	6.7	7.0	31.0	24.5	103.6
H4-10m	Jul-02			10	H	23.7	3.3	2.1	28.6	33.3	51.2
H4-15m	Jul-02			15	H	30.2	2.9	3.2	27.7	34.7	45.2
H4-b	Jul-02			b	H	31.9	2.2	2.4	27.4	35.0	33.3
I1-s	Jul-02	4.01	1	0	I	19.0	7.0	7.4	30.9	24.6	108.5
I1-5m	Jul-02			5	I	18.6	6.2	6.2	30.3	25.4	95.1
I1-b	Jul-02			b	I	25.9	0.6	0.6	27.9	32.9	9.6
I3-s	Jul-02	4.11	1	0	I	20.4	7.5	7.8	30.9	24.8	115.9
I3-5m	Jul-02			5	I	18.4	7.5	8.0	30.7	24.9	115.8
I3-10m	Jul-02			10	I	23.4	5.8	5.8	29.2	31.1	89.6
I3-b	Jul-02			b	I	30.2	1.5	1.3	28.3	33.4	22.5
I5-s	Jul-02	4.22	1	0	I	23.2	6.5	6.5	31.1	25.3	100.9
I5-5m	Jul-02			5	I	22.3	6.3	6.5	31.1	25.2	97.9
I5-10m	Jul-02			10	I	24.5	3.8	3.8	28.6	32.4	59.0
I5-15m	Jul-02			15	I	24.2	4.3	4.5	28.2	34.4	67.3
I5-20m	Jul-02			20	I	26.1	2.7	2.4	27.6	34.4	41.3
I5-b	Jul-02			b	I	32.4	1.7	1.7	27.5	34.4	26.3
I6-s	Jul-02	4.29	274	0	I	22.7	6.7	6.8	30.5	23.7	101.8
I6-5m	Jul-02			5	I	21.8	6.0	6.7	30.8	24.3	91.7
I6-10m	Jul-02			10	I	23.3	6.1		30.0	27.5	93.4
I6-15m	Jul-02			15	I	25.3	4.2	5.7	29.3	30.8	65.3
I6-20m	Jul-02			20	I	25.2	5.5	5.4	28.7	34.1	86.4
I6-b	Jul-02			b	I	36.3	0.7	0.8	27.2	34.4	11.1
I7-s	Jul-02	4.34	305	0	I	22.6	6.7	6.7	30.8	25.0	103.2
I7-5m	Jul-02			5	I	21.6	6.2	6.2	30.2	27.3	96.6
I7-10m	Jul-02			10	I	23.0	6.2	6.3	29.8	29.8	95.9
I7-15m	Jul-02			15	I	24.4	5.2	5.6	29.2	32.3	81.8
I7-20m	Jul-02			20	I	28.0	3.0	3.2	27.9	34.1	46.6
I7-25m	Jul-02			25	I	27.4	2.9	1.7	27.3	34.5	43.9
I7-b	Jul-02			b	J	27.6	3.3	3.5	26.9	34.9	50.4
J1-s	Jul-02	4.78	50	0	J	22.2	6.8	6.9	30.3	24.5	104.2
J1-5m	Jul-02			5	J	21.7	6.2	6.6	30.4	24.8	95.1
J1-b	Jul-02			b	J	22.5	2.9	0.9	28.4	31.7	44.6
J3-s	Jul-02	4.70	502	0	J	22.4	6.7	6.8	30.3	23.9	102.0
J3-5m	Jul-02			5	J	21.8	6.2	6.7	30.3	23.9	94.1
J3-10m	Jul-02			10	J	21.4	4.0	1.1	28.0	33.5	62.1
J3-b	Jul-02			b	J	37.2	0.8	1.0	27.9	34.0	13.0
J5-s	Jul-02	4.59	640	0	J	23.3	6.7	6.7	30.2	24.2	101.7
J5-5m	Jul-02			5	J	22.0	6.8	6.7	30.3	24.2	102.8
J5-10m	Jul-02			10	J	20.5	7.1	5.8	29.6	29.2	110.2
J5-15m	Jul-02			15	J	39.4	0.3	1.3	27.9	33.2	4.6
J5-b	Jul-02			b	J	37.2	0.5	0.7	27.2	34.3	7.1
J7-s	Jul-02	4.45	1068	0	J	22.3	6.8	6.7	30.7	25.1	104.9
J7-5m	Jul-02			5	J	22.1	6.3	6.4	30.5	26.6	97.8
J7-10m	Jul-02			10	J	22.8	6.1	6.0	30.1	29.6	95.3
J7-15m	Jul-02			15	J	23.8	6.0	5.9	29.4	32.2	94.2
J7-20m	Jul-02			20	J	25.4	5.5	5.4	28.6	34.2	85.7
J7-25m	Jul-02			25	J	26.9	3.8	4.0	27.7	34.6	58.1
J7-b	Jul-02			b	J	27.9	3.3	3.4	27.4	34.7	51.4
K2-s	Jul-02	4.94	1	0	K	21.8	5.9	5.8	29.6	27.0	89.6
K2-5m	Jul-02			5	K	21.6	5.8		29.5	27.4	88.9
K2-b	Jul-02			b	K	29.2	0.9	0.5	29.0	29.0	13.5
K4-s	Jul-02	5.07	1	0	K	22.8	6.6	6.5	29.9	26.3	100.2
K4-5m	Jul-02			5	K	22.7	6.5		29.8	27.0	99.9
K5-10m	Jul-02			10	K	22.7	4.9	5.0	29.6	27.9	75.9
K5-b	Jul-02			b	K	32.5	0.4	0.5	27.4	33.7	6.4
K5-s	Jul-02			0	K	23.4	6.5	6.5	29.9	27.0	99.1
K5-5m	Jul-02			5	K	23.4	6.5	6.4	29.9	27.0	99.8
K5-10m*	Jul-02			10	K	23.3	6.5	6.4	29.9	27.0	100.0
K5-15m	Jul-02			15	K	28.4	2.1	1.7	28.1	33.2	32.4
K5-b*	Jul-02			b	K	34.7	0.9	1.0	27.8	33.6	14.3
K6-s	Jul-02	5.14	1	0	K	23.2	6.6	6.5	29.6	27.7	100.9
K6-5m	Jul-02			5	K	23.3	6.6	6.5	29.5	27.7	100.5
K6-10m	Jul-02			10	K	22.5	6.6	6.6	29.6	28.9	101.5
K6-15m	Jul-02			15	K	24.0	4.4	5.0	28.7	30.1	67.1
K6-20m	Jul-02			20	K	33.9	1.9	2.1	27.7	34.2	28.8

Sample	Date	Time	PAR	Depth m	Transect	IRMS δ18O ‰	IRMS O2 mg/L	Hydrolab O2 mg/L	Hydrolab Temp C	Hydrolab Salinity ‰	IRMS O2 %
K6-b	Jul-02			b	K	33.6	1.8	2.0	27.6	34.2	28.2
P4-s	Jul-02	5.58	1201	0	P	22.4		6.6	30.1	28.7	
P4-b	Jul-02			10	P	23.0		0.7	28.6	32.0	0.0
P5-s	Jul-02	5.53	1356	0	P	23.2	6.6	6.5	29.9	27.3	101.1
P5-b	Jul-02			b	P	29.3	0.6	0.5	27.7	33.4	8.7
MR-1	Jul-02			0	MR	23.3					
MR-2	Jul-02			0	MR	23.4					
MR-3	Jul-02			0	MR	23.2					
MR-a	Jul-02			0	MR	23.0					
MR-b	Jul-02			0	MR	22.8					
C3-s	Aug-02			0	C	23.8	6.2	6.2	28.8	26.5	93.1
C3-5m	Aug-02			5	C	24.0	6.1	6.1	28.8	26.5	91.5
C3-b	Aug-02			b	C	24.4	6.0	6.0	28.8	26.6	90.5
C6b-s	Aug-02			0	C	22.4	6.8	6.7	29.0	27.7	102.5
C6b-5m	Aug-02			5	C	22.3	6.6	6.5	29.0	27.7	100.8
C6b-10m	Aug-02			10	C	23.7	6.2	6.1	29.1	27.7	93.7
C6b-15m	Aug-02			15	C	26.9	3.6	3.5	29.5	31.5	55.5
C6b-b	Aug-02			b	C	38.9	0.4	0.5	28.7	34.1	6.9
C7-s	Aug-02			0	C	23.7	6.4	6.2	28.8	26.7	95.8
C7-5m	Aug-02			5	C	24.0	6.4	6.2	28.8	26.8	95.7
C7-10m	Aug-02			10	C	25.2	5.6	6.0	29.1	27.3	85.2
C7-15m	Aug-02			15	C	29.7	2.7	4.3	29.9	33.1	42.8
C7-b	Aug-02			b	C	39.0	0.4	0.5	28.5	34.4	6.6
C9-s	Aug-02			0	C	24.0	6.3	6.3	29.2	29.0	97.1
C9-5m	Aug-02			5	C	24.4	6.2	6.3	29.2	29.0	95.3
C9-10m	Aug-02			10	C	24.7	6.0	5.8	29.5	30.2	92.4
C9-15m	Aug-02			15	C	25.8	5.3	5.2	29.2	34.5	84.1
C9-20m	Aug-02			20	C	27.1	4.5	2.4	28.2	34.7	70.3
C9-25m	Aug-02			25	C	30.2	1.7	1.2	27.9	34.7	26.0
C9-b	Aug-02			b	C	32.0	1.4	1.5	27.3	34.9	21.8
F2-s	Aug-02			0	F	21.3	6.9	7.1	29.0	25.4	103.2
F2-5m	Aug-02			5	F	21.5	6.7	6.7	28.9	25.4	100.4
F2-b	Aug-02			b	F	22.0	6.5	5.3	28.9	25.6	97.6
F3-s	Aug-02			0	F	23.9	6.1	5.9	29.2	28.7	93.3
F3-5m	Aug-02			5	F	24.0	5.9	5.9	29.3	28.7	91.2
F3-10m	Aug-02			10	F	24.1	6.1	5.9	29.2	29.1	93.4
F3-15m	Aug-02			15	F	24.1	6.1	6.1	29.2	29.6	93.5
F3-b	Aug-02			b	F	26.1	3.6	0.4	29.1	32.1	55.7
F5-s	Aug-02			0	F	23.4	6.5	6.5	29.4	27.5	99.1
F5-5m	Aug-02			5	F	23.4	6.2	6.5	29.4	27.7	95.0
F5-10m	Aug-02			10	F	23.9	6.4	6.3	29.5	31.7	100.2
F5-15m	Aug-02			15	F	24.6	5.5	5.4	29.4	32.5	85.5
F5-20m	Aug-02			20	F	33.1	0.7	0.8	27.9	34.5	10.6
F5-25m	Aug-02			25	F	35.7	0.5	0.7	27.8	34.7	8.4
F5-b	Aug-02			b	F	34.6	0.8	0.9	27.5	34.7	11.7
F6-s	Aug-02			0	F	23.7	6.5	6.5	29.5	27.6	99.6
F6-5m	Aug-02			5	F	23.8	6.5	6.4	29.6	32.2	101.8
F6-10m	Aug-02			10	F	23.7	6.5	6.4	29.6	32.8	102.3
F6-15m	Aug-02			15	F	23.8	6.5	6.5	29.6	33.4	102.7
F6-20m	Aug-02			20	F	23.9	6.2	6.4	29.2	33.7	97.6
F6-25m	Aug-02			25	F	24.0	6.7	6.7	27.4	34.7	102.8
F6-30m	Aug-02			30	F	24.0	6.5	6.6	26.8	34.9	99.2
F6-35m	Aug-02			35	F	26.8	3.8	4.0	25.5	35.1	56.7
F6-b	Aug-02			b	F	27.9	3.2	3.2	25.4	35.1	48.1
C3 s	Sep-02			0	C	22.8	6.8	6.8	29.7	28.1	105.0
C3 5m	Sep-02			5	C	22.4	6.6	6.4	29.3	29.1	101.9
C3 b	Sep-02			b	C	31.4	1.8	1.8	29.2	31.4	27.5
C3 b (rep)	Sep-02			10	C	31.3	1.8	1.8	29.2	31.4	28.1
C6b s	Sep-02			0	C	23.2	6.8	6.7	29.3	29.4	104.8
C6b 5m	Sep-02			5	C	23.2	6.7	6.7	29.2	29.7	103.6
C6b 10m	Sep-02			10	C	22.8	6.6	6.7	29.3	33.0	103.3
C6b 15m	Sep-02			15	C	22.9	5.3	4.9	29.2	33.8	83.2
C6b b	Sep-02			b	C	33.5	1.8	1.8	28.9	34.5	28.4
C7 s	Sep-02			0	C	23.4	6.7	6.6	29.2	29.8	103.3
C7 5m	Sep-02			5	C	23.2	6.8	6.6	29.2	29.9	104.3
C7 10m	Sep-02			10	C	22.4	6.0	5.6	29.2	34.3	95.3

Sample	Date	Time	PAR	Depth m	Transect	IRMS δ18O ‰	IRMS O2 mg/L	Hydrolab O2 mg/L	Hydrolab Temp C	Hydrolab Salinity ‰	IRMS O2 %
C7 15m	Sep-02			15	C	25.8	4.3	4.4	29.0	34.8	67.6
C7 b	Sep-02			b	C	30.9	2.7	2.6	28.9	34.7	42.6
C7 b (rep)	Sep-02			20	C	31.0	2.7	2.6	28.9	34.7	42.1
C9-s	Sep-02			0	C	23.6	6.5	6.4	28.9	29.9	99.6
C9-s (rep)	Sep-02			0	C	23.6	6.5	6.4	28.9	29.9	99.7
C9-5m	Sep-02			5	C	23.8	6.5	6.4	29.1	30.7	101.3
C9-10m	Sep-02			10	C	23.7	6.5	6.3	29.3	34.5	103.0
C9-15m	Sep-02			15	C	22.7	6.6	6.3	29.3	34.8	104.9
C9-20m	Sep-02			20	C	23.5	6.5	6.4	29.0	34.7	102.4
C9-25m	Sep-02			25	C	23.5	5.8	5.9	29.0	34.9	91.2
C9-b	Sep-02			b	C	25.6	4.4	3.9	28.8	35.0	68.6
C3-s	Oct-02			0	C	22.0	7.4	7.7	26.0	28.7	106.9
C3-5m	Oct-02			5	C	22.6	7.1	7.3	25.3	30.4	102.2
C3-5m (rep)	Oct-02			5	C	22.8	7.1	7.3	25.3	30.4	102.4
C3-b	Oct-02			b	C	24.7	6.0	5.9	25.3	30.6	87.2
C6b-s	Oct-02			0	C	22.3	7.1	7.3	25.7	30.3	104.2
C6b-5m	Oct-02			5	C	22.7	7.0	7.1	25.8	30.8	103.1
C6b-10m	Oct-02			10	C	23.5	6.6	7.1	25.8	31.1	97.1
C6b-15m	Oct-02			15	C	28.1	4.5	4.4	26.8	33.0	67.9
C6b-b	Oct-02			b	C	30.0	3.8	3.8	26.7	32.2	57.2
C6b-b (rep)	Oct-02			20	C	30.2	3.8	3.8	26.7	32.2	57.2
C7-s	Oct-02			0	C	22.9	7.0	7.2	25.6	30.8	102.5
C7-s (rep)	Oct-02			0	C	23.0	7.0	7.2	25.6	30.8	102.8
C7-5m	Oct-02			5	C	23.2	7.0	7.2	25.6	30.9	102.1
C7-10m	Oct-02			10	C	27.1	4.8	4.3	27.3	33.2	73.8
C7-15m	Oct-02			15	C	28.7	4.3	4.1	27.5	33.5	65.2
C7-b	Oct-02			b	C	29.9	3.7	3.9	27.3	33.9	55.9
C9-s	Oct-02			0	C	23.6	6.6	6.7	26.2	33.2	98.6
C9-5m	Oct-02			5	C	23.8	6.6	6.6	26.2	33.5	98.3
C9-10m	Oct-02			10	C	23.7	6.6	6.6	26.3	33.6	98.4
C9-10m (rep)	Oct-02			10	C	23.7	6.5	6.6	26.3	33.6	97.5
C9-15m	Oct-02			15	C	23.7	6.5	6.6	26.3	33.6	97.4
C9-20m	Oct-02			20	C	24.0	6.3	6.5	26.7	33.9	95.1
C9-25m	Oct-02			25	C	24.5	5.8	5.5	27.3	34.6	89.2
C9-b	Oct-02			b	C	28.3	3.9	4.1	27.6	35.4	60.4
F2-s	Oct-02			0	F	24.1	6.5	6.6	24.8	31.0	94.4
F2-5m	Oct-02			5	F	24.2	6.5	6.5	24.7	31.1	93.0
F2-5m(rep)	Oct-02			5	F	24.2	6.4	6.5	24.7	31.1	92.6
F2-b	Oct-02			b	F	24.4	6.4	6.5	24.7	31.1	91.5
F3-s	Oct-02			0	F	23.5	6.5	6.5	26.3	33.4	96.8
F3-5m	Oct-02			5	F	23.4	6.4	6.5	26.3	33.5	96.4
F3-10m	Oct-02			10	F	23.7	6.4	6.4	26.1	33.6	96.2
F3-10m(rep)	Oct-02			10	F	23.5	6.4	6.4	26.1	33.6	96.0
F3-15m	Oct-02			15	F	23.9	6.3	6.4	26.1	33.6	94.8
F3-b	Oct-02			b	F	24.0	6.2	6.3	26.1	33.7	93.1
F5-s	Oct-02			0	F	23.5	6.5	6.6	26.5	34.0	98.6
F5-5m	Oct-02			5	F	23.7	6.4	6.6	26.6	34.1	96.6
F5-10m	Oct-02			10	F	23.3	6.4	6.5	26.7	34.4	97.7
F5-15m	Oct-02			15	F	24.0	6.1	5.5	26.9	35.2	93.8
F5-20m	Oct-02			20	F	24.0	6.3	6.3	26.6	35.3	95.7
F5-25m	Oct-02			25	F	24.2	6.2	6.3	26.5	35.6	94.8
F5-25m(rep)	Oct-02			25	F	24.1	6.2	6.3	26.5	35.6	95.1
F5-b	Oct-02			b	F	24.2	6.2	6.3	26.5	35.6	94.2
C5-s	Dec-02			0	C	23.1					
C6-s	Dec-02			0	C	23.8					
C7-s	Dec-02			0	C	23.9					
C8-s	Dec-02			0	C	24.0					
C9-s	Dec-02			0	C	24.2					
C9-15m	Dec-02			15	C	24.7					
C9-20m	Dec-02			20	C	24.3					
C9-20m (rep)	Dec-02			20	C	24.4					
C9-25m	Dec-02			25	C	24.4					
C9-b	Dec-02			b	C	24.9					
F2-s	Dec-02			0	F	24.0	8.7	9.1	13.4	27.0	98.5
F2-s (rep)	Dec-02			0	F	23.8	8.7	9.1	13.4	27.0	98.9
F2-5m	Dec-02			5	F	23.6	7.9	8.3	15.0	30.0	93.9

Sample	Date	Time	PAR	Depth m	Transect	IRMS δ18O ‰	IRMS O2 mg/L	Hydrolab O2 mg/L	Hydrolab Temp C	Hydrolab Salinity ‰	IRMS O2 %
F2-b	Dec-02			b	F	24.2	7.8	7.2	15.7	31.8	95.8
F3-s	Dec-02			0	F	23.5	8.0	8.8	15.9	30.7	97.7
F3-5m	Dec-02			5	F	22.2	7.6	8.5	16.0	30.7	92.4
F3-10m	Dec-02			10	F	23.5	7.8	8.0	16.8	31.1	97.2
F3-15m	Dec-02			15	F	24.0	7.6	7.7	17.2	31.3	95.2
F3-15m (rep)	Dec-02			15	F	23.5	7.4	7.7	17.2	31.3	92.5
F3-b	Dec-02			b	F	24.3	7.0	7.0	19.1	32.8	92.2
F5-s	Dec-02			0	F	22.2	8.4	8.3	18.4	32.3	108.5
F5-5m	Dec-02			5	F	22.2	8.4	8.2	18.4	32.3	108.6
F5-10m	Dec-02			10	F	23.2	7.8	7.7	18.9	33.1	102.2
F5-15m	Dec-02			15	F	24.4	6.9	6.9	19.9	33.7	92.6
F5-20m	Dec-02			20	F	24.3	6.7	6.7	20.1	33.8	90.3
F5-25m	Dec-02			25	F	24.7	6.5	6.3	20.4	34.0	88.6
F5-25m (rep)	Dec-02			25	F	24.7	6.5	6.3	20.4	34.0	88.7
F5-b	Dec-02			b	F	25.0	6.4	6.2	20.7	34.1	86.9
C3-s	Feb-03			0	C	23.6	8.2	8.7	15.4	30.5	99.1
C3-5m	Feb-03			5	C	23.3	8.3	9.2	15.4	30.0	99.7
C3-b	Feb-03			b	C	23.3	8.2	8.8	15.4	30.4	98.7
C6b-s	Feb-03			0	C	23.1	8.2	8.6	15.8	31.1	99.9
C6b-5m	Feb-03			5	C	23.0	8.2	9.0	15.8	30.6	100.0
C6b-10m	Feb-03			10	C	23.2	8.2	8.8	15.8	30.7	99.7
C6b-15m	Feb-03			15	C	24.0	7.5	8.7	15.8	30.9	91.2
C6b-b	Feb-03			b	C	27.4	5.5	5.9	17.1	34.0	70.2
C7-s	Feb-03			0	C	23.2	7.7	8.2	17.1	33.2	98.1
C7-5m	Feb-03			5	C	23.2	7.8	8.2	17.0	32.6	97.8
C7-10m	Feb-03			10	C	24.0	7.3	7.9	17.0	32.6	91.7
C7-15m	Feb-03			15	C	27.2	5.7	5.9	17.0	35.1	72.8
C7-b	Feb-03			b	C	27.9	5.1	5.4	18.0	35.7	66.4
C9-s	Feb-03			0	C	22.7	8.0	8.2	17.3	34.9	103.0
C9-5m	Feb-03			5	C	22.6	8.0	8.2	17.3	34.5	102.5
C9-5m (rep)	Feb-03			5	C	22.7	8.1	8.2	17.3	34.5	103.3
C9-10m	Feb-03			10	C	22.7	8.0	8.1	17.3	34.5	102.8
C9-15m	Feb-03			15	C	22.7	8.0	7.8	17.4	34.6	102.3
C9-20m	Feb-03			20	C	25.8	6.0	6.3	18.0	35.7	78.9
C9-25m	Feb-03			25	C	26.5	5.7	6.0	18.2	35.8	75.2
C9-25m (rep)	Feb-03			25	C	26.4	5.8	6.0	18.2	35.8	76.1
C9-b	Feb-03			b	C	26.4	5.8	6.1	18.1	36.1	75.7
C3-s	Mar-03			0	C	20.5	9.3	10.4	17.8	17.3	108.8
C3-s(rep)	Mar-03			0	C	20.6	9.2	10.4	17.8	17.3	107.2
C3-5m	Mar-03			5	C	21.2	8.6	9.1	17.4	21.0	102.3
C3-b	Mar-03			b	C	30.1	4.4	4.7	17.4	31.3	55.5
C6b-s	Mar-03			0	C	21.9	8.6	9.3	17.5	23.2	103.9
C6b-5m	Mar-03			5	C	25.0	7.1	7.5	17.2	29.6	88.4
C6b-10m	Mar-03			10	C	25.0	6.8	7.1	17.5	31.2	85.3
C6b-15m	Mar-03			15	C	25.4	6.6	6.4	17.8	32.5	84.3
C6b-b	Mar-03			b	C	28.5	5.0	5.3	18.0	33.9	64.5
C7-s	Mar-03			0	C	20.2	9.1	9.5	18.5	28.0	114.4
C7-5m	Mar-03			5	C	22.9	7.8	8.1	17.7	28.8	97.5
C7-10m	Mar-03			10	C	25.4	6.8	7.1	17.6	32.1	86.6
C7-10m(rep)	Mar-03			10	C	25.4	6.8	7.1	17.6	32.1	87.0
C7-15m	Mar-03			15	C	24.1	6.9	7.3	19.2	34.3	92.0
C7-b	Mar-03			b	C	25.9	6.0	6.6	18.7	35.0	79.2
C9-s	Mar-03			0	C	22.1	7.9	8.3	19.7	33.5	105.7
C9-5m	Mar-03			5	C	22.3	7.8	8.1	19.6	33.7	103.8
C9-10m	Mar-03			10	C	23.1	7.3	7.7	19.4	34.3	97.3
C9-15m	Mar-03			15	C	23.4	7.3	7.5	19.4	34.5	96.9
C9-20m	Mar-03			20	C	26.7	5.9	6.0	18.5	35.5	78.3
C9-25m	Mar-03			25	C	29.0	4.7	4.9	18.6	35.7	62.8
C9-b	Mar-03			b	C	27.7	5.2	5.4	18.9	36.0	69.4
F2-s	Mar-03			0	F	20.9	8.9	9.6	18.6	24.2	110.4
F2-5m	Mar-03			5	F	21.2	8.5	9.0	18.2	25.8	105.8
F3-s	Mar-03			0	F	21.2	8.5	9.2	18.7	26.9	107.4
F3-5m	Mar-03			5	F	22.6	7.8	8.3	18.4	30.2	99.8
F3-10m	Mar-03			10	F	23.4	7.3	8.0	18.3	33.0	95.2
F3-15m	Mar-03			15	F	24.7	7.0	7.4	17.8	33.7	90.6
F3-15m (rep)	Mar-03			15	F	24.9	6.9	7.4	17.8	33.7	88.7

Sample	Date	Time	PAR	Depth m	Transect	IRMS δ18O ‰	IRMS O2 mg/L	Hydrolab O2 mg/L	Hydrolab Temp C	Hydrolab Salinity ‰	IRMS O2 %
F3-b	Mar-03			b	F	25.5	6.5	6.9	17.9	34.4	83.9
F5-s	Mar-03			0	F	24.3	7.2	7.5	18.2	34.6	94.1
F5-5m	Mar-03			5	F	24.3	7.2	7.5	18.2	34.7	94.1
F5-10m	Mar-03			10	F	24.4	7.2	7.6	18.4	34.7	94.2
F5-15m	Mar-03			15	F	24.3	7.2	7.6	18.4	34.7	94.3
F5-20m	Mar-03			20	F	24.8	7.0	7.2	17.8	34.7	90.5
F5-25m	Mar-03			25	F	25.6	6.6	6.9	17.8	34.7	85.6
F5-25m (rep)	Mar-03			25	F	25.7	6.6	6.9	17.8	34.7	85.5
F5-b	Mar-03			b	F	27.3	5.6	6.1	18.4	35.3	74.1
C3-S	Apr-03			0	C	22.3	7.8	7.7	19.3	27.7	99.8
C3-5	Apr-03			5	C	23.9	6.9	7.6	19.3	27.7	88.5
C3-B	Apr-03			b	C	32.9	3.2	3.1	19.8	34.2	42.6
C6b-S	Apr-03			0	C	24.4	7.4	7.6	19.7	29.1	95.7
C6b-5	Apr-03			5	C	24.6	7.1	7.5	19.5	29.1	92.0
C6b-10	Apr-03			10	C	28.9	4.6	7.3	19.4	30.7	59.5
C6b-14	Apr-03			15	C	33.4	3.2	4.0	19.7	33.5	42.7
C6b-B	Apr-03			b	C	33.9	3.1	3.3	19.9	35.0	41.4
C7-S	Apr-03			0	C	24.1	7.5	7.7	19.4	28.8	96.4
C7-5	Apr-03			5	C	24.5	7.4	7.7	19.4	28.8	95.0
C7-10	Apr-03			10	C	27.7	5.3	7.6	19.3	29.0	68.7
C7-15	Apr-03			15	C	30.7	4.0	4.2	20.0	35.2	53.9
C7-B	Apr-03			b	C	30.8	4.0	4.3	20.0	35.2	53.8
C9-S	Apr-03			0	C	24.5	7.4	7.7	19.1	28.5	94.6
C9-5	Apr-03			5	C	24.5	7.4	7.7	19.0	28.5	94.8
C9-15	Apr-03			15	C	26.8	5.9	6.6	20.0	31.1	77.8
C9-20	Apr-03			20	C	27.8	5.2	5.3	20.0	36.0	70.3
C9-25	Apr-03			25	C	28.2	5.1	5.3	20.0	36.1	69.6
C9-30	Apr-03			b	C	27.9	5.2	5.3	20.0	36.1	70.3
C3 surf	May-03			0	C	21.4	7.1	7.6	27.3	24.6	103.5
C3 5m	May-03			5	C	22.3	6.9	7.3	27.2	27.0	101.3
C3 bot	May-03			b	C	24.3	5.8	5.8	27.0	27.5	84.8
C6b surf	May-03			0	C	22.5	6.8	7.3	27.1	27.8	100.2
C6b surf	May-03			0	C	22.5	6.8	7.3	27.1	27.8	99.9
C6b 5m	May-03			5	C	22.8	6.7	7.2	26.8	27.8	98.0
C6b 10m	May-03			10	C	24.6	6.1	6.4	26.5	28.3	89.1
C6b 15m	May-03			15	C	28.8	4.2	4.4	22.9	31.5	58.5
C6b bot	May-03			b	C	41.9	1.0	1.2	20.7	34.7	13.9
C7 surf	May-03			0	C	22.3	6.9	7.4	27.5	27.3	101.6
C7 5m	May-03			5	C	22.4	6.6	7.0	26.7	28.1	97.2
C7 10m	May-03			10	C	24.3	6.4	6.7	26.1	31.8	94.6
C7 15m	May-03			15	C	32.9	2.3	2.3	20.7	34.2	31.2
C7 15m	May-03			15	C	33.1	2.3	2.3	20.7	34.2	31.1
C7 bot	May-03			b	C	40.5	1.4	1.5	20.6	35.0	18.5
C9 surf	May-03			0	C	23.8	6.5	6.9	26.5	32.0	97.7
C9 5m	May-03			5	C	23.4	6.6	7.0	25.9	32.0	98.1
C9 10m	May-03			10	C	22.7	6.4	6.7	24.3	33.4	92.6
C9 15m	May-03			15	C	28.1	4.2	4.5	20.3	35.6	58.0
C9 20m	May-03			20	C	31.1	3.7	3.9	20.1	35.8	49.9
C9 25m	May-03			25	C	32.1	3.6	3.8	20.1	35.8	48.6
C 9 bottom	May-03			b	C	32.4	3.4	3.6	20.1	35.8	46.9
F2 surf	May-03			0	F	22.6	6.5	6.9	26.8	30.4	97.0
F2 surf	May-03			0	F	22.8	6.5	6.9	26.8	30.4	97.2
F2 5m	May-03			5	F	22.7	6.5	7.0	26.7	30.3	96.7
F2 bottom	May-03			b	F	22.8	6.5	7.0	26.7	30.4	96.0
F3 surf	May-03			0	F	24.4	6.5	6.8	25.4	34.9	96.0
F3 5m	May-03			5	F	24.6	7.3	6.8	25.2	35.0	108.3
F3 10m	May-03			10	F	24.4	6.5	6.8	25.2	34.9	96.5
F3 15m	May-03			15	F	24.4	6.5	6.9	24.8	34.9	96.4
F3 bottom	May-03			b	F	23.7	6.3	6.7	24.1	35.1	91.2
F5 surf	May-03			0	F	24.4	6.4	6.8	25.1	34.2	95.1
F5 5m	May-03			5	F	24.4	6.4	6.8	25.0	34.5	94.8
F5 10m	May-03			10	F	24.4	6.5	6.9	24.3	35.0	95.2
F5 15m	May-03			15	F	24.4	6.6	6.9	24.3	35.1	96.6
F5 20m	May-03			20	F	24.4	6.7	7.0	23.5	35.4	96.6
F5 20m	May-03			20	F	24.1	6.8	7.0	23.5	35.4	98.1
F5 25m	May-03			25	F	21.9	6.7	6.9	20.8	35.6	92.1

Sample	Date	Time	PAR	Depth m	Transect	IRMS δ18O ‰	IRMS O2 mg/L	Hydrolab O2 mg/L	Hydrolab Temp C	Hydrolab Salinity ‰	IRMS O2 %
F5 bottom	May-03			b	F	22.9	5.9	6.0	20.6	35.7	81.1
C3 surf	Jun-03			0	C	20.6	6.8	7.0	29.9	24.3	102.6
C3 surf	Jun-03			0	C	20.8	6.8	7.0	29.9	24.3	103.3
C3 5m	Jun-03			5	C	20.9	6.3	6.3	29.6	25.1	94.8
C3 bottom	Jun-03			b	C	44.1	0.2	0.3	25.6	33.1	2.8
C6b surf	Jun-03			0	C	23.4	6.3	6.5	29.5	27.8	96.3
C6b 5m	Jun-03			5	C	23.1	6.4	6.6	29.4	28.1	98.2
C6b 10m	Jun-03			10	C	23.5	5.9	6.2	27.9	32.7	91.1
C6b 15m	Jun-03			15	C	23.4	4.6	4.9	27.9	34.4	71.7
C6b bottom	Jun-03			b	C	46.0	0.2	0.3	23.1	34.7	2.2
C6b bottom	Jun-03			20	C	34.8	0.2	0.3	23.1	34.7	3.5
C7 surf	Jun-03			0	C	23.8	6.1	6.4	30.0	27.4	94.5
C7 5m	Jun-03			5	C	23.7	6.2	6.5	29.6	27.4	95.1
C7 5m	Jun-03			5	C	23.7	6.2	6.5	29.6	27.4	94.8
C7 10m	Jun-03			10	C	22.9	4.9	5.3	28.1	29.9	74.9
C7 15m	Jun-03			15	C	24.4	3.2	5.2	28.0	34.2	49.3
C7 bottom	Jun-03			b	C	27.9	1.5	1.7	24.3	34.6	21.4
C9 surf	Jun-03			0	C	23.6	6.3	6.5	29.2	27.1	96.3
C9 5m	Jun-03			5	C	23.7	6.3	6.5	29.2	27.0	95.9
C9 10m	Jun-03			10	C	23.2	5.4	6.0	28.4	30.3	82.3
C9 15m	Jun-03			15	C	23.7	5.9	6.2	26.3	35.1	88.7
C9 20m	Jun-03			20	C	28.0	3.1	3.8	23.4	35.3	44.9
C9 25m	Jun-03			25	C	33.4	1.8	4.3	21.6	35.9	25.0
C9 25m	Jun-03			25	C	33.5	1.8	4.3	21.6	35.9	24.8
C9 bottom	Jun-03			b	C	32.7	2.0	1.8	21.0	35.9	27.3
A'1 s	Jul-03	0.57	241	0	AA	21.1	7.6	7.8	29.1	5.4	102.4
A'2 s	Jul-03	0.60	167	0	AA	19.1	8.4	7.6	29.2	18.7	122.5
A'2 5m	Jul-03			5	AA	20.1	7.9	7.8	29.2	18.9	115.1
A'2 b	Jul-03			b	AA	24.0	5.5	6.2	28.5	25.1	81.7
A'3 s	Jul-03	0.64	904	0	AA	22.6	6.6	6.3	28.8	22.1	96.9
A'4 s	Jul-03	0.67	446	0	AA	22.6	6.6	6.1	28.9	21.6	96.9
A'4 5m	Jul-03			5	AA	22.9	6.4	6.3	28.9	21.7	94.0
A'4 10m	Jul-03			10	AA	26.6	5.2	5.5	28.2	31.2	80.0
A'4 15m	Jul-03			15	AA	25.8	5.3	5.4	27.9	33.8	82.0
A'4 20m	Jul-03			20	AA	31.9	2.9	2.6	26.8	34.8	44.6
A'4 25m	Jul-03			25	AA	29.7	3.9	4.1	23.6	35.7	57.0
A'4 30m	Jul-03			30	AA	25.7	6.2	6.3	21.6	36.0	86.8
A'4 b	Jul-03			b	AA	35.5	2.2	2.8	21.6	36.0	31.3
A'5 s	Jul-03	0.70	127	0	AA	22.1	6.5	6.6	28.9	28.7	99.3
A1 s	Jul-03	1.09	1	0	A	23.5	6.4	6.5	28.3	23.1	93.6
A2 s	Jul-03	1.06	1	0	A	23.8	6.1	6.1	28.3	29.4	92.7
A2 s	Jul-03	1.06	1	0	A	23.8	6.1	6.1	28.3	29.4	92.5
A2 5m	Jul-03			5	A	23.7	6.2	6.1	28.3	29.4	93.9
A2 b	Jul-03			b	A	23.6	6.0	5.8	28.3	31.2	92.2
A3 s	Jul-03	1.03	1	0	A	23.8	6.2	5.9	28.2	29.4	93.5
A4 s	Jul-03	0.99	1	0	A	23.8	6.3	6.3	28.3	29.0	95.7
A4 5m	Jul-03			5	A	23.6	6.4	6.3	28.4	33.1	98.7
A4 10m	Jul-03			10	A	24.4	6.0	5.9	28.2	33.6	92.8
A4 15m	Jul-03			15	A	25.3	5.6	5.8	27.9	34.7	86.2
A4 b	Jul-03			b	A	40.0	0.8	0.2	25.5	35.6	12.1
A5 s	Jul-03	0.95	1	0	A	23.5	6.5	6.3	28.4	31.7	99.9
A5 5m	Jul-03			5	A	23.6	6.4	6.3	28.4	33.7	99.0
A5 10m	Jul-03			10	A	23.1	6.4	6.3	28.3	33.8	99.3
A5 15m	Jul-03			15	A	25.1	6.1	6.0	27.8	35.0	94.2
A5 20m	Jul-03			20	A	26.1	5.3	5.0	27.5	35.4	81.7
A5 25m	Jul-03			25	A	35.4	2.1	2.0	24.6	35.5	30.6
A5 b	Jul-03			b	A	38.4	1.4	1.8	22.3	35.9	19.7
A6 s	Jul-03	0.91	1	0	A	22.1	6.7	6.6	28.2	31.9	103.1
A6 5m	Jul-03			5	A	22.4	6.6	6.6	28.2	32.0	102.0
A6 10m	Jul-03			10	A	23.6	6.2	6.1	28.4	32.4	95.2
A6 15m	Jul-03			15	A	25.1	5.9	5.8	28.1	34.5	91.8
A6 20m	Jul-03			20	A	24.7	6.1	6.0	27.3	35.2	94.1
A6 25m	Jul-03			25	A	32.0	2.4	2.5	24.0	35.8	34.8
A6 30m	Jul-03			30	A	30.7	3.6	3.3	22.7	35.8	51.4
A6 35m	Jul-03			35	A	34.0	2.8	2.8	21.4	36.0	39.3
A6 b	Jul-03			b	A	34.9	2.6	2.7	21.2	36.1	36.1

Sample	Date	Time	PAR	Depth m	Transect	IRMS δ18O ‰	IRMS O2 mg/L	Hydrolab O2 mg/L	Hydrolab Temp C	Hydrolab Salinity ‰	IRMS O2 %
A7 s	Jul-03	0.86	1	0	A	22.0	6.7	6.5	28.5	30.2	102.4
A8 s	Jul-03	0.78	8	0	A	22.2	6.7	6.5	28.8	28.7	102.6
B1 s	Jul-03	1.24	11	0	B	26.5	4.0	4.3	27.1	31.6	59.4
B2 s	Jul-03	1.27	21	0	B	25.4	4.6	4.4	27.2	31.0	68.6
B2 5m	Jul-03			5	B	27.8	3.3	3.3	26.6	32.7	49.4
B2 5m(rep)	Jul-03			5	B	27.8	3.3	3.3	26.6	32.7	49.5
B2 b	Jul-03			b	B	29.3	3.8	3.8	26.6	35.7	58.2
B4 s	Jul-03	1.30	58	0	B	23.9	6.1	6.0	28.2	27.8	92.0
B6 s	Jul-03	1.33	374	0	B	23.6	6.3	6.1	28.4	29.3	95.6
B6 5m	Jul-03			5	B	23.6	6.3	6.3	28.2	29.1	95.7
B6 10m	Jul-03			10	B	24.4	5.5	5.7	28.2	32.1	83.7
B6 15m	Jul-03			15	B	25.8	4.9	5.0	26.8	35.8	75.2
B6 b	Jul-03			b	B	28.0	4.1	5.5	26.5	36.0	62.1
B8 s	Jul-03	1.38	730	0	B	23.1	6.9	6.9	28.5	25.0	102.6
B8 5m	Jul-03			5	B	22.9	6.9	6.7	28.7	25.0	102.3
B8 10m	Jul-03			10	B	24.5	5.4	5.1	28.4	30.0	81.9
B8 15m	Jul-03			15	B	24.9	5.9	5.8	27.6	34.4	91.3
B8 20m	Jul-03			20	B	24.7	6.0	6.0	27.0	35.4	92.8
B8 25m	Jul-03			25	B	24.5	6.2	6.3	27.0	36.2	95.7
B8 b	Jul-03			b	B	28.1	3.9	5.2	25.5	36.2	58.1
C3 s	Jul-03	1.77	50	0	C	20.9	6.1	5.9	28.3	30.2	92.9
C3 5m	Jul-03			5	C	28.2	3.2	3.4	27.8	32.2	49.0
C3 b	Jul-03			b	C	35.0	1.6	1.7	25.5	35.1	23.7
C4 s	Jul-03	1.74	275	0	C	20.4	6.8	6.5	28.6	28.7	103.2
C5 s	Jul-03	1.71	748	0	C	18.6	7.9	7.9	29.0	27.2	119.4
C6b s	Jul-03	1.64	865	0	C	19.0	8.0	7.8	28.7	26.4	119.7
C6b 5m	Jul-03			5	C	24.3	6.0	5.6	28.7	27.5	91.1
C6b 10m	Jul-03			10	C	24.2	5.5	5.6	27.8	33.9	85.5
C6b 15m	Jul-03			15	C	26.5	4.2	3.6	27.4	34.8	63.9
C6b b	Jul-03			b	C	41.9	1.1	1.3	24.8	35.5	15.5
C7 s	Jul-03	1.59	1688	0	C	21.3	7.3	7.4	28.8	23.1	108.4
C8 s	Jul-03	1.53	1120	0	C	19.5	8.2	7.7	28.8	23.8	121.3
C9 s	Jul-03	1.48	1170	0	C	21.4	7.5	7.6	28.9	23.7	111.0
C9 5m	Jul-03			5	C	24.0	6.7	6.4	28.8	25.3	99.4
C9 10m	Jul-03			10	C	24.0	6.4	6.3	28.8	34.2	100.4
C9 15m	Jul-03			15	C	23.7	6.4	6.2	28.3	34.5	100.0
C9 20m	Jul-03			20	C	24.0	6.2	6.2	27.8	35.1	96.8
C9 25m	Jul-03			25	C	28.3	4.0	4.3	24.5	35.7	58.6
C9 b	Jul-03			b	C	30.0	3.4	3.9	23.4	35.7	49.6
D'1 s	Jul-03	1.90	1	0	DD	20.7	7.3	7.1	28.7	21.6	107.3
D'2 s	Jul-03	1.94	1	0	DD	20.2	7.8	8.2	28.8	21.7	113.8
D'3 s	Jul-03	1.98	1	0	DD	23.3	6.8	6.9	29.0	22.6	100.1
D'3 5m	Jul-03			5	DD	23.7	6.4	6.6	29.0	24.0	94.8
D'3 10m	Jul-03			10	DD	24.2	6.1	6.3	28.3	33.0	94.3
D'3 15m	Jul-03			15	DD	24.9	4.7	5.1	26.2	34.7	70.4
D'3 15m(rep)	Jul-03			15	DD	24.8	4.7	5.1	26.2	34.7	70.8
D'3 b	Jul-03			b	DD	30.6	2.1	2.1	22.9	35.7	30.7
D'4 s	Jul-03	2.03	1	0	DD	24.3	6.6	6.6	28.8	19.2	95.5
D'4 5m	Jul-03			5	DD	23.7	6.1	6.2	29.0	22.6	89.3
D'4 10m	Jul-03			10	DD	22.8	6.4	6.5	28.4	33.4	98.6
D'4 15m	Jul-03			15	DD	23.0	6.1	6.3	28.0	33.8	95.0
D'4 20m	Jul-03			20	DD	25.6	4.9	5.5	27.8	34.5	76.4
D'4 25m	Jul-03			25	DD	24.1	4.4	6.2	25.0	35.8	65.9
D'4 bottom	Jul-03			b	DD	22.9	6.9	2.0	21.8	35.8	97.0
D'5 surf	Jul-03	2.07	1	0	DD	23.6	6.7	6.7	28.5	18.7	95.5
D'6 surf	Jul-03	2.14	1	0	DD	23.7	6.7	6.5	28.6	20.3	96.5
D'6 5m	Jul-03			5	DD	22.9	6.7	6.6	28.9	22.5	98.8
D'6 10m	Jul-03			10	DD	23.0	6.2	6.3	28.2	34.4	96.6
D'6 15m	Jul-03			15	DD	23.4	6.2	6.3	27.9	34.6	96.7
D'6 20m	Jul-03			20	DD	23.4	6.4	6.4	27.0	35.1	98.0
D'6 25m	Jul-03			25	DD	23.0	6.2	6.3	27.0	35.1	94.4
D'6 30m	Jul-03			30	DD	22.8	6.4	6.5	25.5	35.5	96.4
D'6 35m	Jul-03			35	DD	22.8	6.4	6.4	23.1	36.0	91.6
D'6 40m	Jul-03			40	DD	23.9	4.7	5.0	21.4	35.9	65.4
D'6 bottom	Jul-03			b	DD	23.7	4.7	4.9	21.4	35.9	65.5
D0 surf	Jul-03	2.59	2143	0	D	19.4	7.1	5.4	28.6	27.5	107.4

Sample	Date	Time	PAR	Depth m	Transect	IRMS δ18O ‰	IRMS O2 mg/L	Hydrolab O2 mg/L	Hydrolab Temp C	Hydrolab Salinity ‰	IRMS O2 %
D1 surf	Jul-03	2.56	2330	0	D	19.2	7.3	7.3	28.6	26.0	108.4
D1N surf	Jul-03	2.53	2344	0	D	20.0	6.9	7.0	28.7	25.8	103.8
D1N 5m	Jul-03			5	D	27.5	3.2	3.7	28.7	27.4	47.8
D1N b	Jul-03			b	D	38.8	0.4	0.2	26.9	33.7	5.8
D2 surf	Jul-03	2.49	2344	0	D	23.4	6.6	6.7	28.8	25.1	98.7
D2 5m	Jul-03			5	D	24.0	4.5	5.8	28.9	28.2	68.3
D2 10m	Jul-03			10	D	28.9	2.4	2.9	27.3	33.7	36.6
D2 b	Jul-03			b	D	37.5	1.1	1.0	26.1	34.6	16.2
D3 surf	Jul-03	2.43	2239	0	D	23.7	6.3	6.1	28.7	28.1	95.3
D4 surf	Jul-03	2.38	1776	0	D	23.5	6.4	6.4	28.3	29.1	97.1
D4 5m	Jul-03			5	D	23.6	6.3	6.3	28.3	29.1	94.9
D4 10m	Jul-03			10	D	25.1	5.2	5.7	28.5	30.2	78.7
D4 15m	Jul-03			15	D	28.0	3.1	3.1	26.4	34.2	46.6
D4 b	Jul-03			b	D	24.2	4.9	5.4	26.1	34.6	73.5
D5 surf	Jul-03	2.31	1115	0	D	23.4	6.6	6.5	28.5	26.5	99.0
D5 5m	Jul-03			5	D	23.6	6.4	6.5	28.8	29.8	98.4
D5 10m	Jul-03			10	D	23.4	6.3	6.4	28.6	34.1	99.0
D5 15m	Jul-03			15	D	23.7	6.3	6.4	28.5	34.7	99.4
D5 20m	Jul-03			20	D	23.7	6.5	6.4	27.9	34.9	100.7
D5 25m	Jul-03			25	D	23.7	6.2	6.3	27.6	35.0	95.1
D5 30m	Jul-03			30	D	24.0	5.4	5.7	23.8	35.8	78.1
D5 b	Jul-03			b	D	23.9	5.5	5.8	22.0	35.8	77.8
D6 surf	Jul-03	2.25	220	0	D	23.6	6.7	6.5	28.3	26.0	99.5
D6 5m	Jul-03			5	D	23.6	6.4	6.4	28.5	33.5	99.8
D6 10m	Jul-03			10	D	23.6	6.4	6.3	28.3	34.5	100.0
D6 15m	Jul-03			15	D	23.5	6.4	6.4	28.1	34.5	98.9
D6 20m	Jul-03			20	D	23.7	6.4	6.3	28.2	35.0	100.0
D6 25m	Jul-03			25	D	23.7	6.4	6.5	28.3	35.5	100.6
D6 30m	Jul-03			30	D	23.7	6.4	6.4	27.8	36.0	100.2
D6 35m	Jul-03			35	D	23.0	5.0	5.6	24.0	36.0	73.8
D6 40m	Jul-03			40	D	23.5	6.0	6.2	21.0	36.0	82.6
D6 b	Jul-03			b	D	23.9	5.9	6.2	21.0	36.0	82.3
E1 surf	Jul-03	2.70	960	0	E	16.7	8.5	8.7	31.1	27.2	133.7
E2 surf	Jul-03	2.74	350	0	E	19.3	7.0	7.2	29.2	31.7	108.6
E2 5m	Jul-03			5	E	23.6	5.1	5.1	28.3	32.1	78.6
E2 b	Jul-03			b	E	26.9	4.0	4.0	27.8	33.8	61.8
E2a surf	Jul-03	2.79	18	0	E	23.3	6.5	6.3	28.9	28.8	98.5
E3 surf	Jul-03	2.83	1	0	E	23.2	6.8	6.7	28.6	28.5	103.5
E3 5m	Jul-03			5	E	23.4	6.6	6.5	28.3	29.3	99.5
E3 10m	Jul-03			10	E	24.3	5.7	6.3	28.5	30.6	87.5
E3 15m	Jul-03			15	E	25.5	4.8	5.0	27.6	34.2	73.7
E3 b	Jul-03			b	E	25.9	2.9	3.2	23.0	35.5	42.1
E4 surf	Jul-03	2.87	1	0	E	23.0	6.7	6.5	29.0	28.6	102.5
E4 5m	Jul-03			5	E	23.1	6.7		28.7	30.5	102.5
E4 10m	Jul-03			10	E	23.1	6.5	6.5	28.5	32.5	100.5
E4 15m	Jul-03			15	E	24.6	5.4	5.5	27.9	33.1	83.6
E4 20m	Jul-03			20	E	23.4	5.5	5.7	26.8	34.8	83.6
E4 25m	Jul-03			25	E	23.8	4.5	5.1	24.7	35.3	66.3
E4 b	Jul-03			b	E	25.8	3.2	3.5	20.9	35.7	44.7
F0 surf	Jul-03	3.30	721	0	F	24.2	5.8	5.5	29.3	29.9	89.0
F1 surf	Jul-03	3.26	210	0	F	24.9	4.8	6.0	29.0	29.9	73.9
F2 surf	Jul-03	3.20	1	0	F	22.4	6.5	6.1	28.6	30.0	98.6
F2 5m	Jul-03			5	F	23.1	6.1	6.3	28.6	30.0	93.2
F2 b	Jul-03			b	F	27.1	3.8	4.1	27.9	32.3	58.7
F3 surf	Jul-03	3.14	1	0	F	22.7	6.7	6.4	29.3	27.0	102.2
F3 5m	Jul-03			5	F	23.8	6.6	6.2	28.9	29.1	101.5
F3 10m	Jul-03			10	F	23.6	6.2	6.1	28.4	32.4	95.6
F3 15m	Jul-03			15	F	24.7	4.5	5.4	27.9	33.0	69.5
F3 b	Jul-03			b	F	25.4	3.3	3.5	25.4	34.9	49.2
F4 surf	Jul-03	3.09	1	0	F	22.2	7.0	6.8	29.4	25.7	105.9
F5 surf	Jul-03	3.04	1	0	F	22.9	7.6	7.0	29.5	25.0	115.3
F5 5m	Jul-03			5	F	22.3	7.2	6.9	28.9	25.9	107.9
F5 10m	Jul-03			10	F	23.3	6.5	6.4	28.0	33.1	100.4
F5 15m	Jul-03			15	F	23.5	7.1	6.4	27.8	33.4	108.4
F5 20m	Jul-03			20	F	24.0	6.5	6.4	27.8	34.3	99.6
F5 25m	Jul-03			25	F	23.6	6.4	6.5	27.0	34.8	97.7

Sample	Date	Time	PAR	Depth m	Transect	IRMS δ18O ‰	IRMS O2 mg/L	Hydrolab O2 mg/L	Hydrolab Temp C	Hydrolab Salinity ‰	IRMS O2 %
F5 b	Jul-03			b	F	23.9	5.2	5.5	23.1	35.6	75.3
F6 surf	Jul-03	2.97	1	0	F	22.9	7.1	6.7	29.7	25.9	107.6
F6 5m	Jul-03			5	F	23.1	6.8	6.7	28.8	28.0	103.5
F6 10m	Jul-03			10	F	23.3	6.4	6.5	29.2	29.8	98.9
F6 15m	Jul-03			15	F	23.5	6.2	6.4	28.7	33.5	96.9
F6 20m	Jul-03			20	F	23.6	6.4	6.5	27.8	27.9	95.9
F6 25m	Jul-03			25	F	23.7	6.5	6.3	26.9	25.5	94.5
F6 30m	Jul-03			30	F	23.6	6.5	6.9	23.9	35.6	94.5
F6 35m	Jul-03			35	F	25.3	4.8	5.0	20.7	35.7	66.1
F6 b	Jul-03			b	F	26.1	4.6	4.9	20.4	35.8	62.6
G1 surf	Jul-03	3.41	2111	0	G	21.0	6.7	6.5	29.3	30.1	103.1
G2 surf	Jul-03	3.46	2344	0	G	22.0	6.6	6.4	29.6	27.8	102.0
G2 5m	Jul-03			5	G	22.3	4.6	6.1	28.2	31.5	70.2
G2 b	Jul-03			b	G	39.0	0.5	0.5	26.0	33.0	7.3
G3 surf	Jul-03	3.52	2344	0	G	23.4	6.8	6.6	29.3	25.9	102.8
G3 5m	Jul-03			5	G	22.4	6.0	6.0	29.2	26.3	91.4
G3 10m	Jul-03			10	G	24.3	5.7	5.8	28.8	32.0	88.4
G3 15m	Jul-03			15	G	24.5	4.9	5.2	27.4	33.6	74.9
G3 b	Jul-03			b	G	28.3	2.1	2.3	24.9	34.6	31.6
G4 surf	Jul-03	3.56	2271	0	G	23.6	6.7	6.7	29.2	26.9	101.0
G5 surf	Jul-03	3.61	1900	0	G	24.0	6.4	6.3	29.6	31.4	99.7
G5 5m	Jul-03			5	G	23.9	6.4	6.4	29.2	31.7	99.0
G5 10m	Jul-03			10	G	23.8	6.4	6.5	28.8	31.8	99.7
G5 15m	Jul-03			15	G	23.7	6.4	6.4	28.6	31.9	99.1
G5 20m	Jul-03			20	G	23.1	6.4	6.3	28.2	33.0	98.7
G5 25m	Jul-03			25	G	23.3	4.0	4.5	27.5	34.0	61.8
G5 b	Jul-03			b	G	25.0	2.6	2.8	23.7	35.0	38.0
G6 surf	Jul-03	3.67	1300	0	G	23.5	6.4	6.2	31.0	28.3	101.4
G6a surf	Jul-03	3.73	605	0	G	23.4	6.5	6.5	29.4	31.1	101.3
G6a 10m	Jul-03			10	G	23.7	6.4	6.4	28.9	31.7	99.0
G6a 15m	Jul-03			15	G	22.9	6.4	6.4	28.1	32.8	97.9
G6a 20m	Jul-03			20	G	23.2	6.4	6.3	27.8	33.4	97.9
G6a 25m	Jul-03			25	G	23.5	6.2	6.4	27.6	34.0	95.5
G6a 30m	Jul-03			30	G	25.2	2.4	4.0	27.4	34.5	36.3
G6a b	Jul-03			b	G	31.2	2.1	1.9	20.6	35.6	28.7
G8 surf	Jul-03	3.78	43	0	G	23.4	6.5	6.4	29.8	30.1	100.7
G8 b	Jul-03			b	G	26.6	4.2	4.5	20.6	35.8	58.3
H0 surf	Jul-03	4.32	371	0	H	17.9	7.9	8.1	29.6	30.0	123.2
H1 surf	Jul-03	4.27	73	0	H	19.6	7.3	7.2	29.6	27.0	111.4
H1 5m	Jul-03			5	H	18.6	5.7	6.7	29.0	29.0	87.2
H1 b	Jul-03			b	H	32.7	2.1	2.0	28.4	31.6	31.9
H2 surf	Jul-03	4.23	11	0	H	22.2	6.7	6.5	29.4	24.7	100.2
H3 surf	Jul-03	4.17	1	0	H	21.7	7.1	6.8	29.6	24.1	106.4
H4 surf	Jul-03	4.12	1	0	H	21.0	7.2	7.6	29.6	25.7	109.3
H4 5m	Jul-03			5	H	24.1	5.6	5.6	29.1	29.4	85.5
H4 10m	Jul-03			10	H	23.2	6.1	6.0	28.4	32.9	94.1
H4 15m	Jul-03			25	H	23.3	6.1	6.1	27.8	33.9	93.8
H4 20m	Jul-03			20	H	24.4	5.1	5.3	25.4	34.8	76.2
H4 b	Jul-03			b	H	25.9	3.5	3.9	25.0	34.8	52.4
H5 surf	Jul-03	4.06	1	0	H	23.2	6.7	6.4	29.5	26.5	101.6
H5 10m	Jul-03			5	H	23.5	6.3	6.4	29.5	31.7	99.1
H5 10m	Jul-03			10	H	23.8	6.4	6.4	28.7	32.2	99.2
H5 15m	Jul-03			15	H	23.2	6.4	6.4	27.7	34.5	98.4
H5 20m	Jul-03			20	H	22.8	5.2	5.9	26.6	34.7	79.0
H5 25m	Jul-03			25	H	22.8	5.1	5.4	23.4	35.5	73.0
H5 b	Jul-03			b	H	22.8	4.8	5.1	22.8	35.4	68.7
H6 surf	Jul-03	4.01	1	0	H	23.8	6.5	6.7	29.5	26.8	99.4
H7 surf	Jul-03	3.96	1	0	H	23.1	6.7	6.5	29.7	25.9	102.0
H7 5m	Jul-03			5	H	23.6	6.4	6.4	29.1	32.2	99.2
H7 10m	Jul-03			10	H	22.8	6.2	6.3	27.5	34.6	95.9
H7 15m	Jul-03			15	H	23.7	6.5	6.5	27.6	35.8	101.5
H7 20m	Jul-03			20	H	23.7	6.6	6.6	27.6	36.0	102.4
H7 25m	Jul-03			25	H	23.7	6.6	6.6	27.2	36.0	102.0
H7 30m	Jul-03			30	H	23.7	6.7	6.7	26.9	36.0	102.2
H7 bottom	Jul-03			b	H	23.2	6.0	6.2	24.0	35.9	87.6
H8 surf	Jul-03	3.90	1	0	H	23.6	6.6	6.7	29.9	26.2	101.2

Sample	Date	Time	PAR	Depth m	Transect	IRMS δ18O ‰	IRMS O2 mg/L	Hydrolab O2 mg/L	Hydrolab Temp C	Hydrolab Salinity ‰	IRMS O2 %
I1 surf	Jul-03	4.43	2182	0	I	21.9	6.8	6.6	29.1	27.0	102.6
I1 5m	Jul-03			5	I	20.9	6.3	6.8	29.0	29.0	95.7
I1 bottom	Jul-03			b	I	36.5	1.5	1.3	28.4	31.6	22.8
I2 surf	Jul-03	4.47	2344	0	I	22.1	6.9	6.9	29.1	26.7	104.5
I3 surf	Jul-03	4.52	2344	0	I	23.0	6.7	6.8	29.9	26.0	101.7
I4 surf	Jul-03	4.56	2344	0	I	22.4	6.8	6.7	30.2	25.3	103.2
I4 5m	Jul-03			5	I	22.1	6.7	6.8	29.8	25.3	102.0
I4 10m	Jul-03			10	I	24.0	6.1	5.4	29.3	28.1	93.0
I4 15m	Jul-03			15	I	24.4	5.3	6.0	28.7	32.3	82.1
I4 bottom	Jul-03			b	I	32.6	1.2	1.7	25.6	34.3	18.0
I5 surf	Jul-03	4.61	2025	0	I	22.3	7.0	6.9	30.2	23.1	105.2
I6 surf	Jul-03	4.67	1596	0	I	22.1	7.0	7.0	30.9	23.0	106.1
I7 surf	Jul-03	4.72	861	0	I	22.9	6.9	6.8	30.2	23.5	104.2
I7 5m	Jul-03			5	I	22.7	6.7	6.5	29.7	25.3	101.4
I7 10m	Jul-03			10	I	23.1	6.8	6.2	28.8	33.4	106.1
I7 15m	Jul-03			15	I	23.4	6.9	6.5	27.7	34.4	106.2
I7 20m	Jul-03			20	I	23.6	6.4	6.6	26.7	34.7	97.0
I7 25m	Jul-03			25	I	24.1	6.1	6.2	25.8	35.3	91.1
I7 bottom	Jul-03			b	I	24.3	6.1	6.0	25.9	35.8	92.1
J0 surf	Jul-03	5.15	1	0	J	18.7	8.1	7.6	28.9	27.1	122.4
J1 surf	Jul-03	5.10	1	0	J	19.6	7.5	6.6	29.5	28.4	115.6
J1 5m	Jul-03			5	J	19.3	7.3	6.9	29.5	28.4	111.7
J1 bottom	Jul-03			b	J	28.1	0.5	0.1	27.6	32.7	7.9
J2 surf	Jul-03	5.05	1	0	J	21.4	6.8	6.2	29.0	28.7	103.2
J3 surf	Jul-03	5.00	1	0	J	23.2	6.6	6.6	29.5	26.8	100.3
J3 5m	Jul-03			5	J	21.7	6.7	6.8	29.4	27.5	103.0
J3 10m	Jul-03			10	J	21.6	6.3	6.2	28.9	28.7	96.1
J3 bottom	Jul-03			b	J	29.7	2.3	2.3	27.6	32.7	35.1
J4 surf	Jul-03	4.95	1	0	J	22.9	6.8	7.0	29.5	24.8	102.7
J5 surf	Jul-03	4.88	1	0	J	23.4	6.5	6.7	29.9	27.4	99.6
J5 5m	Jul-03			5	J	23.2	6.6	6.6	29.2	28.3	101.6
J5 10m	Jul-03			10	J	23.0	6.4	6.3	29.0	30.0	97.7
J5 15m	Jul-03			15	J	23.1	5.8	6.0	28.4	32.1	89.3
J5 bottom	Jul-03			b	J	26.9	2.0	4.4	27.4	33.2	31.1
J6 surf	Jul-03	4.83	1	0	J	23.6	6.6	6.6	29.9	27.9	101.4
J6 5m	Jul-03			5	J	23.2	6.5	6.5	29.2	29.2	99.1
J6 10m	Jul-03			10	J	22.9	6.0	6.0	28.7	30.8	91.9
J6 15m	Jul-03			15	J	24.0	5.6	5.8	28.3	31.6	85.3
J6 20m	Jul-03			20	J	25.8	4.5	4.7	26.5	34.7	68.5
J6 bottom	Jul-03			b	J	26.6	3.9	4.0	26.2	35.0	59.5
K1 surf	Jul-03	5.24	73	0	K	21.8	6.5	6.1	29.4	29.2	99.4
K2 surf	Jul-03	5.28	460	0	K	23.1	5.7	5.4	29.2	30.2	87.6
K2 5m	Jul-03			5	K	23.1	5.6	5.6	29.2	30.2	86.3
K2 bottom	Jul-03			b	K	23.5	5.3	5.0	29.1	30.2	81.5
K3 surf	Jul-03	5.34	1271	0	K	23.5	6.4	6.2	29.3	28.0	98.2
K4 surf	Jul-03	5.40	2024	0	K	23.7	6.5	6.4	29.1	27.1	98.5
K4 5m	Jul-03			5	K	23.2	6.4	6.3	29.1	27.2	97.5
K4 10m	Jul-03			10	K	22.6	5.9	4.6	28.9	29.1	90.6
K4 15m	Jul-03			15	K	24.8	3.9	2.4	28.5	31.4	59.8
K4 bottom	Jul-03			b	K	27.8	3.3	3.2	28.0	32.2	49.8
M1 surf	Jul-03	5.69	486	0	M	20.5	7.2	7.1	30.3	30.0	113.5
M2 surf	Jul-03	5.65	530	0	M	21.0	6.6	6.2	30.4	31.0	104.4
M2 5m	Jul-03			5	M	20.7	6.6	6.5	29.0	31.0	101.9
M2 bottom	Jul-03			b	M	23.1	5.5	5.8	28.8	31.1	84.5
M3 surf	Jul-03	5.59	2170	0	M	21.4	6.6	6.5	29.8	29.3	102.7
M4 surf	Jul-03	5.54	2344	0	M	23.4	6.6	6.6	30.2	26.7	101.3
M5 surf	Jul-03	5.48	2344	0	M	23.2	6.8	6.7	29.9	25.6	102.9
M5 5m	Jul-03			5	M	23.1	6.7	6.7	29.7	25.8	101.3
M5 10m	Jul-03			10	M	23.2	6.2	6.3	29.1	30.6	96.4
M5 15m	Jul-03			15	M	22.9	6.3	6.2	28.7	31.9	96.9
M5 bottom	Jul-03			b	M	24.5	4.8	4.8	27.8	32.9	73.7

APPENDIX II
PROTOCOL FOR STABLE OXYGEN ISOTOPES ANALYSES

FIELD PROCEDURE

1. At 8 mg of oxygen per liter, 125 ml bottles contain 31.25 micromoles of dissolved oxygen; 0.7 ml of air contains the same amount of oxygen. Hence, small amounts of normal air that is very rich in oxygen can and will contaminate samples. It is imperative to watch out for and prevent bubbles.
2. Wrap tape around bottles and label with a permanent (water-proof) marker: date, station and depth.
3. Prepare blue stoppers by inserting a 1-inch needle through top.
4. Attach tubing to bottom of Niskin bottle and open air-vent at top of it. For surface water samples a bucket can be used to collect the water.
5. Start water flow, and get all bubbles out of the line. For surface samples a 20 ml syringe can be used to start water flow through the tubing previously inserted into the bucket.
6. Put end of tube in bottom of bottle and fill 3 volumes, letting water overflow. Estimate time to fill bottle initially and multiply by 3 to get time needed for 3 volumes. Using a 20 ml syringe, collect additional water in case toping off is necessary.
7. As soon as possible, take bottles into lab for acidification/preservation.
8. Prepare 1 ml of 6 N HCl (50% concentrated HCl) in a 1 ml syringe. Hold syringe upright and tap to remove bubbles. Inject 1 ml into bottle. Water should overflow a little bit and build a small cap due to surface tension.
9. Press blue stopper into top of filled bottle; some water will squirt out the needle.

10. Remove needle slowly and carefully so it does not suck up air into the bottle. Only use needles once, they loose their sharpness after first use and become difficult to remove from the stopper leading to air bubbles in the sample because of sucked up air.
11. Check for bubbles immediately. If there are bubbles, remove stopper and top off the bottle with water from the 20 ml syringe. Reinsert the stopper with needle as describe previously. Later on, bubbles may appear due to over-saturation of oxygen or CO_2.
12. Crimp on metal cap; use a light touch in the crimping, as water expands and the stopper needs some flex room.
13. Store bottles in box (or cooler) inside cool cabin. Bottles are pressurized and may crack if they warm up, especially samples filled with cold water from bottom.

LABORATORY PROCEDURE

1. Once in the lababoratory, store samples in the fridge. Prepare and analyze as soon as possible.
2. Check mass spectrometer setup ~3 days before running samples (see part III below).
3. Start preparation of standards and samples two days before the analysis.
4. Take samples out of refrigerator and let them acclimate to room temperature. Creating a head space in a cold sample leads to inaccuracies in the volume of the head space
5. Attach a 4-way stop cock to a 20-ml syringe and flush syringe three times (He from reference side, 150 kPa), fill, pressurize it and close valve.
6. Weigh the sample before and after adding the headspace. The difference in weight should be 10 g (after weighing hundreds of samples there was no significant difference from 10 g, so this step could be skipped).

7. Attach a 4-inch needle to syringe, open valve, push out He to 10 ml, and immediately push into rubber stopper. With help of pliers, push needle all the way through stopper into the pressurize bottle. Insert a 1-inch needle into stopper and turn bottle upside down. Inject He into the bottle, water will drain out through small needle. When water starts dripping, remove small 1-inch needle, turn bottle around, and quickly remove syringe with 4-inch needle.
8. Before flushing and filling syringe with He for next sample, remove any water from 4-inch needle and syringe.
9. Prepare standards by filling 4L beaker with deionized water, put in on stirrer at low speed overnight to equilibrate dissolved gases with the laboratory atmosphere. Add 132.5 g of NaCl to adjust salinity to 36 psu for marine samples. Record temperature, salinity, adjust pH to 9, and add 0.848 g Na_2CO_3 (2000 µmol C L^{-1}) from "carbonate standard" vial. Make sure that carbonate is completely dissolved before proceeding.
10. Take beaker off stirrer and fill standard bottles with tygon tubing by overflowing bottles three times.
11. Add 1 ml of 6N HCl to each bottle immediately before sealing with thick blue rubber stopper that is penetrated by a 1-inch needle do drain excess water. Check bottle for air bubbles before crimping with aluminum cap. In case of air bubble, discard standard. Never re-use 1-inch needles for penetrating rubber stoppers.
12. Add headspace to standards as described above.
13. Prepare zero-oxygen water by dissolving 100 g of Na_2SO_3 in 2L of tap water (put on stirrer at slow speed). Proceed with filling zero-oxygen standards, and adding headspace as described above.

14. In the afternoon before the analyses, place all samples and standards in shaker (100 rpm) and let headspace equilibrate with dissolved gases overnight.
15. The following morning, start CNO sequence with 1.0 ml air injection and standards, check $\delta^{18}O$ values.
16. Adjust Excel output file to accommodate CNO Macro.
17. Use CNO Macro to analyze the data (blank correction if necessary and size-dependency).

MASS SPECTROMETER SETUP

Do not attempt CON analyses right after running sulfur samples; $\delta^{18}O$ values will be too low. It takes 10 to 14 days to flush sulfur off the source and reach stable $\delta^{18}O$ values. Carbon and nitrogen samples do not cause problems. Make sure that gas pressure on all needed gas cylinders is sufficient.

1. Close sample and standard valves in mass spectrometer.
2. Switch flow to reference side (100 kPa) and turn off flow on sample side.
3. Set furnace temperatures to 200 ºC, they are not needed for analysis.
4. Ignore EA settings, none of this is needed for the analysis.
5. Switch 1/8 fittings between O_2 and SO_2 cylinders to have oxygen standard in middle injector (at gas bench).
6. Set pressure on O_2 cylinder to 20 kPa.
7. Set He pressure on gas bench to 8 psi.
8. Set pressure for He and N_2 on ConFlo to 7 and 0 psi, respectively.
9. Disconnect sample He flow from autosampler.
10. Insert injector, water trap (filled with magnesium perchlorate), and 1.5m GC column (for CNS analyses, at room temperature) into sample train.

11. Connect sample train to connector on top of gas bench (next to cryofocus trap).
12. Insert second water trap (filled upstream with ascarite and magnesium perchlorate downstream) and 2m GC column for O_2–N_2 separation (5 å mesh, at room temperature) into cryofocus loop.
13. Connect gas bench back to ConFlo.
14. Set pressure on EA for sample train to 115 kPa and check for leaks.
15. Switch back to sample flow.
16. Open sample and standard valve in mass spectrometer.
17. Refocus machine as necessary for C, then O, then N. For each gas, peak center, autofocus (with extraction boxes off), then again peak center (pass HV and magnet settings to gas configuration), again autofocus (with extraction boxes off) and pass this to gas configuration.
18. Check O_2-N_2 jump (instrument control, scan, green arrow, N_2 standard on, and write down settings for the new jump).
19. Open CON sequence and inject 5ml of CNO-gas cylinder at 10 sec. to check timing for peak retention. Adjust timing if necessary, or if retention times are extremely long, bake out 2m 5å column at 400 ºC in muffle furnace overnight (have slow He flow set up through column to flush out water residues). To avoid water contamination of GC column, keep it always tightly closed if not in use. If open to the atmosphere, the column sucks up water like a sponge.
20. Inject several air samples (1ml) at 10 sec. and check if $\delta^{18}O$ values are stable.
21. Update and save sequence information.

SAMPLE INJECTIONS

The actual sample that will be injected into the mass spectrometer is obtained from the headspace in the 125 ml bottles.

1. Using a 5 ml syringe, inject into the headspace the same amount of He as the sample that will be analyzed.
2. Flush the syringe five times to mix the He with the headspace and withdraw the appropriate amount of sample into the syringe.
3. Immediately injected the headspace-sample gas through the instrument's septum into the sample train.

APPENDIX III
MARINE ECOLOGY PROGRESS SERIES COPYRIGHT RELEASE AUTHORIZATION

Dear Zoraida,

We herewith give publisher permission for you to use your article mentioned below in your PhD thesis, provided proper acknowledgement is being made to the original source of publication.

Kind regards
Marianne Hiller
Permission Department

==========
Inter-Research Science Center
Nordbuente 23, D-21385 Oldendorf/Luhe , Germany

Tel: (+49) (4132) 7127 Email: Marianne@int-res.com
Fax: (+49) (4132) 8883 http://www.int-res.com
==========

From: "Zoraida Quinones" <zquino1@lsu.edu>
To: "Angela Fromm" <angela@int-res.com>
Date: Mon, 28 Jan 2008 09:51:41 -0600
Subject: M 6840 Copyrights

Hello Angela,

I am writing in regards to manuscript 6840, published in MEPS in 2007 (Vol 342: 69-83). This manuscript is part of my PhD work and I would like for it to be one of the chapters of my dissertation. I believe I need authorization from MEPS first, so could you please tell me how should I proceed.

Best regards and best wishes for the new year,

Zoraida

VITA

Zoraida J. Quiñones-Rivera was born July 12, 1973, in San Juan, Puerto Rico. She obtained a Bachelor of Science degree in ecology, evolution and organismal biology with a second major in Spanish literature at Tulane University, New Orleans, Louisiana, in 1996. She entered the graduate program at Louisiana State University, Baton Rouge, Louisiana, where she obtained a Master of Science degree in the Department of Zoology and Physiology in 2000. In 2002, Zoraida started her degree of Doctor of Philosophy at the Department of Oceanography and Coastal Sciences at Louisiana State University. In the spring of 2005, Zoraida and her husband Dr. Björn Wissel moved to Saskatchewan, Canada. Currently she has a full time position as a Research Scientist and Laboratory Manager of the Limnology Laboratory at the University of Regina, Regina, Saskatchewan, under the direction of Dr. Peter Leavitt. Presently, she is a candidate for the degree of Doctor of Philosophy in the Department of Oceanography and Coastal Sciences at Louisiana State University.